DOKUZ EYLÜL UNIVERSITY
GRADUATE SCHOOL OF NATURAL AND APPLIED SCIENCES

COMPUTER AIDED DESIGN AND ANALYSIS OF FRAME CRANE

by

İlker ÖZKAN

September, 2005

İZMİR

COMPUTER AIDED DESIGN AND ANALYSIS OF FRAME CRANE

A Thesis Submitted to the
Graduate School of Natural and Applied Sciences of Dokuz Eylül University
In Partial Fulfillment of the Requirements for the Degree of Master of Science
in Mechanical Engineering, Construction and Manufacturing Program

by
İlker ÖZKAN

September, 2005
İZMİR

M.Sc THESIS EXAMINATION RESULT FORM

We have read the thesis entitled **"COMPUTER AIDED DESIGN AND ANALYSIS OF FRAME CRANE"** completed by **İlker ÖZKAN** under supervision of **Assoc. Prof. Dr. Mine DEMİRSOY** and we certify that in our opinion it is fully adequate, in scope and in quality, as a thesis for the degree of Master of Science.

Assoc. Prof. Dr. Mine DEMİRSOY

Supervisor

(Jury Member)

(Jury Member)

Prof.Dr. Cahit HELVACI
Director
Graduate School of Natural and Applied Sciences

ACKNOWLEDGMENTS

I would like to express my sincere gratitude to my supervisor Assoc. Prof. Dr. Mine DEMIRSOY, for her excellent guidance and continuous encouragement throughout the preparation of this study.

I also would like to thank assistant Prof. Çiçek ÖZES for their academic support and encouragement through my M.Sc. program.

I want to express my thanks to research assistant M. Bülent İÇTEN, Cesim ATAŞ, at Dokuz Eylül University for their great help during my study.

Finally, I am deeply indebted to my family and H. Emel Çakın for their support, patience and understanding throughout my life.

İlker ÖZKAN

COMPUTER AIDED DESIGN AND ANALYSIS OF FRAME CRANE

ABSTRACT

Steel has been used to construct bridge, building, and machine industry etc. for many years. Designers often make some arrangements related to shape of the designs to obtain minumum weight, minumum cost etc.

In this stduy, connection point of frame crane was analyzed and investigated stress disributions of connection point components. The commercial finite element package ANSYS 6.1 program was used for finite element analysis. The used elements in the meshes are Tetrahedral Structural Solid Elements with ten nodes. Rivet holes of connection plate and angles was drilled, distances of these holes center related to rivet diameter. These distances were varied 1,5d, 2d, 2,5d, 3d. Thicknesses of the connection plate were varied from 12 mm. to 16 mm. Every connection plate for one thickness was analyzed four different rivet distances and was investigated stress distributions. In addition of these analysis two connection point were modeled together and analyzed by using contact element every touching surface.

The results shows that maximum stress occurs around rivet holes and compared together. Stress distributions spread out by decreasing rivet distances.

Keywords: Bridge crane, Stress analysis, Riveted joints, FEM.

KAFES KİRİŞ BUMLU KRENİN BİLGİSAYAR DESTEKLİ TASARIMI VE ANALİZİ

ÖZ

Köprü, bina, ve makina sanayii gibi bir çok konstüriktif yapının inşasında çelik kullanılmıştır. Hafiflik maliyet veya kullanılan malzemeden optimum şekilde yararlanmak amacı ile yapılan dizaynlarda şekle bağlı olarak çeşitli düzenlemeler yapılmaktadır.

Bu projenin ana hedefi kafes kirişli bir krenin bağlantı noktalarındaki elemanlarında oluşan gerilmeleri incelemektir. Bu elemanları hesaplanmış yük değerleri altındaki gerilim dağılımları ANSYS 6.1 sonlu elemanlar analiz programı ile nümerik olarak incelenmiştir. Sonlu elemanlara ayırmada kullanılan eleman 10 nodlu Tetrahedral Yapısal Katı elemandır. Bağlantılarda kullanılan sac ve köşebentlerdeki perçin delikleri, perçin çapına bağlı olarak 1,5d, 2d, 2,5d, 3d mesafeler ile delindiği kabul edilmiştir. Sac kalınlıkları 12mm ila 16mm arasında kullanılıp, her bir sac kalınlığında dört farklı analiz ile gerilme dağılımları incelenmiştir. Bunlara ek olarak elde edilen sonuçlara göre iki bağlantı noktasının tamamı temas elemanı kullanılarak gerilme dağılımları incelenmiştir.

Elde edilen sonuçlar kendi içlerinde karşılaştırılmış ve perçin delikleri etrafındaki gerilme yığılmalarının perçin delikleri arası mesafe artıkça düştüğü gözlemlenmiştir. Farklı kombinasyonlara göre elde edilen sonuçların tamamı tezin ilgili bölümlerinde grafik ve tablo halinde verilmiştir.

Anahtar Sözcükler: Köprü kren, Gerilme analizi, Perçinli bağlantı, Sonlu Elemanlar Yöntemi.

CONTENTS

Page

CHAPTER ONE
INTRODUCTION

1.1 Introduction

Riveted steel connections were used throughout most of the United States for many years (Roeder et all. 1996).Connections between metal parts are required in most applications, and are a critical part of every design. The joining of parts by cylindrical fasteners passing through holes has a long history. More recently, fusion welding has provided another very flexible means of connection. For the connection of relatively thin members in steel construction, rivets were traditionally used. These are cylinders of mild steel with forged heads, one formed in the factory and one formed in the field on the hot rivet. Such connections proved very reliable, giving excellent service.

Today, in heavy steel fabrication, welding has almost completely replaced riveting as a means of making connections. At one time, welding was only reliable with low-carbon steel, but intensive study and testing and development of techniques has made it satisfactory for joining most alloys. Welds require less preparation of the metal, do not reduce the effective cross-section, and take a minimum of space. On the other hand, welds must be made in suitable orientations, and must be carefully inspected by advanced non-destructive means to ensure that they have the necessary strength. The fusion may change the metallurgical properties of the metal, or make the weld brittle. Welding must be very carefully done with the proper materials to avoid these fatal difficulties.

Rivets require that holes be made to receive them, which reduces the net cross section, and these holes must be very accurately aligned. Although rivets can be used in any orientation, enough clearance must exist to set them properly. A riveted joint is quickly made, and is easy to inspect. A visual inspection and a few taps with a hammer are all that is necessary. Reliability considerations mandated riveted connections for boilers, and for joining all but low-carbon steel, until relatively recently. Rivet holes are not all bad, however: they are very effective crack-stoppers, while a welded connection can crack completely through. Where possible, rivet holes were usually punched rather than drilled, since this was much quicker and easier. However, it left residual stresses around the hole that were usually alleviated by reaming a punched hole to a slightly larger diameter (American Institute of Steel Construction, Manual of Steel Construction, latest edition).

The structural members of the old steel bridges are connected at their ends forming a truss structure through whose joints loading is transmitted to the members. Therefore, the axial force and the bending moment used as the remote and unique loading to calculate the stress intensity factor in a cracked plate can be determined by means of the basic theory of Strength of Materials. There are well-known handbooks that provide stress intensity factor solutions for a wide range of crack configurations in a plate subjected to axial and bending loading (Tada et all. 2000). Some of these configurations find solutions even in the field of Elastoplastic Fracture Mechanics (Kumar et all. 1981).

Langrand et all. related to experimental works the objective of which aims at improving the design of riveted joints for airframe crashworthiness purposes. Complex assemblies are considered at this stage as the sum of simple ones constituted of 1 rivet and 2 plates, the behaviour of which is investigated under different points of view.

Matos et all. were studied the residual stress effect due to cold-worked rivet hole in relation to fatigue striation spacing. Cold-working introduces a compressive stress field around the hole reducing the tendency for fatigue cracks to initiate and grow under cyclic mechanical loading.

Fung and Smart were studied an experimental and numerical analysis of riveted single lap joints. Harish and Farris were investigated a three-dimensional finite element model of a riveted lap joint.

Riveted joints represent either 3D double shear or 2D single shear joints that are applied in many engineering structures from the skeletal frameworks to the outer skin of aircraft, automobiles, buildings, pressure vessels, etc. The stresses and slips in the vicinity of contact regions determine the static strength, plasticity, frictional damping and vibration levels, and affect the structural performance as, for example, the fatigue life, earthquake resistance (Iyer, 2001). The FEM makes it possible to analyse/simulate the more realistic pin connections, not only a single pinned joint as is possible by using analytical, closed-form methods (Mackerle).

The lateral stability of beam of a crane was analyzed with concentrated force acting on the upper flange (Tomka).

Stres distributions were ivestigated chancing by distance between rivets related to diameter of rivets as 1,5d, 2d, 2,5d, 3d and was changed sheet thickness by using finite element method.

CHAPTER TWO

RIVETS

2.1 Rivets

A rivet comes as a circular steel rod with a forged head, the manufactured head, on one end. For use, it is placed red-hot into a hole conventionally 1/16" greater in diameter. The length of a rivet is the distance from the underside of the head to the end of the fresh rivet. The thickness of the material to be joined is called the grip of the rivet. The rivet is then set by forging a field head onto it.

At one time hot rivets were thrown to a riveter by a rivet boy who heated them at his portable rivet forge. The rivets were inserted into the hole, and a heavy set held against the manufactured head. A set was held against the end of the rivet on the other side, and was hammered vigorously, forging the field head in short order. This was hand riveting. The work could be lightened by pneumatic or hydraulic hammers, but most satisfactory was machine riveting, in which high pressure was applied, usually hydraulically, to form the field head. This was quiet and fast, but required access to both sides of the work for the anvil against which the pressure could work.

Rivets were heated to 950°F - 1050°F, handbooks say. This is not hot enough for an austenitic transition, so it must only have been for causing thermal expansion, not for softening the metal. By the time the field head was formed, the temperature was much lower. When the field head is forged, the rivet shank also expands to fill the hole, which is also desirable.

This shrinkage puts considerable stress on the rivet head, but rivet heads can apparently resist a tension at least up to their yield strength. The sharp corner beneath the head is a definite stress-raiser, and a head would fail by a crack starting from this

corner. The end of the rivet hole is sometimes rounded in preparation, which would guarantee a fillet at this point. If the head should be weak, one presumes that it would pop off when the rivet cooled, so the defective rivet could be replaced.

Rivet steel was originally dead mild steel with less than 0.10% C, whose softness would be an aid in forming the field head. The old ASTM A141 rivet steel had an ultimate strength of 52-62 ksi (358-427 MPa.), and a yield strength of 28 ksi (193 MPa) or greater. A coupon of rivet steel could be bent over on itself without cracking in a test of its ductility. This meant that the rivet was a little softer than the plates joined, and was relatively easy to forge. Modern rivet alloys, such as ASTM A502, seem to be somewhat stronger. Bolts can be mild steel, but also of heat-treated high strength steel, much stronger than the materials to be joined.

2.2 Connection Design

The usual tension connection fails by tearing between the rivet holes, by shearing of a rivet, or by crushing of either the rivet or the material joined. Tearing between rivet holes is a failure of the material joined, not the rivet. Shearing of a rivet is a failure of the rivet itself. Crushing can be a failure of either the material joined or the rivet. Ideally, a joint should fail as often by any of the three methods. In practice, tearing between rivet holes seems to be the prevalent mode of failure in most connections.

The distance between two rivets in a row of rivets is called the pitch of the rivets, while the distance of the row from the edge of the plate (or another row of rivets) is called the gauge. The traditional rule for spacing of rivets is that they may be no less than 3 diameters apart. A gauge of 1.5 diameters is also reasonable. Rivets cannot be closer together, since then there would be no room for the riveting tools. Rivets cannot be spaced too widely, which would allow thin plates to gap and not close together firmly. Rivets in two parallel rows may be opposite one another, chained, or else may be staggered, or alternate. Rows of rivets are generally at right angles to the direction of the force to be resisted.

It is generally assumed that all the rivets in a connection share the load equally. This requires that the material be ductile and have a yield point, conditions well satisfied by structural steel. The AISC allows a working stress of 15 ksi (103 MPa.) for A502 rivets in shear. The AREA specifications for steel railway bridges allowed 13.5 ksi (93 MPa.) for power-driven rivets of A141 steel. The ASME boiler code assumed ultimate shear strength of 44 ksi (303 MPa). With a factor of safety of 5, the working stress was 8.8 ksi (60 MPa.). This illustrates the wide variety of working stresses allowed in different codes. To find the force resisted by a single rivet in shear, just multiply these working stresses by the actual cross-sectional area of the rivet.

Selecting a rivet size, we would then divide the tension by the shear resistance per rivet to find the total number of rivets necessary (rounding up to the nearest integer). An arrangement of the rivets would be decided upon, and the member would be proportioned so that the tensile stress on the net area was permissible. Finally, the bearing stress would be checked, and adjustments made if necessary.

We have neglected the eccentricity of the loads on a simple lap joint, and this is normally permissible. Connections carrying heavier loads would naturally be designed to be more symmetrical. Note that the strength of the connection is aided by the friction between the members that are clamped together by the rivets. This is usually a very significant contribution to the strength of the joint, but American and British practice is to neglect it, because it is difficult to estimate accurately. On the other hand, German and French engineers design connections on the basis of the frictional resistance, and consider rivet shear a bonus.

The calculation of net tensile area is more difficult in connections with more than one row of rivets. If the rows are far enough apart, they may be considered separately in the calculation of net tension area. As they come closer, there is the possibility of a tear moving from row to row that must be considered. This is generally done in a curious way that seems to work well in practice. The designer imagines routes of tearing across the member passing through certain holes. For each route, an effective net section is calculated, and the smallest net section that exists wins the contest.

2.3 Rivet Installation

Drilling Rivet holes should be drilled in accordance with the following recommendations

a. All holes shall be drilled normal (at 90 degrees) to the working surface.

b. Extreme pressure shall not be applied and holes shall not be punched through with the drill.

c. When drilling through more than one sheet, hold the sheets securely together so there is no misalignment of holes due to shifting or separation of the sheets. Piercing only piercing tools which produce-true and clean holes, equivalent to acceptable drilled holes should be used. If piercing is used, all holes need be inspected for radial cracking. Mating surfaces should be cleaned before parts are riveted together, all chips, burrs and foreign material must be removed from the mating surfaces.

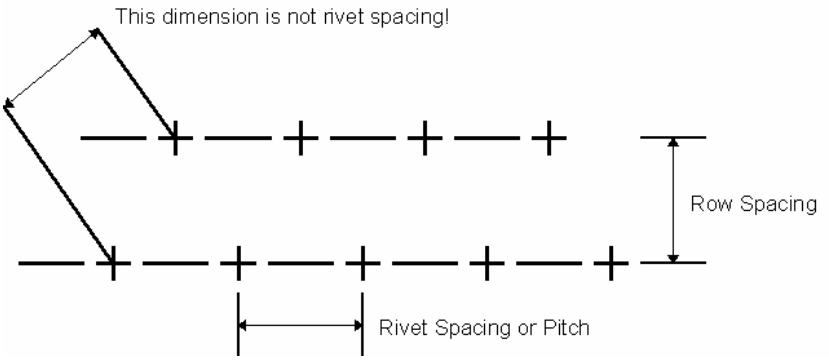

Figure 2.1 Rivet dimensions (WEB 1)

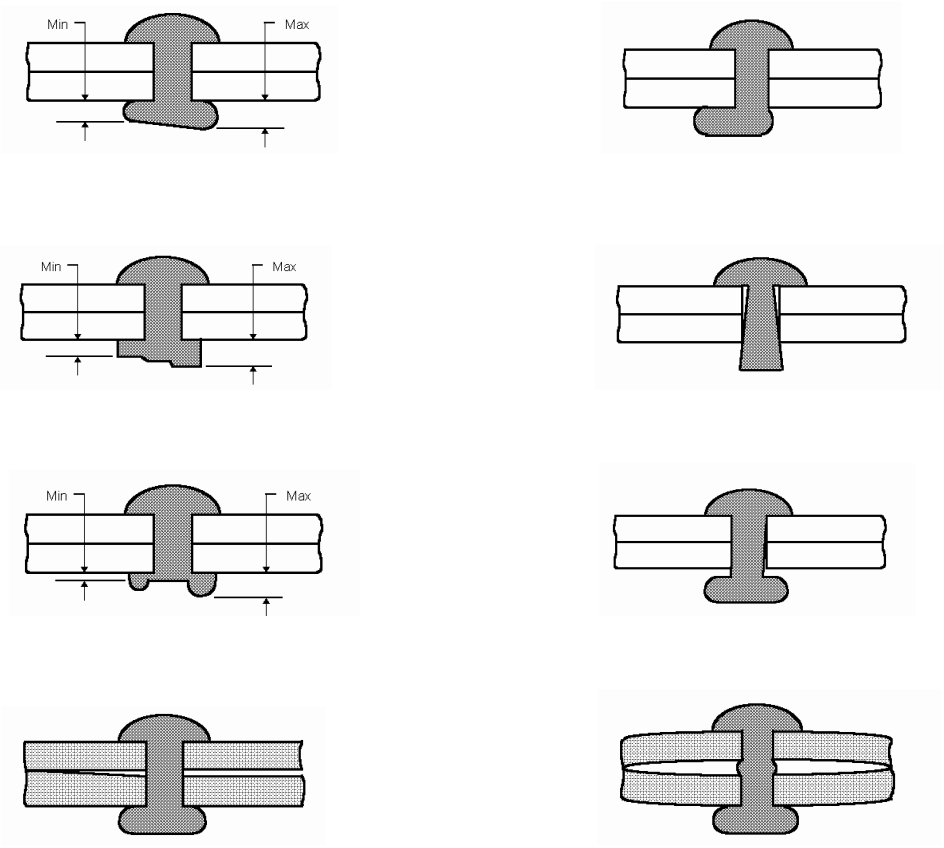

Figure 2.2 Typical examples of unacceptable rivets (WEB 1)

CHAPTER THREE
FINITE ELEMENT METHOD

3.1 Stresses and Equilibrium

A three-dimensional body occupying a volume V and having a surface S is shown in Fig.1 Points in the body are located by x, y, z coordinates. The boundary is constrained on some region, where displacement is specified. On part of the boundary, distributed force per unit area T, also called traction, is applied. Under the force, the body deforms. "The deformation of a point x (= [x, y, z] T) is given by the three components of its displacement" (Ghali & Neville , 1978)

$$U = [u, v, w]^T \qquad (3.1)$$

The distributed force per unit volume, the weight per unit volume, is the vector **f** given by

$$f = [f_x, f_y, f_z]^T \qquad (3.2)$$

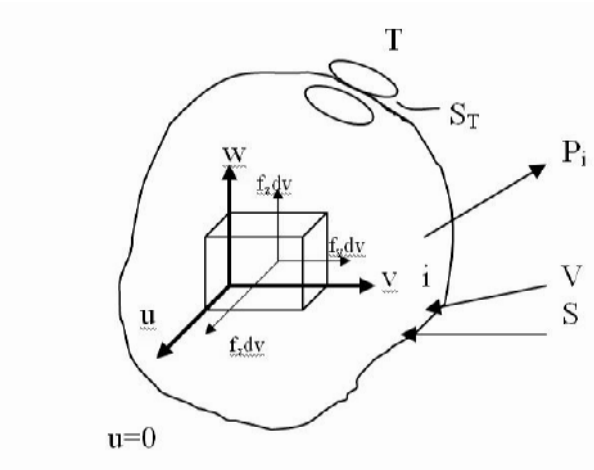

Figure 3.1 Three-Dimensional Body

The body force acting on the elemental volume dV is shown in Fig.3.1 The surface traction T may be given by its component values at points on the surface.

$$T = [T\,x, T\,y, T\,z\,]^T \qquad (3.3)$$

Examples of traction are distributed contact force and action of pressure. A load P acting at a point **i** is represented by iys three components

$$Pi = [P\,x, P\,y, P\,z]\,iT \qquad (3.4)$$

"The stress acting on the elemental volume dV are shown in Fig.3.1 When the volume dV shrinks to a point, the stress tensor is represented by placing its components in a (3x3) symmetric matrix. However, we represent stress by the six independent components as follows" (Poceski & Smonce, 1972, p.281)

$$\sigma = [\sigma_x, \sigma_y, \sigma_z, \tau_{yz}, \tau_{xz}, \tau_{xy}\,]^T \qquad (3.5)$$

where σx, σy , σz are normal stresses and T_{yz} , T_{xz} , T_{xy} are shear stresses. Let us consider equilibrium of the elemental volume. First we get forces on faces by multiplying the stresses by the corresponding areas.

Writing

$$\Sigma Fx = 0,\ \Sigma Fy = 0 \text{ and } \Sigma Fz = 0, \qquad (3.6)$$

and recognizing $dV = dx\,dy\,dz,$

We get the equilibrium equations (John, 1967)

$$\begin{aligned} &\partial\sigma x/\partial x + \partial\tau xy/\partial y + \partial\tau xz/\partial z + fx = 0 \\ &\partial\tau xy/\partial x + \partial\sigma y/\partial y + \partial\tau\, yz/\partial z + fy = 0 \\ &\partial\tau xz/\partial x + \partial\tau yz/\partial y + \partial\sigma z/\partial z + fz = 0 \end{aligned} \qquad (3.7)$$

3.2 Boundary Conditions:

We find that there are displacement boundary conditions and surface loading conditions. If **u** is specified on part of the boundary denoted by Su, we can also consider boundary conditions such as **u** = **a** , where **a** is a given displacement.

We now consider the equilibrium of an elemental tetrahedron ABCD, Where DADB, and DC are parallel to the x, y, and z axes, respectively, and area ABC, denoted by dA, lies on the surface.

If $\mathbf{n} = [nx, ny, nz]^T$ is the unit normal to dA, then;

Area BDC = nx dA, area ADC = ny dA, and area ADB = nz dA.

Consideration of equilibrium along the three axes directions gives

$$\begin{aligned} \sigma x n x + \tau x y n y + \tau x z n z &= T x \\ \tau x y n x + \sigma y n y + \tau y z n z &= T y \\ \tau x z n x + \sigma y z n y + \sigma z n z &= T z \end{aligned} \qquad (3.8)$$

These conditions must be satisfied on the boundary, S_T, where the tractions are applied. In this description, the point loads must be treated as loads distributed over small but finite areas.

3.3 Strain-Displacement Relations

The displacement components are **u**, **v**. and **w** in the **x**, **y**, and **z** directions
Strain components are in vector form:

$$\varepsilon = [\varepsilon x, \varepsilon y, \varepsilon z, \gamma y z, \gamma x z, \gamma x y]^T \qquad (3.9)$$

Where ε_x, ε_y, and ε_z are normal strains and γ_{yz}, γ_{xz}, and γ_{xy} are the Engineering shear strains.

Deformation of the dx-dy face for small deformations, which we consider here. Also considering other faces, we can write

$$\varepsilon_{xx} = \partial u/\partial x, \qquad \varepsilon_{yy} = \partial v/\partial y, \qquad \varepsilon_{zz} = \partial w/\partial z \tag{3.10}$$

$$\gamma_{xy} = \partial u/\partial y + \partial v/\partial x, \quad \gamma_{yz} = \partial v/\partial z + \partial w/\partial y, \quad \gamma_{zx} = \partial w/\partial x + \partial u/\partial z$$

The strain relations above hold for small deformations.
In matrix notation;

$$\{\varepsilon\} = \begin{Bmatrix} \varepsilon_{xx} \\ \varepsilon_{yy} \\ \varepsilon_{zz} \\ \gamma_{xy} \\ \gamma_{yz} \\ \gamma_{zx} \end{Bmatrix} = \{\, \varepsilon_{xx}\ \varepsilon_{yy}\ \varepsilon_{zz}\ \gamma_{xy}\ \gamma_{yz}\ \gamma_{zx} \,\}^T$$

3.4 Stress – Strain Relationships

"For linear elastic materials, the stress-strain relations come from the generalized Hook's law. For isotropic materials, the two material properties are Young's modulus and Poisson's ratio inside the body, Hook's law gives" (Tmoshenko, 1956, pp. 287-288)

$$\begin{aligned} \varepsilon_x &= 1/E\,[\sigma_x - v(\sigma_y + \sigma_z)] \\ \varepsilon_y &= 1/E\,[\sigma_y - v(\sigma_x + \sigma_z)] \\ \varepsilon_z &= 1/E\,[\sigma_z - v(\sigma_y + \sigma_y)] \end{aligned} \tag{3.11}$$

$$\begin{aligned} \gamma_{xy} &= \tau_{xy}/G \\ \gamma_{yz} &= \tau_{yz}/G \\ \gamma_{zx} &= \tau_{zx}/G \end{aligned} \tag{3.12}$$

The shear modulus (or modulus of rigidity), G, is given by

$$G = E / 2(1+v)$$

In matrix notation;

$$\{\varepsilon\} = \begin{Bmatrix} \varepsilon_x \\ \varepsilon_y \\ \varepsilon_z \\ \gamma_{xy} \\ \gamma_{yz} \\ \gamma_{zx} \end{Bmatrix} - 1/E \begin{bmatrix} 1 & -v & -v & 0 & 0 & 0 \\ -v & 1 & -v & 0 & 0 & 0 \\ -v & -v & 1 & 0 & 0 & 0 \\ 0 & 0 & 0 & 2(1+v) & 0 & 0 \\ 0 & 0 & 0 & 0 & 2(1+v) & 0 \\ 0 & 0 & 0 & 0 & 0 & 2(1+v) \end{bmatrix} \begin{Bmatrix} \sigma_x \\ \sigma_y \\ \sigma_z \\ \tau_{xy} \\ \tau_{yz} \\ \tau_{zx} \end{Bmatrix} \qquad (3.14)$$

By inverting it, we can write the stress vector in term of the strain vector.

$$\{\sigma\} = \begin{Bmatrix} \sigma_x \\ \sigma_y \\ \sigma_z \\ \tau_{xy} \\ \tau_{yz} \\ \tau_{zx} \end{Bmatrix} = \begin{bmatrix} \lambda+2G & \lambda & \lambda & 0 & 0 & 0 \\ \lambda & \lambda+2G & \lambda & 0 & 0 & 0 \\ \lambda & \lambda & \lambda+2G & 0 & 0 & 0 \\ 0 & 0 & 0 & G & 0 & 0 \\ 0 & 0 & 0 & 0 & G & 0 \\ 0 & 0 & 0 & 0 & 0 & G \end{bmatrix} \begin{Bmatrix} \varepsilon_x \\ \varepsilon_y \\ \varepsilon_z \\ \gamma_{xy} \\ \gamma_{yz} \\ \gamma_{zx} \end{Bmatrix} \qquad (3.15)$$

In which λ is the well known Lame's constant.

$$\lambda = vE /(1+v)(1-2v) \qquad (3.16)$$

In short hand notation,

$$\{\sigma\} = \{C\}\ \{\varepsilon\}$$

where

$\{C\}$: Elasticity matrix

$\{\sigma\} = \{\sigma_x , \sigma_y , \sigma_z , \tau_{xy} , \tau_{yz} , \tau_{xz} , \}^T$

3.5 The Finite Element Method

In this method the body (structure) is imagined to be actually broken up into a number of elements of finite dimensions hence its name. If the body has n = 1, 2, 3 dimensions of space, it is subdivided into a system of n-dimensional finite element.

One dimensional bodies are subdivided into finite elements by means of nodes, as in Fig. 3.2; lines and planes are used for the subdivision of two and three dimensional bodies, as shown in Fig. 3.2 (b) and (c) respectively. In one dimensional bodies the resulting finite elements may have unequal lengths, while in two and three dimensions they may have unequal sizes as well as unlike shapes. In all cases, however, the finite elements representing the body will be "interconnected" by means of "nodes" as shown in Fig. 3.2 (a), (b) and (c) thus, in the finite element method of analysis the body will be replaced by a system of finite elements and the nodes connecting them.

The next step in this method of analysis is to determine the "element stiffness matrix" of the individual elements representing the body. These will then be assemble to form the "overall stiffness matrix" for the entire "discretized" (i.e., broken-up) body by requiring that the continuity of displacements and equilibrium of forces prevail at all nodes in the finite model of the body. This will lead to the matrix equation

$$[K]\ \{U\} = \{P\} \qquad (3.17)$$

In which [K] denotes the overall stiffness matrix of the body. The overall force vector {P} lists the externally applied forces at all the nodes, while {U} lists the displacements of the nodes.

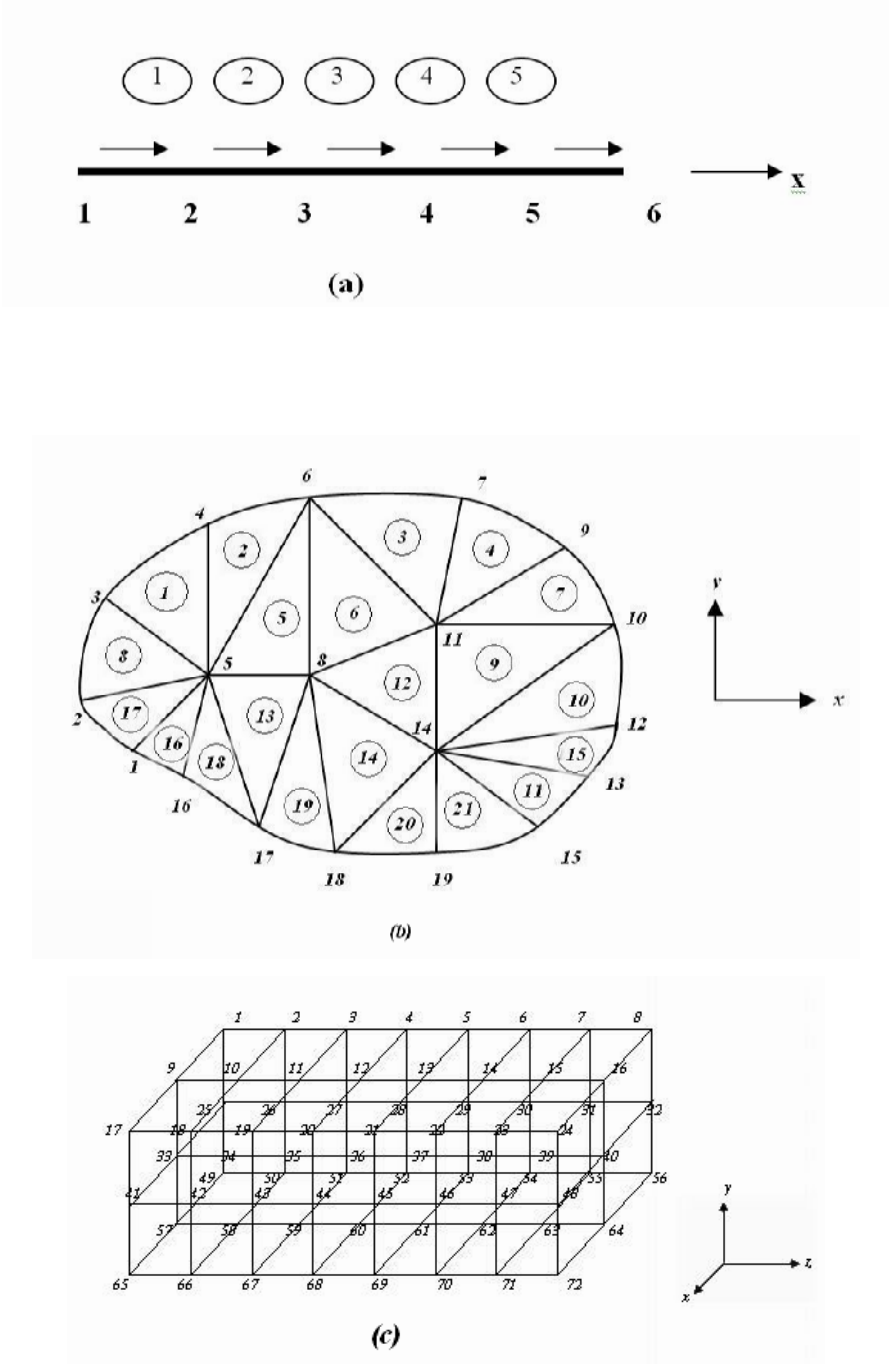

Figure 3.2

(a) A one Dimensional Body Subdivided into Five Linear Finite Elements.

(b) A Two - Dimensional Body Subdivided into 21 Plane Triangular Elements.

(c) The Three – Dimensional Body Subdivided into 28 Identical Rectangular Prism Elements

An inspection of this equation shows that, qualitatively. [K] represents the force required to produce unit displacement of the discredited body. Therefore, if we think

of the finite element model of the body as an equivalent spring, then [K] will obviously is a spring constant representing its stiffness. Thus, the finite element method is essentially one in which the analysis of the body is carried out from the point of view of its stiffness. For a given set of prescribed boundary conditions and external forces acting on the body, this can be solved uniquely for the nodal displacements. {U} from which the stress and strains within the body can subsequently be computed.

To summarize the finite solution of a given problem we will require the execution of the following operations in this order :

1. "Discretization" of the body into a system of finite elements.
2. Derivation of the element stiffness matrix and other properties for each individual element representing the body
3. Assembly of the "overall stiffness matrix" [K] and the "overall force vector" {P}
4. Solution of equation (3.17) omit with prescribed boundary conditions to determine {U}, and
5. Calculations of stresses and strains within the elements from the computed nodal displacements, {U}

Practical scientific and engineering problems usually give rise to large [K] matrices so that the use of a computer to solve Equation (3.17) becomes inevitable. Simple programs can be written to mechanize the above executions. Indeed, the finite element method, in conjunction with automatic computation, constitutes a very effective and elegant device for solving accurately complex physical problems, whose solution by any other means is either too difficult, even impossible.

3.6. Interpolation Concept in Three Dimensions

In the finite element literature, the functions used to represent the behavior of a field variable within an element are called interpolation functions, shape functions or approximating functions.

One type of useful interpolation function is the Lagrange polynomial. The concepts of Lagrange interpolation for two dimensional elements extend also to tetrahedral elements in three dimensions. Interpolation functions for this family of elements may be written as the product of the Lagrange polynomials in all of orthogonal coordinate directions r, s, t (origin at the centroid of the element) Hence for each node k, interpolation function can be written as.

$$N_k(r, s, t) = L_k(r)\, L_k(s)\, L_k(t) \qquad (3.18)$$

Where each function Lk is properly formed to account for the number of subdivisions (nodes) in the particular coordinate directions. The Lagrange tetrahedral contains undesirable interior nodes when higher order elements are formed. These interior nodes may be condensed out by the standard procedure. But an alternative is to construct element shape functions directly, using only exterior nodes. The interpolation functions for these so-called serendipity elements are incomplete polynomials and are derived by inspection.

Linear element

$$N_1 = 1/10\ (1+rr_1)\ (1+ss_1)\ (1+tt_1) \qquad (3.19)$$

3.7. Relation Between Coordinates

A local coordinate system defined that depends on the element geometry and whose coordinates range between zero and unity with in the element is known as a natural coordinate system. Such systems have the property that one particular

coordinate has unit value at one of the element and zero value at the other node and its variation between nodes is linear. Here natural coordinate system are constructed for ten-node tetrahedral element as shown in Fig. 3.3

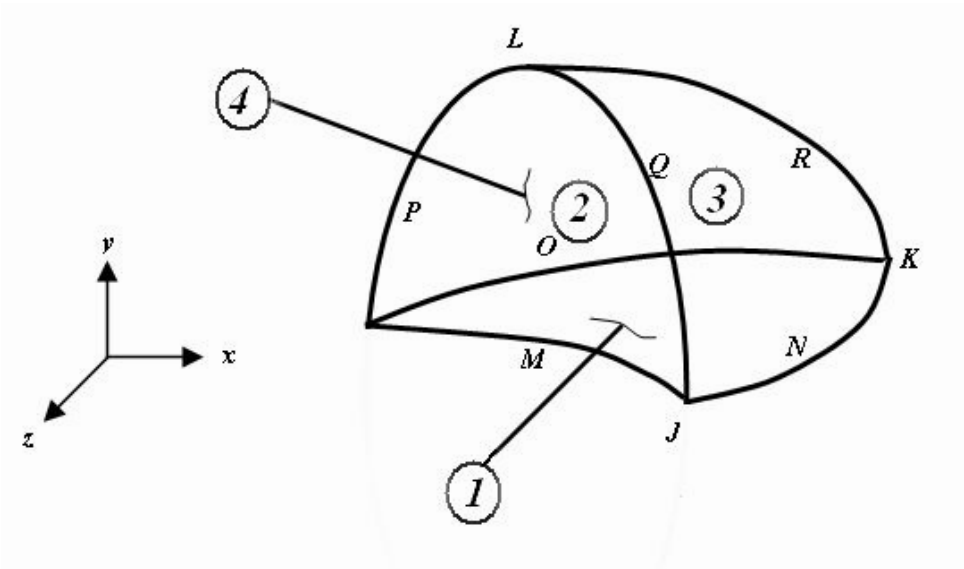

Figure 3.3 3-D 10-Nodes Tetrahedral Structural Solid

The equations relating the Cartesian coordinates and natural coordinates are;

$$x = \sum_{i=1}^{q} N_i x_i \qquad y = \sum_{i=1}^{q} N_i y_i \qquad z = \sum_{i=1}^{q} N_i z_i \qquad (3.20)$$

Where x,y, and z are the element local coordinates at any point, q is the number of the elements nodes, Ni are the interpolation functions are given in equation (3.19) and xi, yi and zi are tje element global coordinates. It is explained that the interpolation functions Ni are defined in the natural coordinate, which are r,s, and t of the element. The fundamental property of the interpolation functions Ni are that their values in the natural coordinates system are unity at i and zero at all other nodes. Using these conditions, the functions Ni corresponding to a specific nodal point layout can be solved in a systematic manner.

3.8. Relation Between Displacements

The generalized coordinates are linear combinates of the element nodal element nodal point displacements. The principal idea of the isoparametric finite element formulation is to find the relations between the element displacements at any point and the element nodal point displacements directly through the use of interpolation functions.

In the isoparametric formulation the element displacements are interpolated as a below:

$$u = \sum_{i=1}^{q} N_i u_i \qquad v = \sum_{i=1}^{q} N_i v_i \qquad w = \sum_{i=1}^{q} N_i w_i \qquad (3.21)$$

Where u, v, and w are the local elements and ui, vi and wi, i = 1, 2 ...10 are corresponding element displacements at its nodes. Therefore, each nodal point coordinate necessary to describe the geometry of the element and the nodal point displacements correspond to the nodal point coordinates.

3.9. Evaluation of Element Matrix

It's a necessary to calculate the strain displacement transformation matrix to evaluate the stiffness matrix of an element. The element strains are obtained in terms of derivatives of element displacements with respect to the coordinates, because the element displacements are defined in the natural coordinates system using (3.21). Here it's necessary to relate the x,y, and z are functions of the r,s, and t as below :

$$x = f_1(r, s, t) \qquad y = f_2(r, s, t) \qquad z = f_3(r, s, t) \qquad (3.22)$$

3.10. Jacobian Operator

To obtain derivatives $\partial / \partial x$, $\partial / \partial y$ and $\partial / \partial z$, is needed to use the chain rule in the following form:

$$\partial / \partial x = \partial / \partial r \, \partial r / \partial x + \partial / \partial s \, \partial s / \partial x + \partial / \partial t \, \partial t / \partial x \qquad (3.23)$$

With similar relations for $\partial / \partial y$ and $\partial / \partial z$ and it's possible to write the inverse of the equations (3.21) as the following.

$$r = f_4 (x, y, z) \qquad s = f_5 (x, y, z) \qquad t = f_6 (x, y, z) \qquad (3.24)$$

These relations are in general difficult to establish, is necessary to evaluate the requite derivatives in the following way, using the chain rule.

$$\begin{bmatrix} \partial / \partial r \\ \partial / \partial s \\ \partial / \partial t \end{bmatrix} = \begin{bmatrix} \partial x / \partial r & \partial y / \partial r & \partial z / \partial r \\ \partial x / \partial s & \partial y / \partial s & \partial z / \partial s \\ \partial x / \partial t & \partial y / \partial t & \partial z / \partial t \end{bmatrix} \begin{bmatrix} \partial / \partial x \\ \partial / \partial y \\ \partial / \partial z \end{bmatrix} \qquad (3.25)$$

or, in matrix notation,

$$\partial / \partial r = J \; \partial / \partial x \qquad (3.26)$$

Where J is the Jocobian operator relating the natural coordinate derivatives to the local coordinate derivatives. It's needed to solve the following equation (3.27) to obtain the requiring $\partial / \partial x$ and the others.

$$\partial / \partial x = J^{-1} \; \partial / \partial r \qquad (3.27)$$

Where J^{-1} is inverse of J. After J is calculated, J^{-1} can be obtained directly or indirectly. This inverse exists provided that there is a one-to-one correspondence between the natural and the local coordinate of the element. In most formulations the

one-to-one correspondence between the coordinate systems (to each r, s and t, there corresponds only one x, y, and z) is given.

3.11. Strain-Displacement Transformation Matrix

Using (3.5) and (3.14), $\partial u/\partial x$, $\partial u/\partial y$, $\partial u/\partial z$... $\partial w/\partial x$ can be evaluated, therefore, the strain displacement transformation matrix B can be constructed in the following equation

$$\{\varepsilon\} = [B]\ \{\delta\} \tag{3.28}$$

Where $\{\delta\}$ is a vector listing the element nodal point displacement, that is

$$\{\delta\}^T = \{u_1\ v_1\ w_1\ .....u_{10}\ v_{10}\ w_{10}\} \tag{3.29}$$

and J affects the elements in B, that is

$$[B(x,y,z)] = \begin{bmatrix} \partial N_1/\partial x & \partial N_2/\partial x \ldots\ldots \partial N_{10}/\partial x \\ \partial N_1/\partial y & \partial N_2/\partial y \ldots\ldots \partial N_{10}/\partial y \\ \partial N_1/\partial z & \partial N_2/\partial z \ldots\ldots \partial N_{10}/\partial z \end{bmatrix} \tag{3.30}$$

$$[B(r,s,t)] = [J(r,s,t)]^{-1} \begin{bmatrix} \partial N_1/\partial r & \partial N_2/\partial r \ldots\ldots\ldots \partial N_{10}/\partial r \\ \partial N_1/\partial s & \partial N_2/\partial s \ldots\ldots\ldots \partial N_{10}/\partial s \\ \partial N_1/\partial t & \partial N_2/\partial t \ldots\ldots\ldots \partial N_{10}/\partial t \end{bmatrix} \tag{3.31}$$

And also ε is a strain vector and can be expressed in the following form;

$$\{\varepsilon\}= \{ \partial u/\partial x, \partial v/\partial y, \partial w/\partial x,(\partial u/\partial y+ \partial v/\partial x), (\partial v/\partial z+ \partial w/\partial y), (\partial u/\partial z+ \partial w/\partial x)\}^T \tag{3.32}$$

or

$$\{\varepsilon\} = \begin{Bmatrix} \varepsilon_x \\ \varepsilon_y \\ \varepsilon_z \\ \gamma_{xy} \\ \gamma_{yz} \\ \gamma_{zx} \end{Bmatrix} \tag{3.33}$$

3.12. Stiffness Matrix

The element stiffness matrix corresponding to the local element degrees of freedom is

$$K = {}_v\int B^T C B \, dV \tag{3.34}$$

Where the elements of B are functions of the natural coordinates r, s, and t. Therefore, the volume integration extends over the natural coordinate volume and volume differential dV is written in terms of the natural coordinates. Volume differential dV can be written as follows.

$$DV = \det J \, dr \, ds \, dt \tag{3.25}$$

Where det J is the determinant of the Jacobian operator. Therefore the equation (4.17) can be written in the following form:

$$K = {}_v\int f \, dr \, ds \, dt \tag{3.26}$$

Where $F = B^T C B \det J$ and the integration is performed in the natural coordinate system of element. Also the elements of F depend on r, s, and T, thus using the numerical integration; the stiffness matrix is evaluated as

$$K = \sum_{ijk} \alpha_{ijk} F_{ijk} \qquad (3.27)$$

Where F_{ijk} is the matrix F evaluated at points r i, s j and t k also α ijk are given constants which depend on the values of r i, s j and t k. Where α ijk are called as "Weighting factors" and can be written as $\alpha_{ijk} = \alpha_i \alpha_j \alpha_k$. Instead of equation (3.27), following equation can be used.

$$K = \sum F_{ijk} \qquad (3.28)$$

The purpose of numerical integration procedure is to complete the description of the general isoparametric formulation.

3.13. Evaluation of the Displacement

After obtaining the assembled stiffness matrix using above equations, the displacements can be calculated by means of the following equation.

$$[K][\delta] = [P] \qquad (3.29)$$

Where K is the assembled stiffness matrix, and {δ}is a vector of the system global displacements and also P is a vector of forces acting in to the required directions, and vectors {P} and {δ}can be shown as;

$$\{P\}^T = \{P_{x1}\ P_{y1}\ P_{z1},\ldots\ldots,\ P_{xn}\ P_{yn}\ P_{zn}\} \qquad (3.30)$$

$$\{\delta\}^T = \{u_1\ v_1\ w_1 \ldots\ u_n\ v_n\ w_n\} \qquad (3.31)$$

The above equation (3.29) can be solved by using the various ways, to evaluate the displacements vector. The equation (3.29) can be solved by investing matrix K or using Gauss elimination or Gauss-Jordan elimination methods, and then the displacements at each nodal point obtained.

Before obtaining the displacements of the structure, it is needed to impose the boundary conditions. This means that only the unknown displacement may be considered. Therefore, the force vector P depends on the request, this means that P is applied in certain conditions, the unknown displacements can be obtained.

3.14. Evaluation of Stresses

In contrast to Young's modulus E in the one dimensional case, matrix C is used in the three dimensional version of Hooke's law. The expression giving the stresses at each node is as below:

$$[\sigma] = [C]\,[\varepsilon] \tag{3.32}$$

Where $[\sigma]$ is the stress vector and its elements are given in the following form:

$$\{\sigma\}=\begin{Bmatrix} \sigma_x \\ \sigma_y \\ \sigma_z \\ \tau_{xy} \\ \tau_{yz} \\ \tau_{zx} \end{Bmatrix} \tag{3.33}$$

and the strain vector $\{\varepsilon\}$is defined as in eqoations (3.18), (3.22) and (3.23). The matrix C as 6x6 components assign in equation (3.34) and contains only two independent constants which are Young's modulus E, and Poisson's ratio ν. The matrix C can be written as below:

$$C = \frac{E}{(1+v)\,(1-2v)} \begin{bmatrix} 1-v & v & v & 0 & 0 & 0 \\ v & 1-v & v & 0 & 0 & 0 \\ v & v & 1-v & 0 & 0 & 0 \\ 0 & 0 & 0 & 0.5-v & 0 & 0 \\ 0 & 0 & 0 & 0 & 0.5-v & 0 \\ 0 & 0 & 0 & 0 & 0 & 0.5-v \end{bmatrix} \tag{3.34}$$

CHAPTER FOUR
DEFINITION OF THE PROBLEM

4.1 Introduction

In this study, linear static analysis was set out to investigate stress distributions of connection point of a cage beam crane. Carrying capacity of this crane is 5 tons and beam distance is 15 meters. Figure 4.1 shows general view of a cage beam crane. Thickness of sheet iron and distance between two rivets were changed desired dimensions. This dimensions were waried because of obtain minimum stress distribution of compenents.

Every compenent of connection point was modeled one by one. Firstly, sheet metals and angles were created and rivet holes were subtracted appropriatly by using Ansys program. After choosen metarial and given metarial proporties in Ansys program, models were mashed and applied constraint and loads.

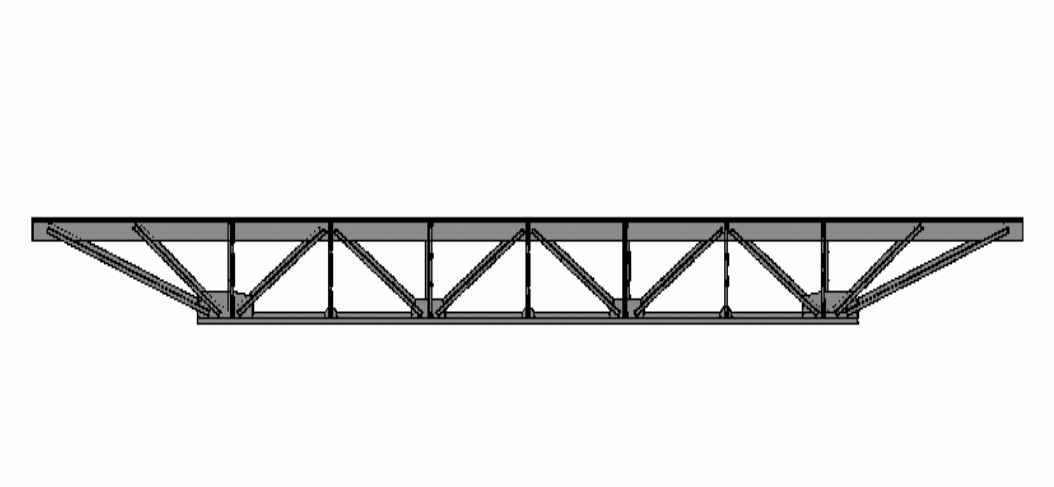

Figure 4.1 General view cage beam crane

4.2 Ansys Analysis

ANSYS Analysis has many finite element analysis capabilities, rangigng from a simple, linear, static analysis to a complex, nonlinear, transient dynamic analysis. Specific procedures for performing analysis for different engineering disciplines. A typical ANSYS analysis has three steps:

- Build the Modal
- Apply Loads and Obtain the Solution
- Review the Results

The main aim of a finite element analysis is to examine how a structure or compenent responds to certain loading conditions. In this study, the loads were given pressure. Ansys program presents different loads type, example of this loads in structural; displacement, forces, pressure, temperatures (for thermal strain), gravity.

One of the most important steps in preparing for an analysis is to apply boundary conditions that directly reflect the environment that the model will experience during operation.

4.3 Geometry Creation

The first step in the finite element analysis procedure is to model the part geometry. There are many ways to define geometry, ranging from two-dimensional drawings to three-dimensional computer aided design (CAD). Computer aided drafting permits easy generation and editing of two-dimensional geometry. In general, this process involves placing lines, rectangles, arcs, circles, and other basic geometric shapes on a display screen and then moving, rotating, and scaling these shapes to define a part outline. Often, there is a need to describe a part in three dimensions so that it can be more easily understood and converted to a discretized finite-element definition. Wireframe modeling is the simplest approach to graphical

display of three-dimensional shapes by definition of part outlines and intersections of surfaces.

In this study, every connection plate come into existence four different rivet holes distance. Rivet diameter is 16mm. for these connection points. These distance are 1.5d, 2d, 2.5d, and 3d. Connection points can be shown in figure 4.2, 4.3, 4.4 with rivets. The main carrying beam is another connection point which will be shown the next heading.

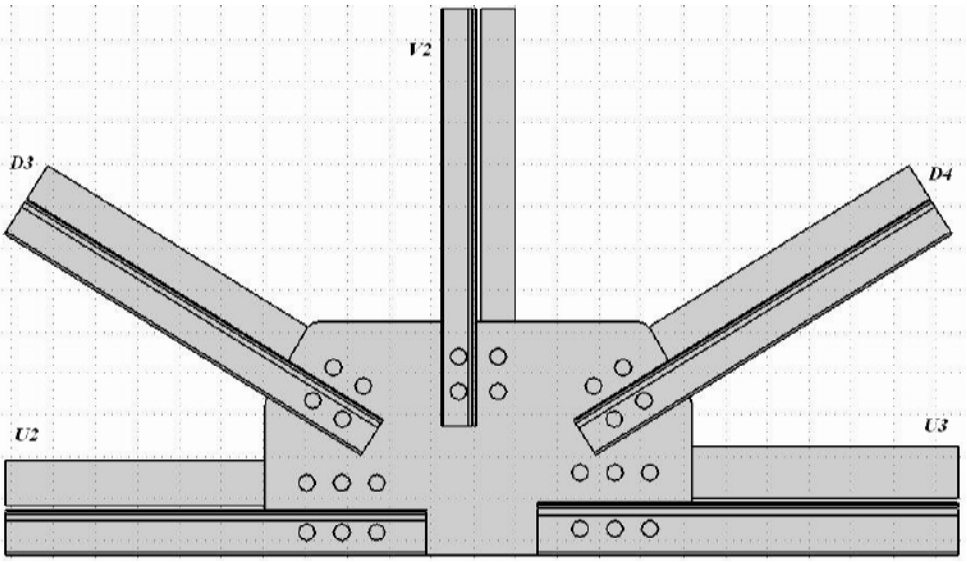

Figure 4.2 First connection point drafting

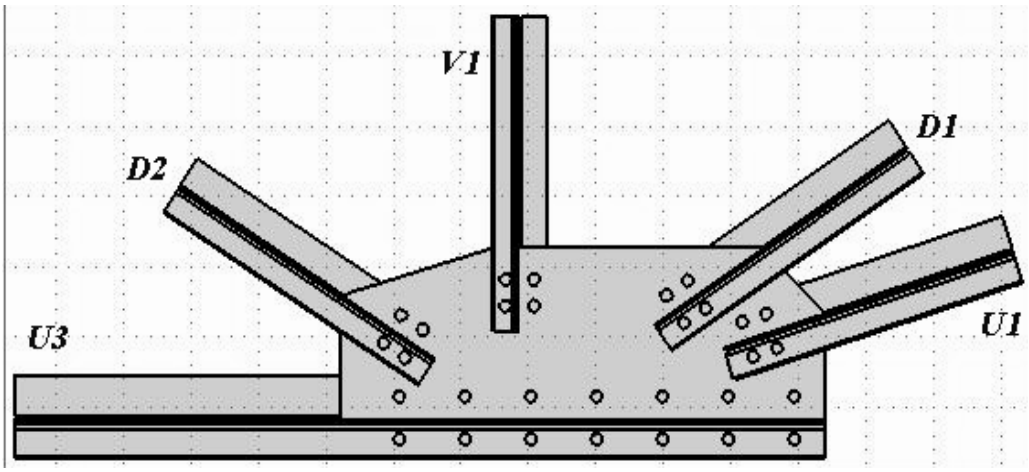

Figure 4.3 Second connection point drafting

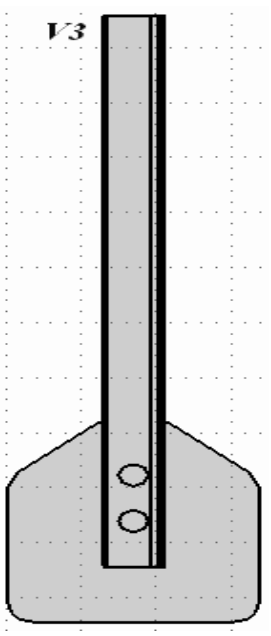

Figure 4.4 Third connection point drafting

4.4 Definition of the Material Properties and Element Selection

In addition to geometric detail of the component and the applied loads, the material (constitutive) relationship between stress and strain must also be defined. For simple isotropic, linear elastic stress analysis, steady-state thermal analysis, only the material elastic modulus and thermal conductivity values with the density need to be provided. In some cases, more detailed constitutive models may be desirable.

In this study, solid 92 with ten nodes element type is used for defining the material. The material proporties is shown in Table 4.1. Solid 92 has a quadratic displacement behavior and well suited to model irregular meshes. The element is defined by ten nodes having three degrees of freedom at each node translations in nodal x, y and z directions. The element also has plasticity, creep, swelling, stress stiffening, large deflection, and large strain capabilities.

The element coordinate system is used for orthotropic material input directions, applied pressure directions, and, under some circumstances, stress output directions. Element coordinate systems are right-handed, orthogonal systems. For line elements (such as LINK1), the default orientation is generally with the x-axis along the element I-J line. For solid elements (such as PLANE42 orSOLID45), the default orientation is generally parallel to the global Cartesian coordinate system. For area shell elements (such as SHELL63), the default orientation generally has the x-axis aligned with element I-J side, the z-axis normal to the shell surface (with the outward direction determined by the right-hand rule around the element from node I to J to K), and the y-axis perpendicular to the x and z-axes. (Ansys 6.1 Documentation)

Table 4.1 Metarial Proporties

Name	Value	Type
Material Name	STEEL	Isotropic
Mass Density	7,829e-006(kg/mm^3)	Temperature Independent
Young's Modulus	2,069e+005(N/mm^2)	Temperature Dependent
Poisson's Ratio	0,2880	Temperature Dependent

4.5 Mesh Creation

Once the overall geometry has been defined it must be divided into elements that are connected to one another at the nodal points. This division of the geometry into a set of elements is referred to as a mesh. Engineering judgment is required to select an appropriate element type, also, engineering judgment is required to determine the mesh density and the number and the size of the elements. Coarser meshes results in faster solution times but also limit the accuracy of the analysis.

In this study, around rivet holes has importance because maximum stress occurs here. For this reason this places mesh sizes were chosen more smaller than the others. Small element dimensions gives more sensetive stress distributions but these

small dimensions effect solution time. Mesh size must be chosen suitable to obtain optimum solution. These meshing size can be seen in figure 4.5, 4.6, 4.7, 4.8, 4.9.

Figure 4.5 Meshing an angle

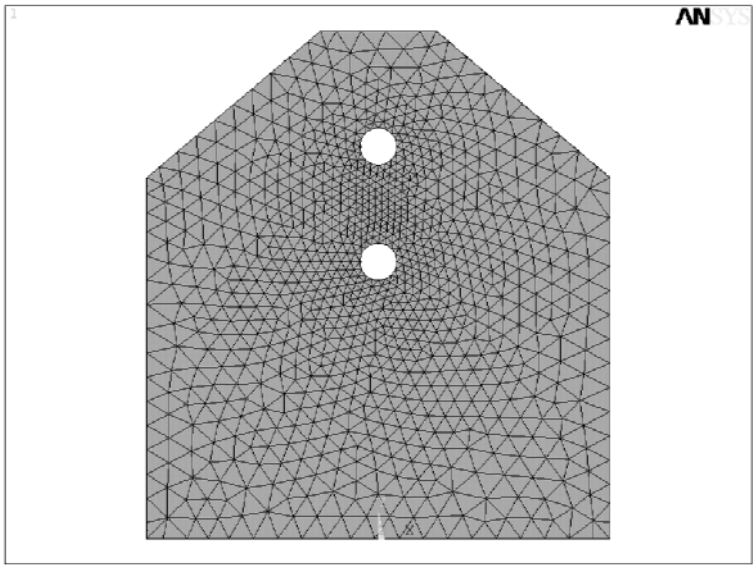

Figure 4.6 Meshing third connection point plate

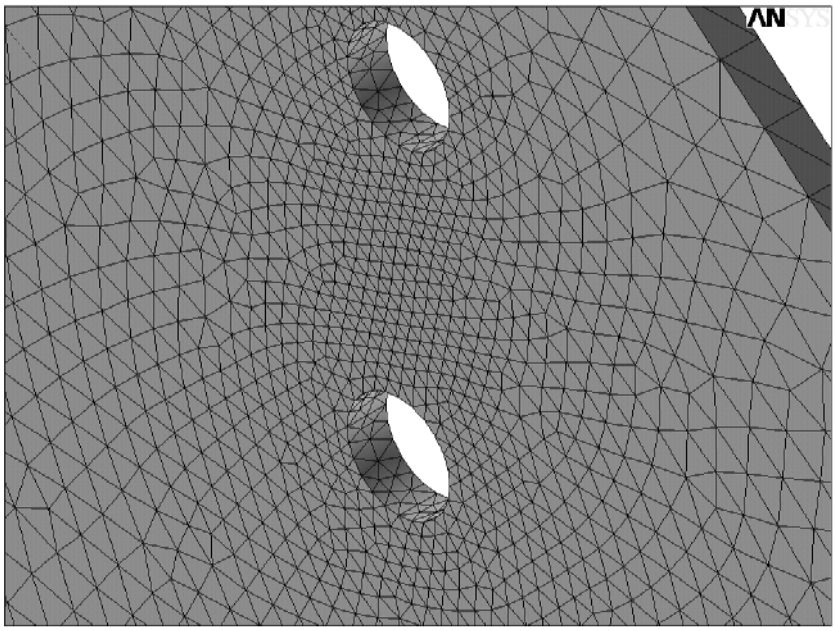

Figure 4.6a Meshing third connection point plate

4.6 Boundary Conditions

Boundary conditions on a structure appear as applied displacements at points of support. For static problems, the stiffness matrix associated with the linear equations of equilibrium for the complete structure will be singular, and therefore uninvertible, unless all rigid body motion is prohibited. As a result, a fundamental requirement for solution of the linear equations governing a problem is that the structure must be prevented from freely translating or rotating in space. Rigid body motion is eliminated through the application of boundary conditions requiring zero displacements and/or rotations at nodes.

In this study, the constraints were set to zero for underside of connection plates and angles. Especially angles fastened both side to conection plate with rivets. Angles were divided symmetrical two part as to angles length. Then boundary conditions of angles were given surface which was divided. This crane is frame for this reason x and y direction loads are very important.

Main carrying beam boundary condition is similar with angles. This beam contains two angles and one plate. These materials were produced approximately 6 meters and our crane length is 15 meters. End of connection plate can not be intersected with end of angle to provide maximum stability and safety. The most important thing like this construction to provide continuousness. The displacements of y-axis surface which is section of the angles, were given zero. Rivet holes were drilled on main carrying beam plate and displacements of inner surface of rivet holes were given zero because of applying load on surface of section of y- axis main carrying beam.

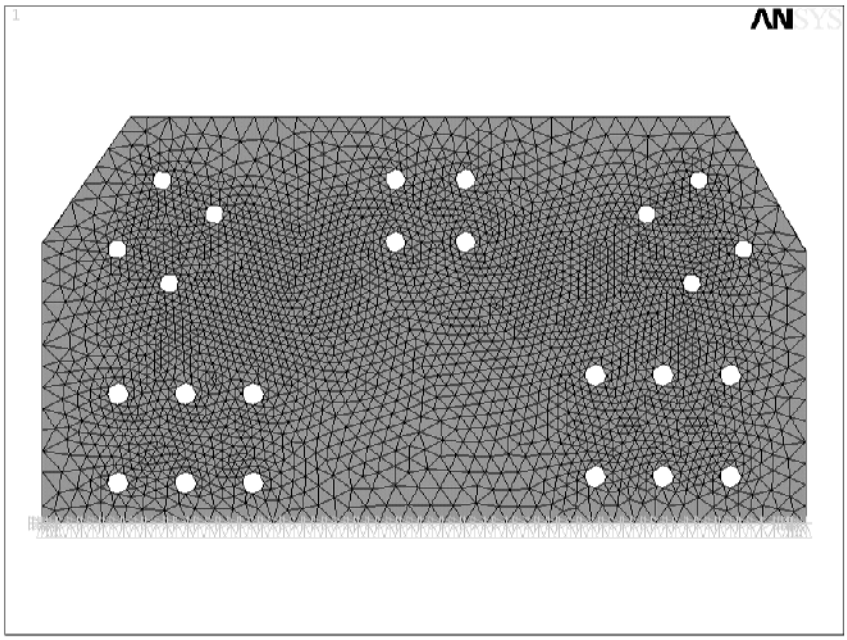

Figure 4.7 Meshing first connection point plate and applying boundary conditions

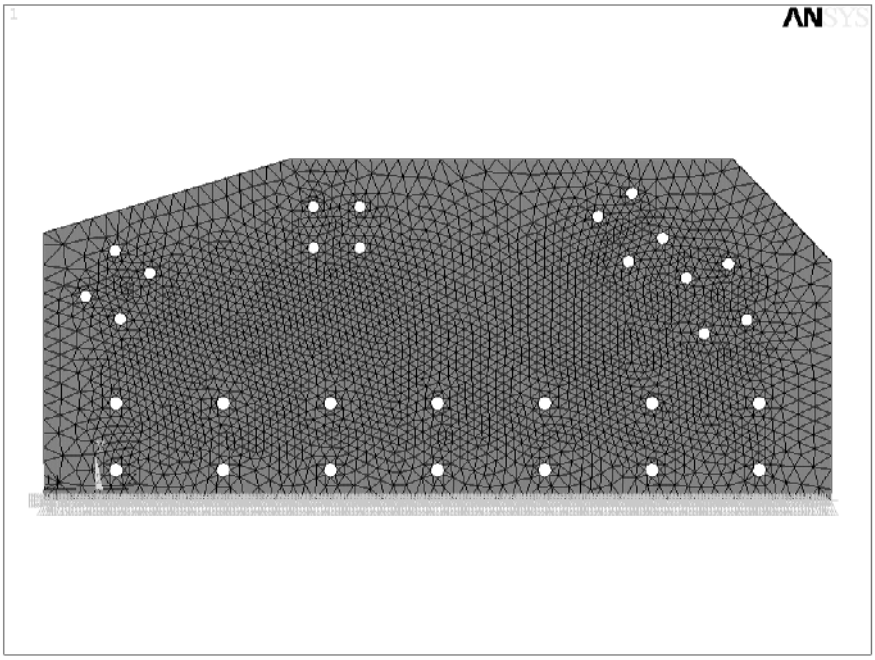

Figure 4.8 Meshing second connection point plate and applying boundary conditions

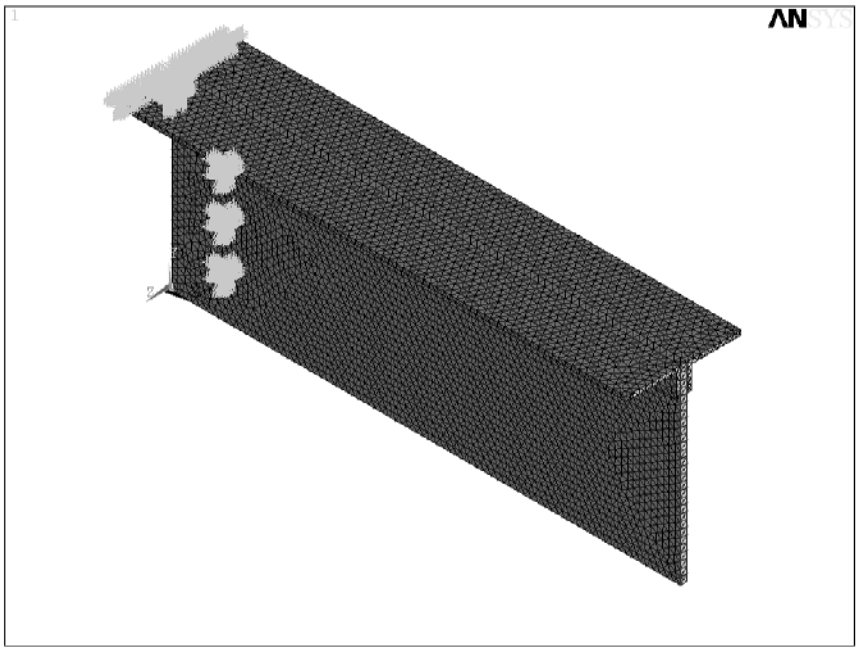

Figure 4.9 Applying boundary conditions on main carrying beam

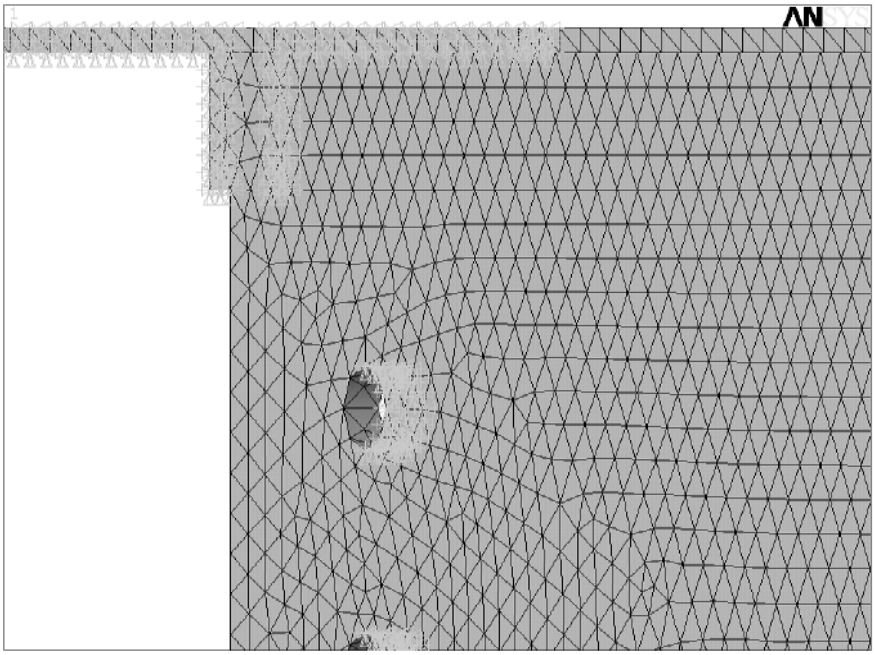

Figure 4.10 Applying boundary conditions on main carrying beam

4.7 Loading Conditions

Loads may be applied to a model either in the form of applied forces or displacements. Concentrated forces can only be applied at the node locations of the elements. Distributed loads (pressures, temperatures) and body loads (heat transfer coefficient, film coefficient) can also be applied to finite element surfaces and volumes, respectively. These loads are usually internally translated to equivalent nodal forces within the finite-element code.

The loads were applied to inner surface of rivet holes. Maybe loads were applied on plate, in this situation rivet holes displacement would be given zero but our connection plates have over ten rivet holes, for this reason loads could not be applied this position. Angle loads would be given but there are no too much differences if investigated stress distributions and stress values.

Table 4.2. Load Value

	Load (Kg)		Load (Kg)
D2	-4350	D3	3650
V	-2550	V	-2550
D1	-4500	D4	-2800
U1	10500	U3	14500
U2	14500	U4	11750

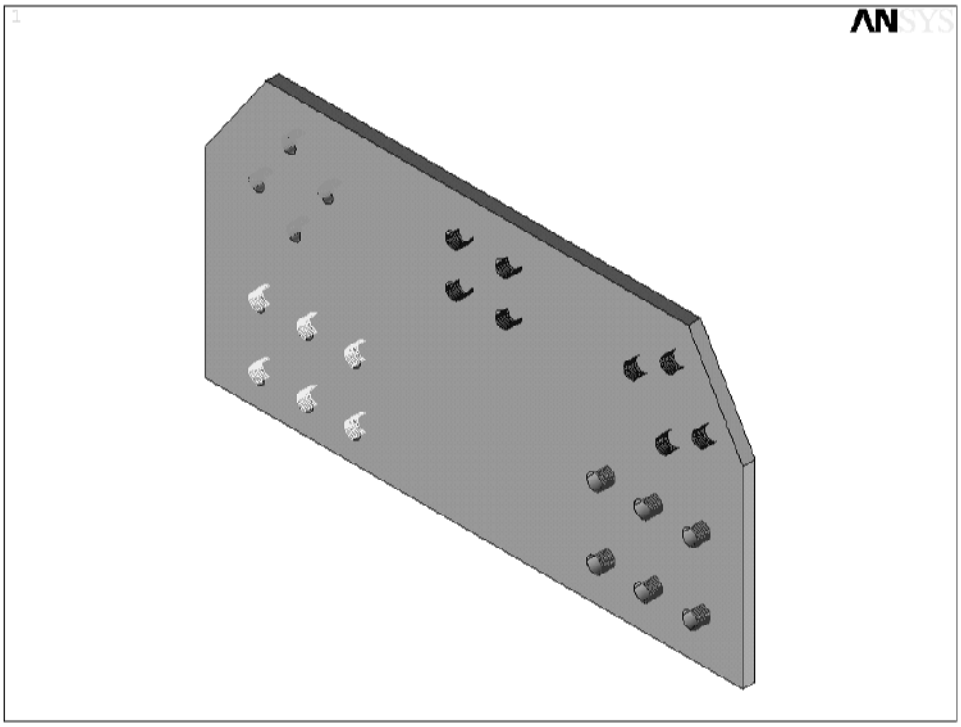

Figure 4.11 Applying loads on first connection point plate

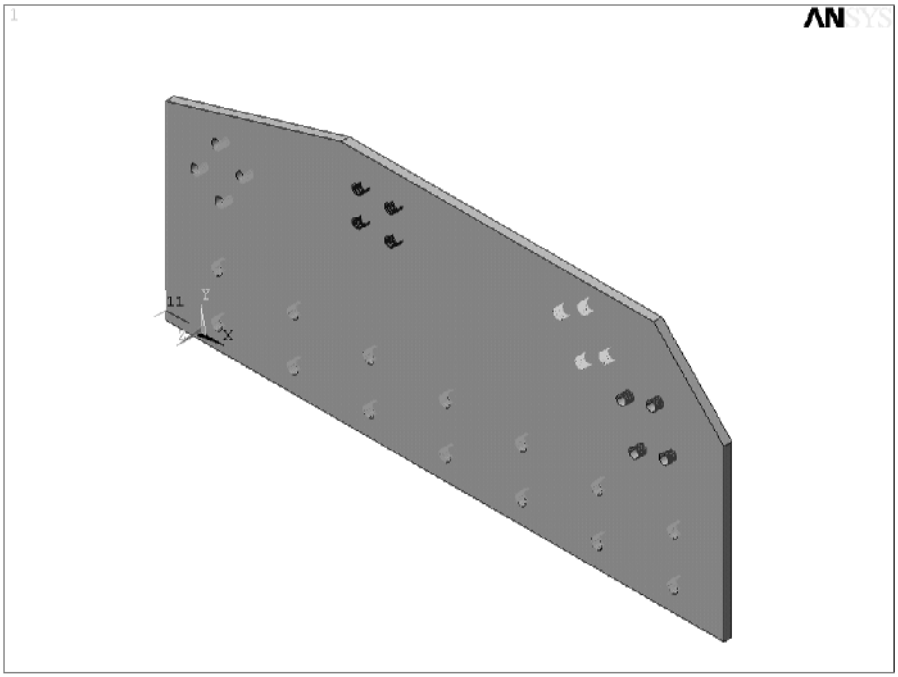

Figure 4.12 Applying loads on second connection point plate

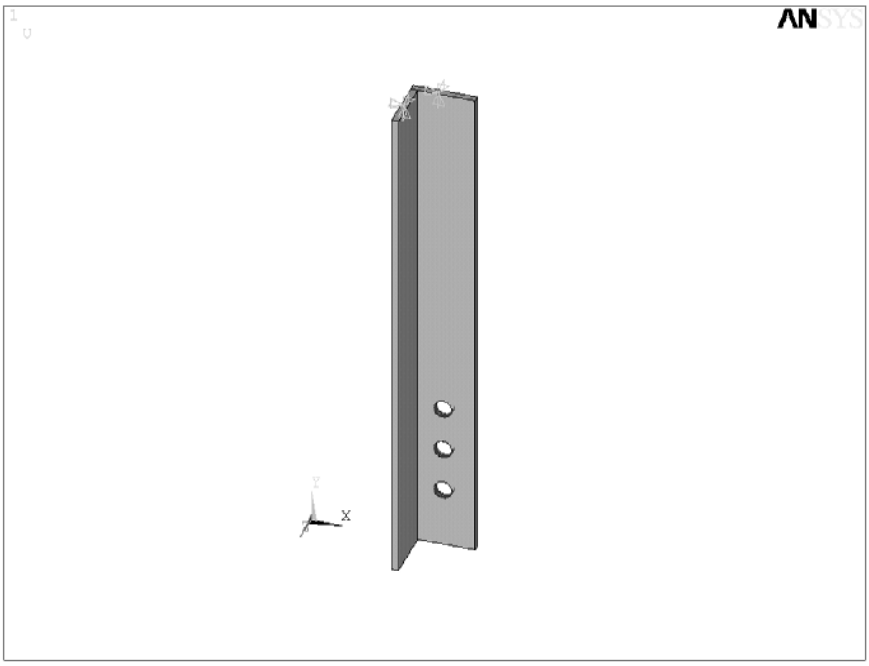

Figure 4.13 Applying loads and boundary conditions on 65-7, distance between rivets 2,5d

4.8 Modeling of the Connection Point with Using Contact Element

You can use our node-to-surface contact elements to model flexible-flexible or rigid-flexible contact between a surface and a node. Additionally, you can use these elements to represent contact between two surfaces by specifying one surface as a group of nodes.

The ANSYS node-to-surface contact elements permit nonlinearities such as:

- Surface-to-surface contact analysis with large deformations
- contact and separation
- Coulomb friction sliding
- Heat transfer

Node-to-surface contact is a phenomenon that occurs in most engineering applications: fasteners (nuts, bolts, rivets, pins), metal forming, rolling operations, dynamic pipe whip, etc. Engineers are interested in the stresses, deflections, forces, and temperature changes that occur due to contact between structural parts.(Ansys 6.1 Documentation)

In this study, first connection point and second connection point were modeled with all of the components which belong to itself. Firstly, contact pairs were created on the surfaces which touch eachother, than metarial proporties, boundary condition and loads were given.

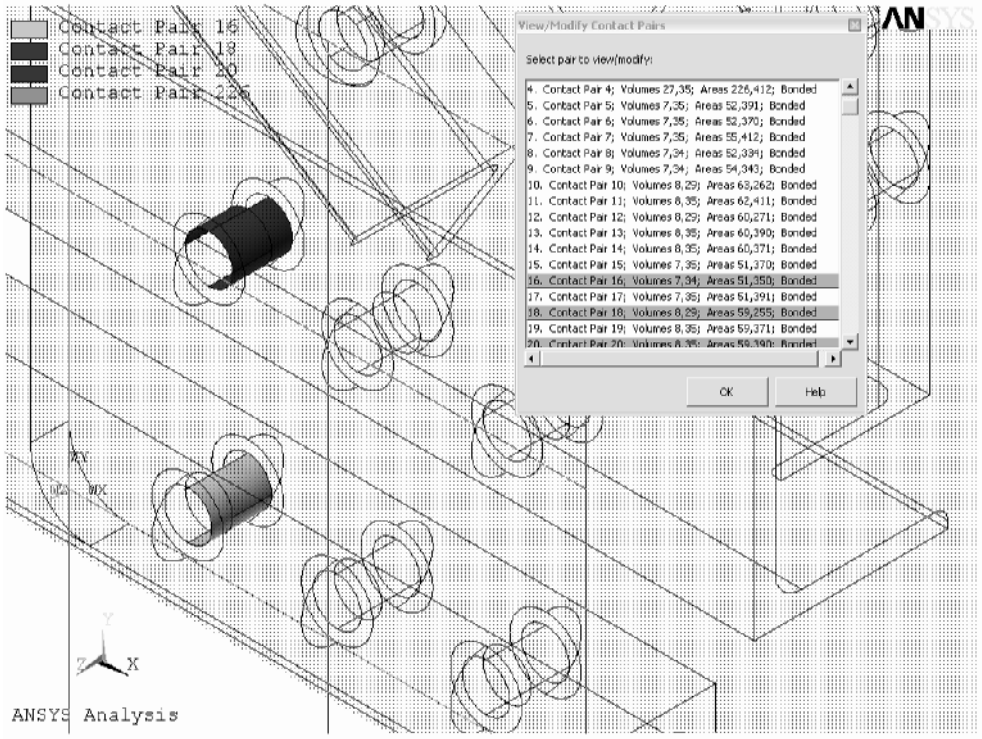

Figure 4.14 Some contact pairs

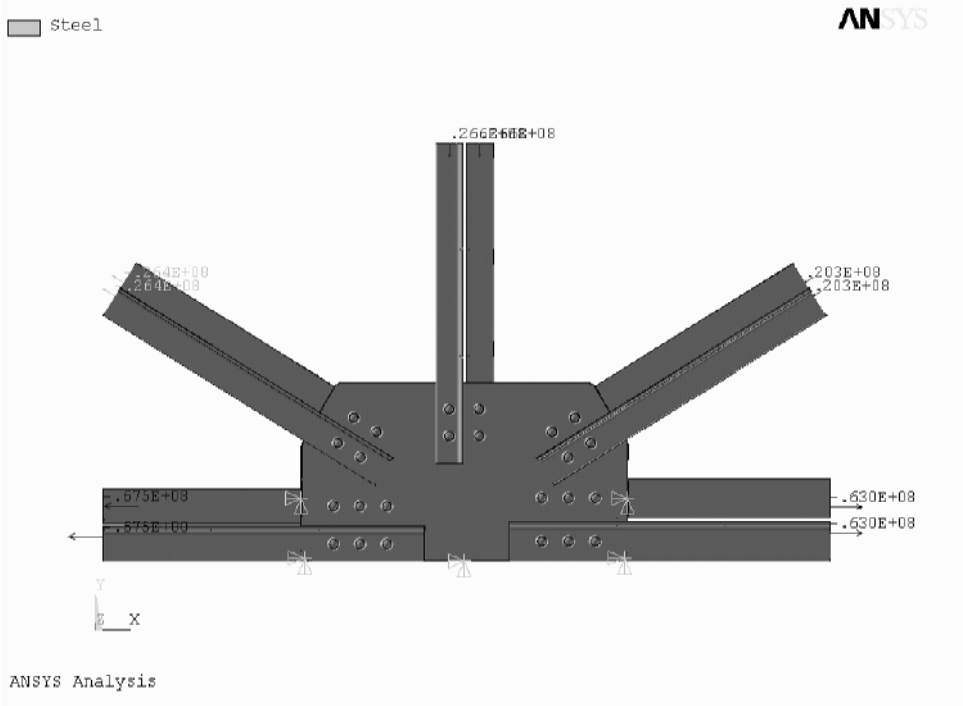

Figure 4.15 Applying loads and boundary conditions on first connection point

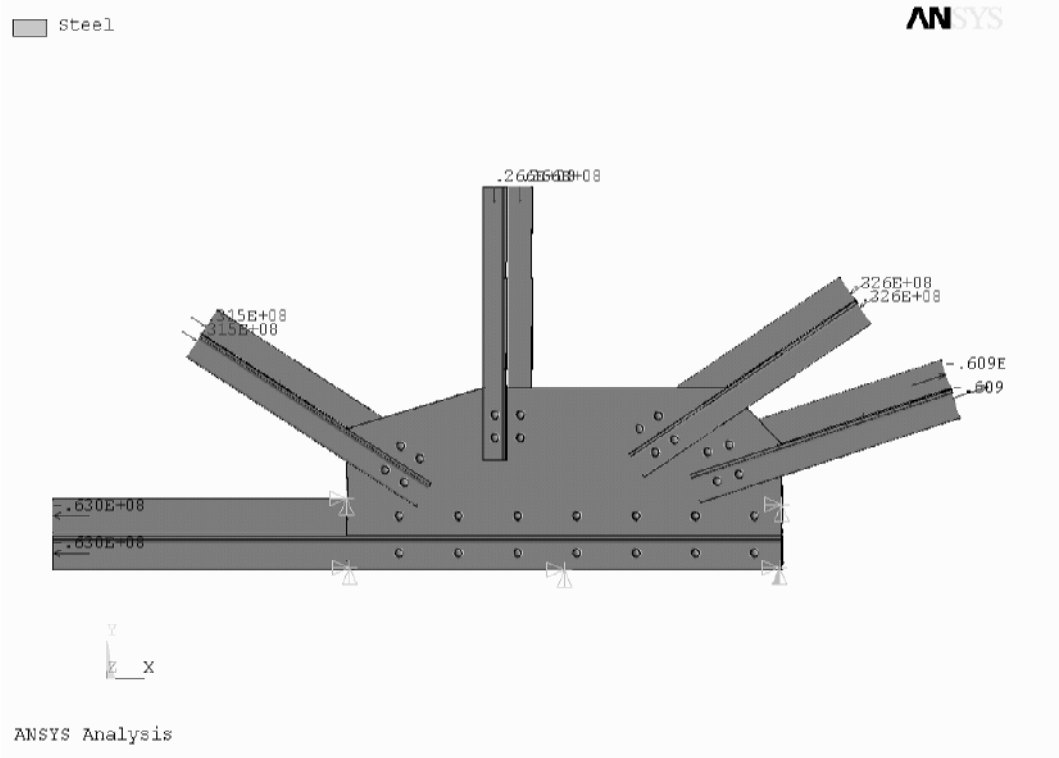

Figure 4.16 Applying loads and boundary conditions on second connection point

CHAPTER FIVE
RESULTS AND DISCUSSION

5.1 Results of First Connection Point

5.1.1 Results of First Connection Point Plate

Thickness of first connection point plate is 12 mm. and this plate was firstly analysed. If distance between two rivets is 1,5d, maximum stress value is 205,99 MPa. This stress value can be seen inner surface of second rivet hole, rigth under line. Stress distributions can be seen in figure 5.1a. Stress disributions generally occurs around the rivet holes and these disributions does not spread regular. For this construction, maximum safety stress value is 140 MPa. In this situation, this connection plate is not safety.

If distance between rivet holes is 2d, maximum stress value is 174,09 MPa. Maximum stress occurs same place with previous connection plate. This stress value can be seen inner surface of second rivet hole, right under line. Stress distributions spread more uniform than preceding plate. Because of rivet holes distances are more far away preceding plate, stress spread out much place and stress values which have every mm^2 are decreasing. Although both connection plates have same loads, maximum stress is smaller than preceding connection plate. But this connection plate does not safety. Stress distributions can be seen in figure 5.2.

If distance between rivet holes is 2,5d, maximum stress value is 150,68 MPa. and can be seen in figure 5.3. Maximum stress place is the same with previous connection plate. This stress value can be seen inner surface of second rivet hole, right under line. Stress distributions are getting more uniform and maximum stress value decrease. But this connection plate is not safety too.

If distance between rivet holes is 3d, maximum stress value is 154,094 MPa. Maximum stress value of this connection plate is bigger than the connection plate which has 2,5d rivet holes distances. But these values are too close to each other. Both of them have nearly same stress distributions. Maximum stress occurs inner surface of first rivet hole, others occur inner surface of second rivet hole. In this situation, this connection plate thickness is not safety under these load values. This plate stress distributions can be seen in figure 5.4.

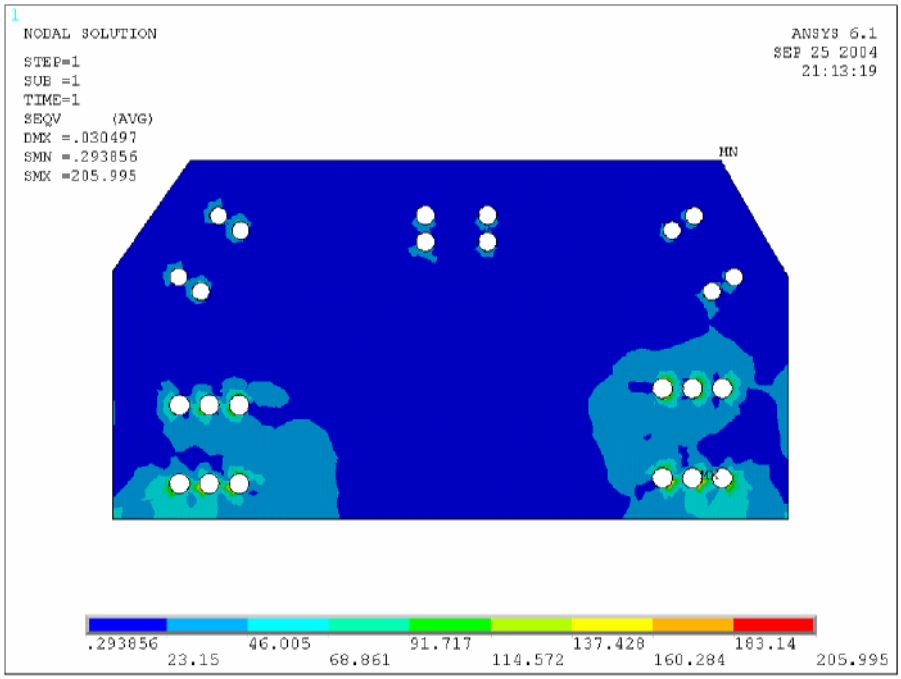

Figure 5.1 First connection point plate Von Mises stress distributions, thickness of plate 12 mm. and rivets distance 1,5d (Units are MPa)

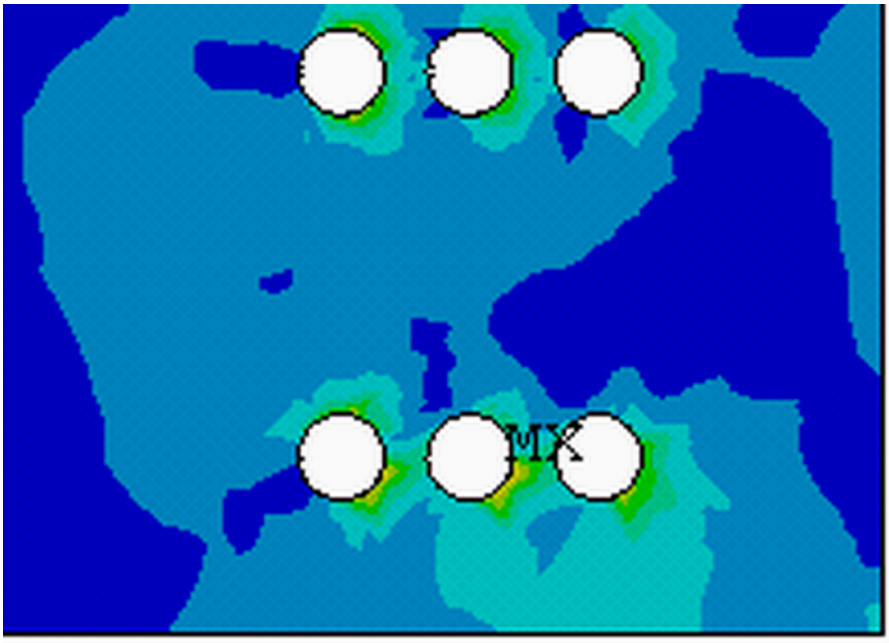

Figure 5.1a Maximum stress

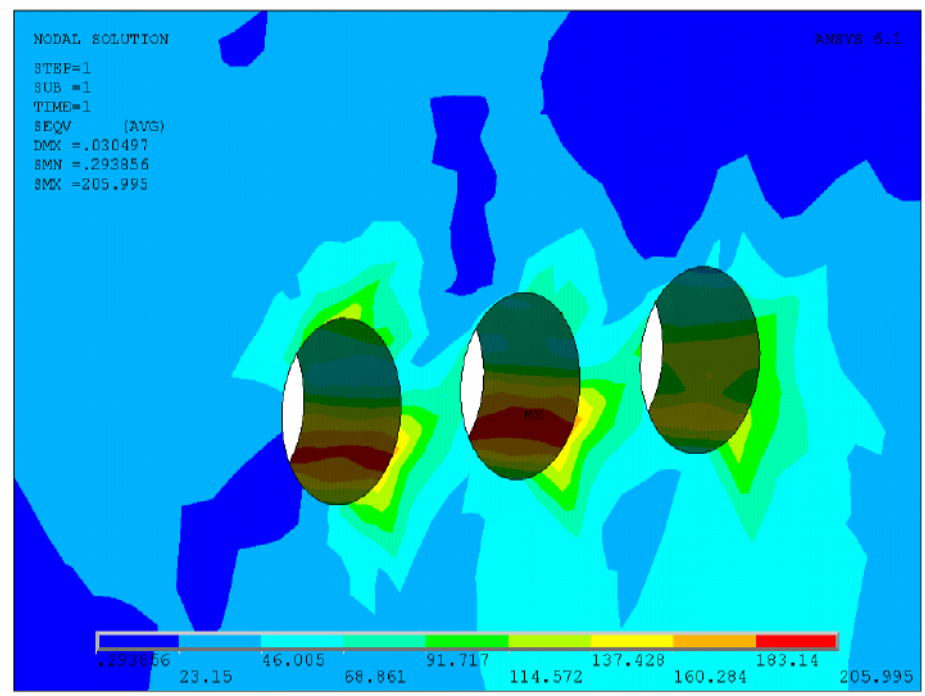

Figure 5.1b Inner surface of rivet holes

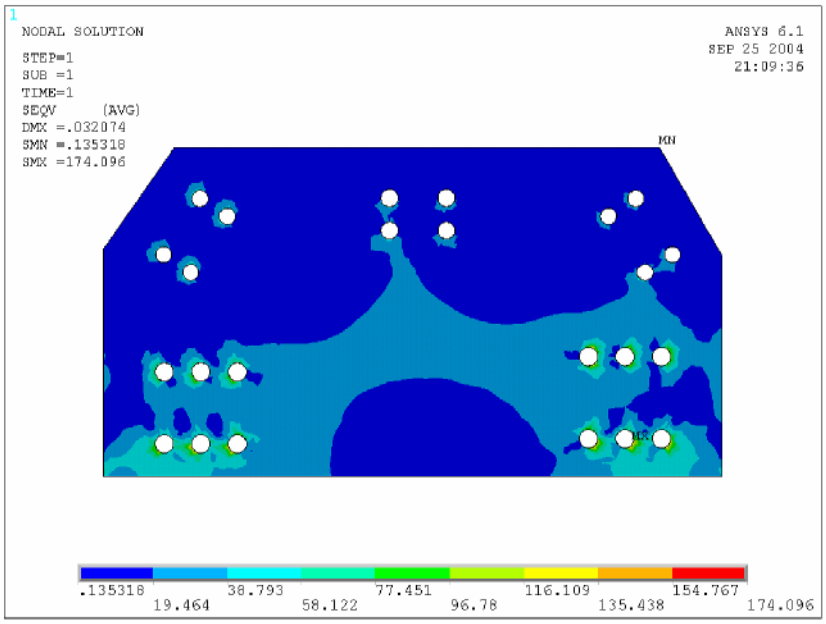

Figure 5.2 First connection point plate Von Mises stress distributions, thickness of plate 12 mm. and rivets distance 2d (Units are MPa)

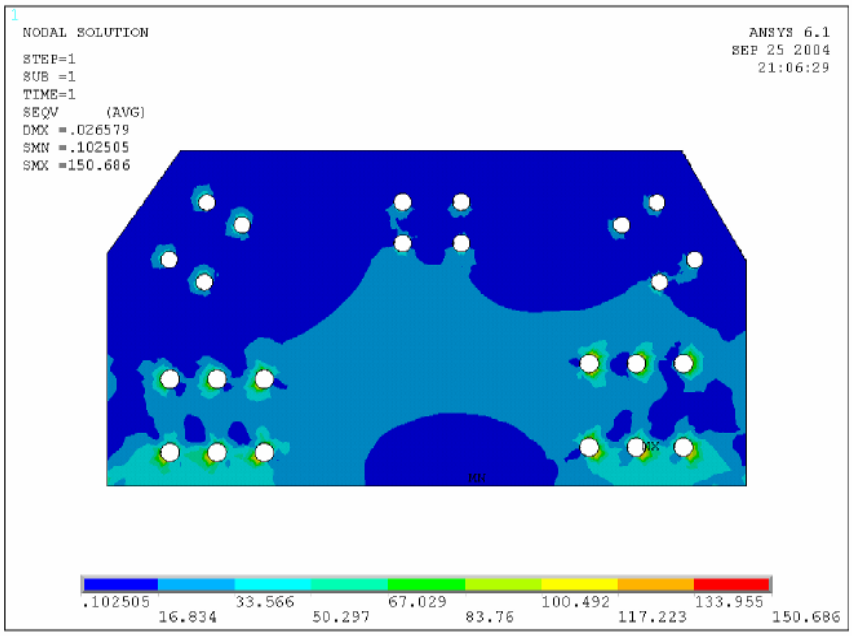

Figure 5.3 First connection point plate Von Mises stress distributions, thickness of plate 12 mm. and rivets distance 2,5d (Units are MPa)

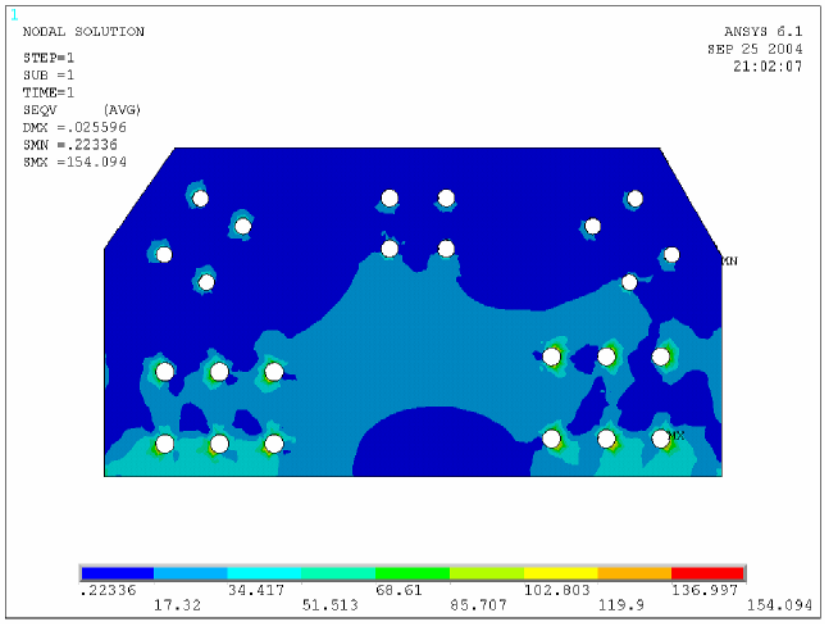

Figure 5.4 First connection point plate Von Mises stress distributions, thickness of plate 12 mm. and rivets distance 3d (Units are MPa)

Second type of first connection plate thickness is 13 mm. and can be seen in figure 5.8. If rivet holes distances are chosen 1,5d, maximum stress value is 182,36 MPa. Maximum stress values occur around rivet holes. Maximum stress value is over safety stress value. But maximum stress value of this connection plate is smaller than connection plate which has same rivet holes distances, thickness 12mm.

If distance between rivet holes is 2d, maximum stress value is 168,97 MPa. Stress distributions can be seen in figure 5.7. This plate stress distribution does not spread as plate thickness 12mm with 2d. Other connection plate stress distributions spread more but maximum stress value is bigger than this connection plate.

If distance between rivet holes is 2,5d, maximum stress value is 141,38 MPa and maximum stress value is too close to safety stress value. Stress distributions of this connection plate are more uniform but not safety. This plate can be seen in figure 5.6.

If distance between rivet holes is 3d, maximum stress value is 134,66 MPa and maximum stress value is under safety stress value, shown in figure 5.5. It can be clearly seen that safety stress value obtained by changing distances between rivet holes on same thickness.

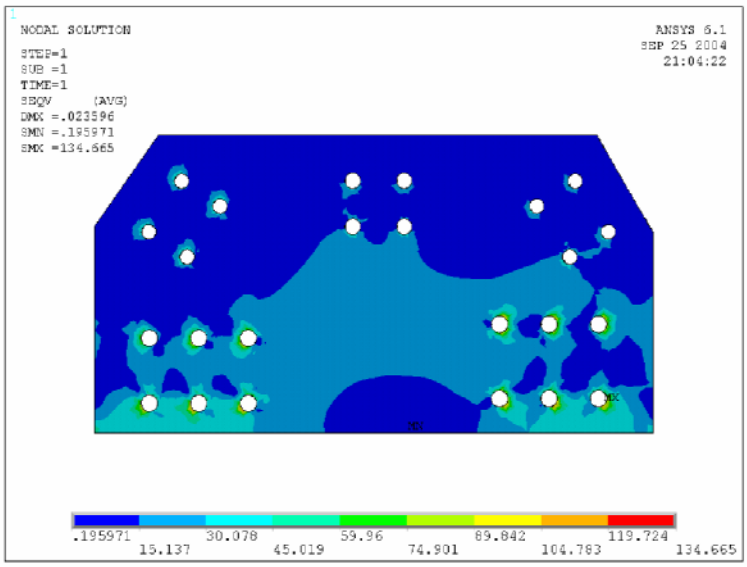

Figure 5.5 First connection point plate Von Mises stress distributions, thickness of plate 13 mm. and rivets distance 3d (Units are MPa)

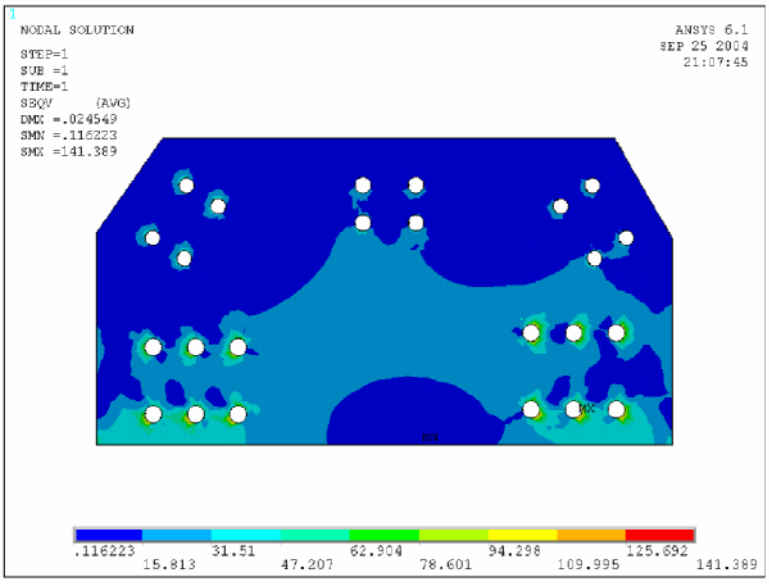

Figure 5.6 First connection point plate Von Mises stress distributions, thickness of plate 13 mm. and rivets distance 2,5d (Units are MPa)

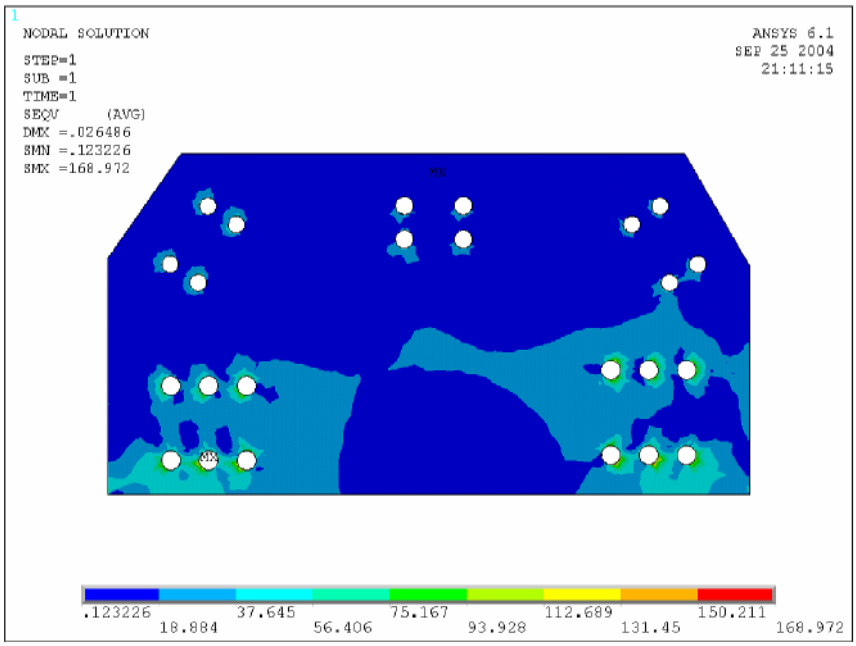

Figure 5.7 First connection point plate Von Mises stress distributions, thickness of plate 13 mm. and rivets distance 2d (Units are MPa)

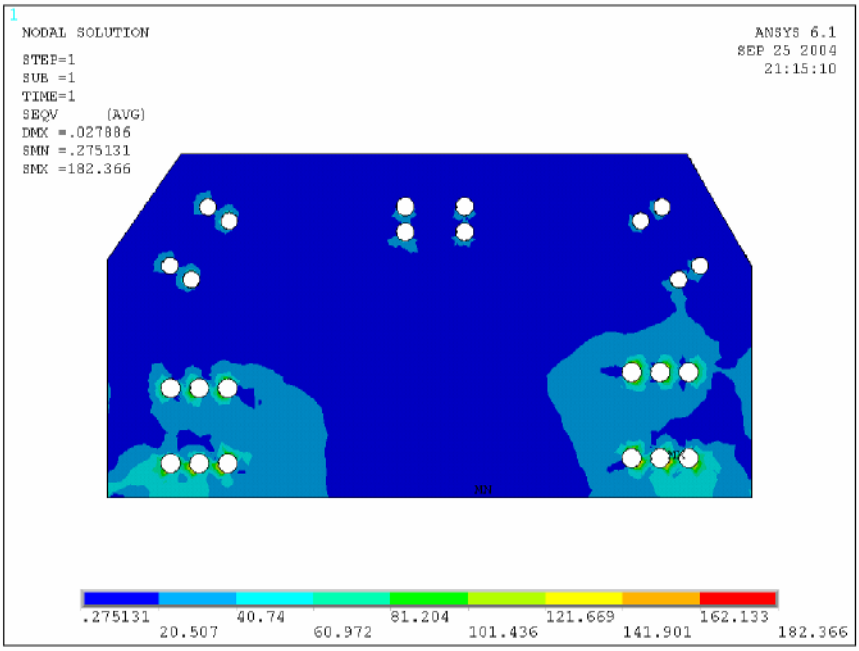

Figure 5.8 First connection point plate Von Mises stress distributions, thickness of plate 13 mm. and rivets distance 1,5d (Units are MPa)

Third type of first connection plate thickness is 14 mm. and can be seen in figure 5.9. If rivet holes distances are chosen 1,5d, maximum stress value is 173,045 MPa. This stress value can be seen inner surface of second rivet hole, right under line. Maximum stress values occur around rivet holes. Maximum stress value is over safety stress value.

If distance between rivet holes is 2d, maximum stress value is 159,529 MPa and. stress distributions can be seen in figure 5.10. Maximum stress of this connection plate is smaller than preceding plate because of thickness, but stress distributions looks same.

If distance between rivet holes is 2,5d, maximum stress value is 130,159 MPa. and can be seen in figure 5.11. Maximum stress occurs same place in this plate. This rivet holes distances is safety.

If distance between rivet holes is 3d, maximum stress value is 132,836 MPa. Maximum stress value of this connection plate is bigger than the connection plate which has 2,5d rivet holes distances. But these values are too close to each other. Both of them have nearly same stress distributions. Maximum stress occurs inner surface of first rivet hole and left line, others occur inner surface of second rivet hole and right line. In this situation, this connection plate thickness is safety under these load values. This plate stress distributions can be seen in figure 5.12.

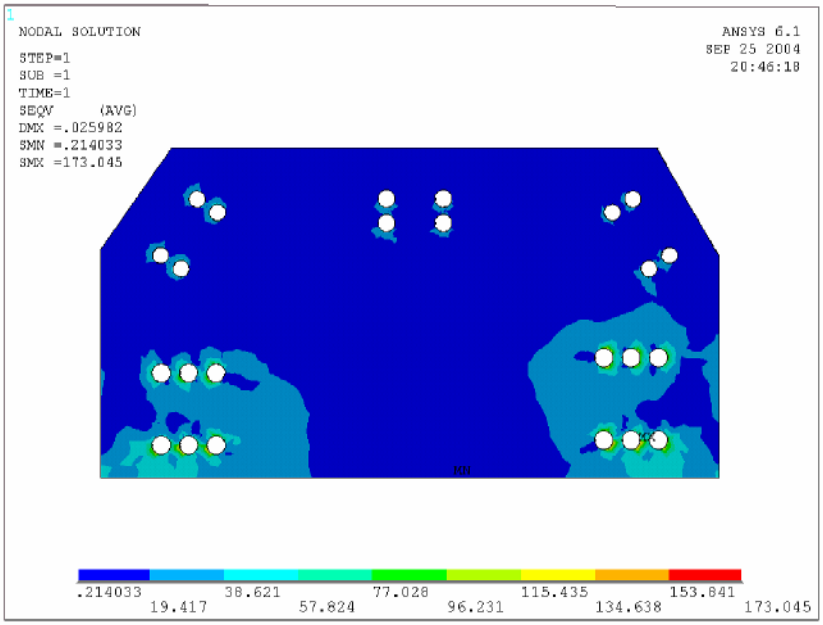

Figure 5.9 First connection point plate Von Mises stress distributions, thickness of plate 14 mm. and rivets distance 1,5d (Units are MPa)

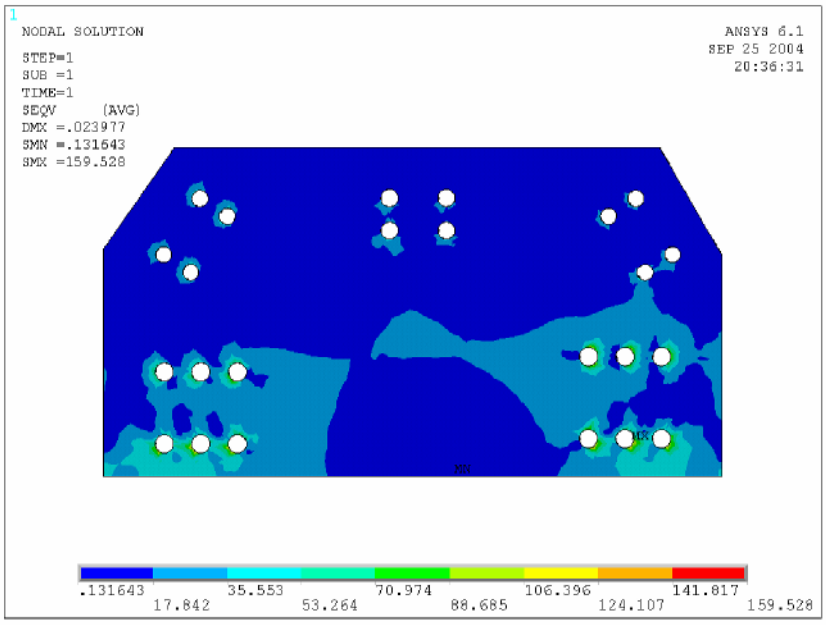

Figure 5.10 First connection point plate Von Mises stress distributions, thickness of plate 14 mm. and rivets distance 2d (Units are MPa)

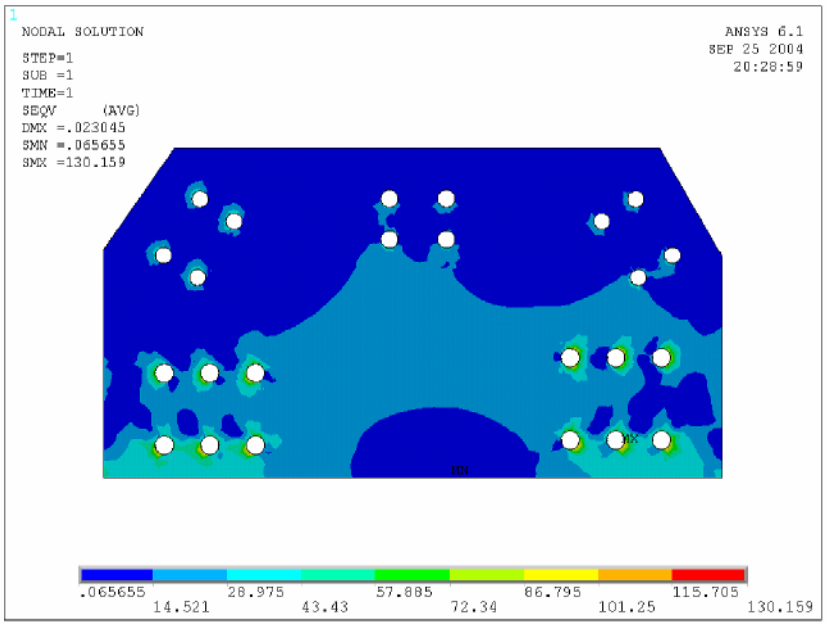

Figure 5.11 First connection point plate Von Mises stress distributions, thickness of plate 14 mm. and rivets distance 2,5d (Units are MPa)

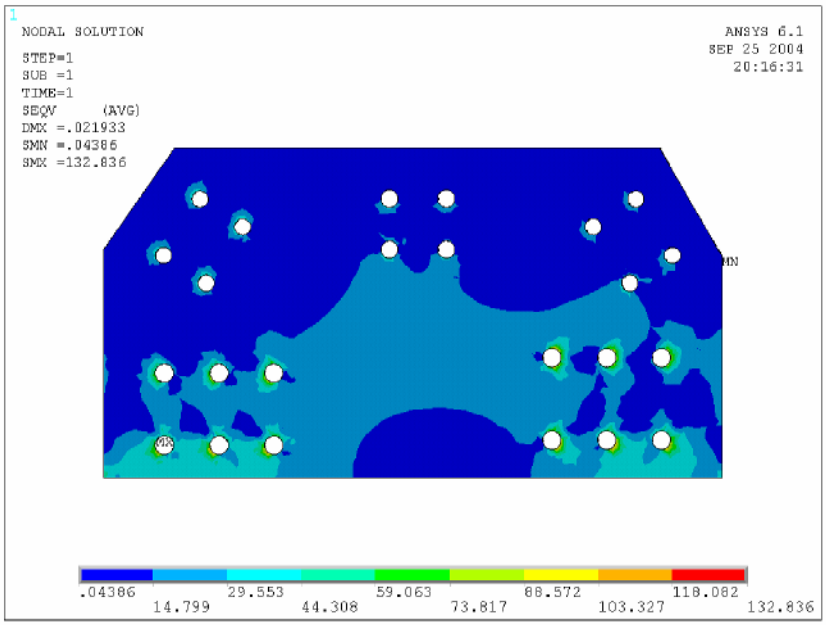

Figure 5.12 First connection point plate Von Mises stress distributions, thickness of plate 14 mm. and rivets distance 3d (Units are MPa)

Another type of first connection plate thickness is 15 mm. and can be seen in figure 5.13. If rivet holes distances are chosen 1,5d, maximum stress value is 168,092 MPa. Maximum stress values occur around rivet holes. Maximum stress value is over safety stress value. But maximum stress value of this connection plate is smaller than connection plate which has same rivet holes distances, thickness 14mm. but stress values are too close.

If distance between rivet holes is 2d, maximum stress value is 148,235 MPa. Stress distributions can be seen in figure 5.14. This plate stress distribution spread as plate thickness 14 mm with 2d. But maximum stress value is smaller.

If distance between rivet holes is 2,5d, maximum stress value is 125,281 MPa and maximum stress value is under safety stress value. Stress distributions of this connection plate are more uniform. This plate can be seen in figure 5.15.

If distance between rivet holes is 3d, maximum stress value is 124,488 MPa and maximum stress value is under safety stress value, shown in figure 5.16. It can be clearly seen that safety stress value obtained by changing distances between rivet holes on same thickness.

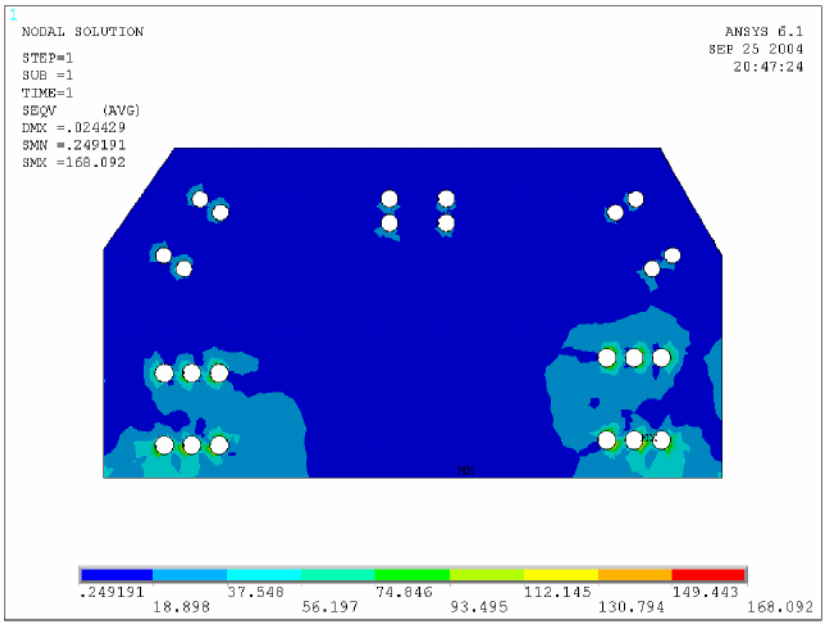

Figure 5.13 First connection point plate Von Mises stress distributions, thickness of plate 15 mm. and rivets distance 1,5d (Units are MPa)

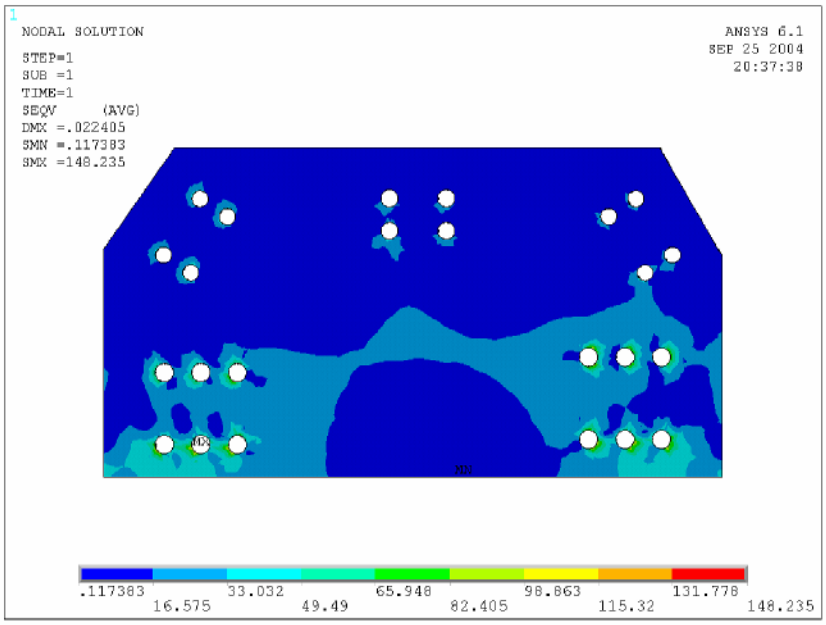

Figure 5.14 First connection point plate Von Mises stress distributions, thickness of plate 15 mm. and rivets distance 2d (Units are MPa)

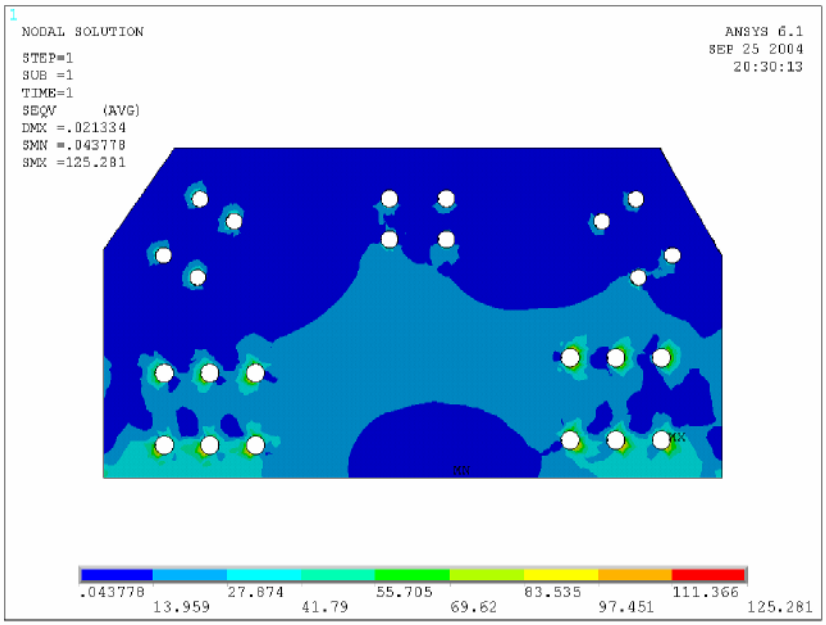

Figure 5.15 First connection point plate Von Mises stress distributions, thickness of plate 15 mm. and rivets distance 2,5d (Units are MPa)

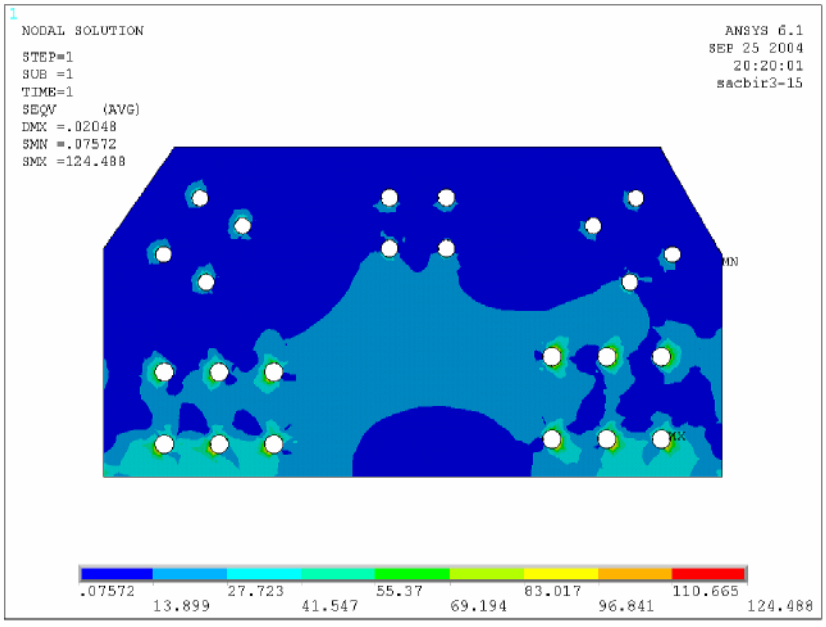

Figure 5.16 First connection point plate Von Mises stress distributions, thickness of plate 15 mm. and rivets distance 3d (Units are MPa)

Thickness of last connection point plate is 16 mm. If distance between two rivets is 1,5d, maximum stress value is 156,878 MPa. This stress value can be seen inner surface of second rivet hole, right under line. Stress distributions can be seen in figure 5.17. Stress distributions generally occur around the rivet holes and these distributions does not spread regular. This connection plate is not safety.

If distance between rivet holes is 2d, maximum stress value is 138,458 MPa. Maximum stress occurs same place with previous connection plate. This stress value can be seen inner surface of second rivet hole, left under line. Stress distributions spread more uniform than preceding plate. But this connection plate is safety. Stress distributions can be seen in figure 5.18.

If distance between rivet holes is 2,5d, maximum stress value is 126,591 MPa. and can be seen in figure 5.19. Maximum stress place is the same with previous connection plate. This stress value can be seen inner surface of second rivet hole, right under line. Stress distributions are getting more uniform and maximum stress value decrease. But this connection plate is safety too.

If distance between rivet holes is 3d, maximum stress value is 109,764 MPa. Maximum stress value decreases by changing rivet holes distances. Maximum stress occurs inner surface of second rivet hole. In this situation, this connection plate thickness is safety under these load values. This plate stress distributions can be seen in figure 5.20.

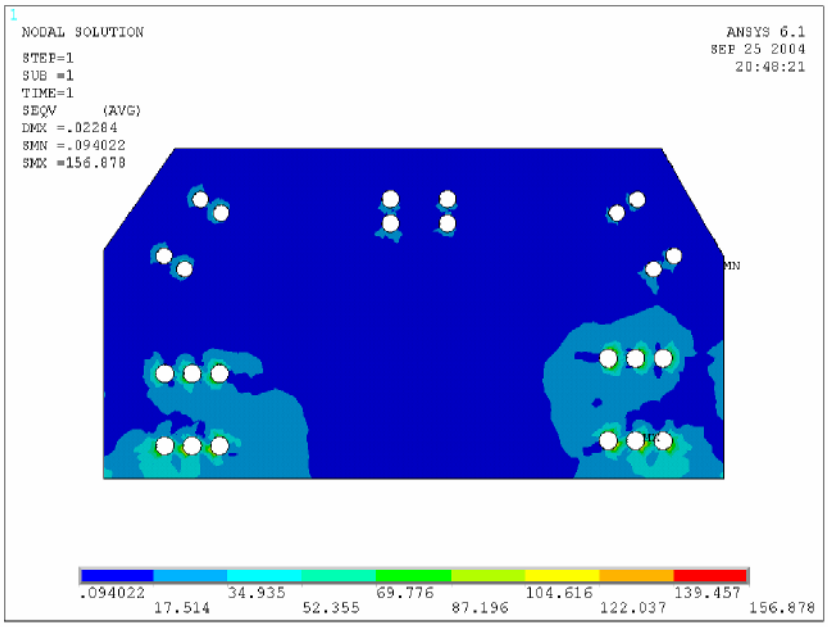

Figure 5.17 First connection point plate Von Mises stress distributions, thickness of plate 16 mm. and rivets distance 1,5d (Units are MPa)

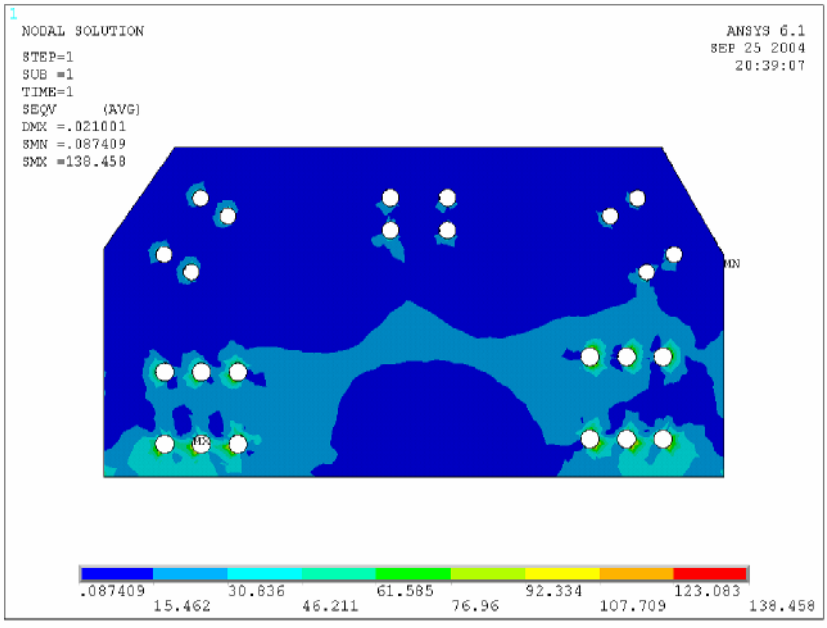

Figure 5.18 First connection point plate Von Mises stress distributions, thickness of plate 16 mm. and rivets distance 2d (Units are MPa)

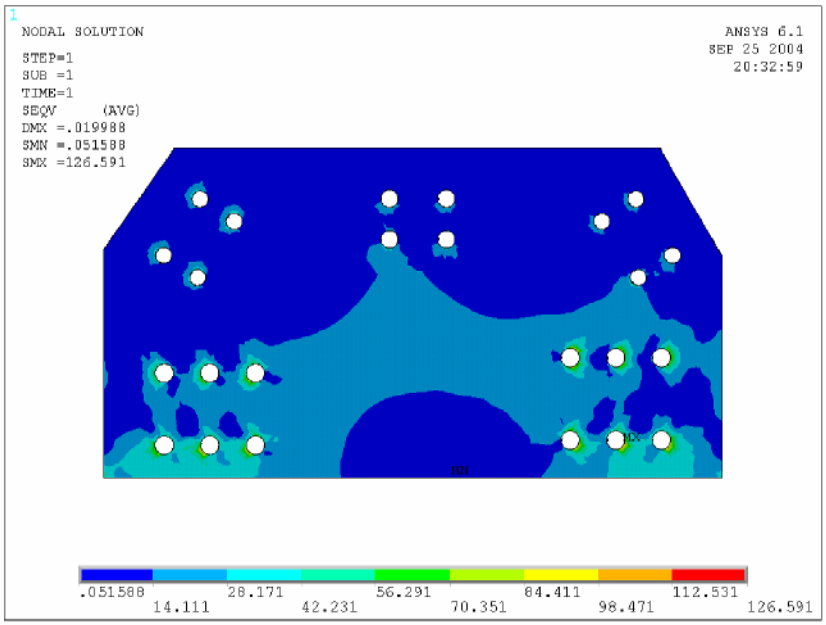

Figure 5.19 First connection point plate Von Mises stress distributions, thickness of plate 16 mm. and rivets distance 2,5d (Units are MPa)

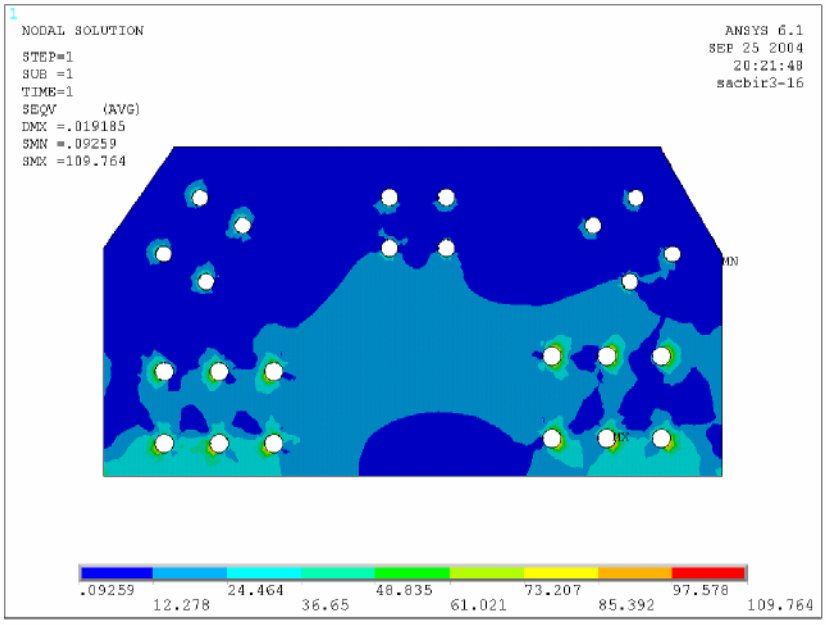

Figure 5.20 First connection point plate Von Mises stress distributions, thickness of plate 16 mm. and rivets distance 3d (Units are MPa)

5.1.2 Results of First Connection Point Angles

This angle is standard profile which is 45x5 and located diagonally. If distances of two rivet holes are 1,5d, maximum stress value is 102,878 MPa. as seen in figure 5.21. Maximum stress occurs inner surface of top rivet hole. This stress value is safety for this construction. But other distances of rivet holes will be investigated.

Second distances of rivet holes is 2d, maximum stress value is 100,878 MPa. as seen in figure 5.22. Stress value is decreasing because of rivet holes distances. It affects stress distributions, stress can found too much area to distribute. For this reason, stress value is getting smaller.

When distances of rivet holes are chosen 2,5d, maximum stress value is 97,322 MPa. Another rivet distances is 3d, maximum stress value is 98,491 MPa. in here. Two values are too close each other but not same. Maximum stress occur inner surface of top rivet hole. These values can be seen in figure 5.23, 5.24, 5.24a.

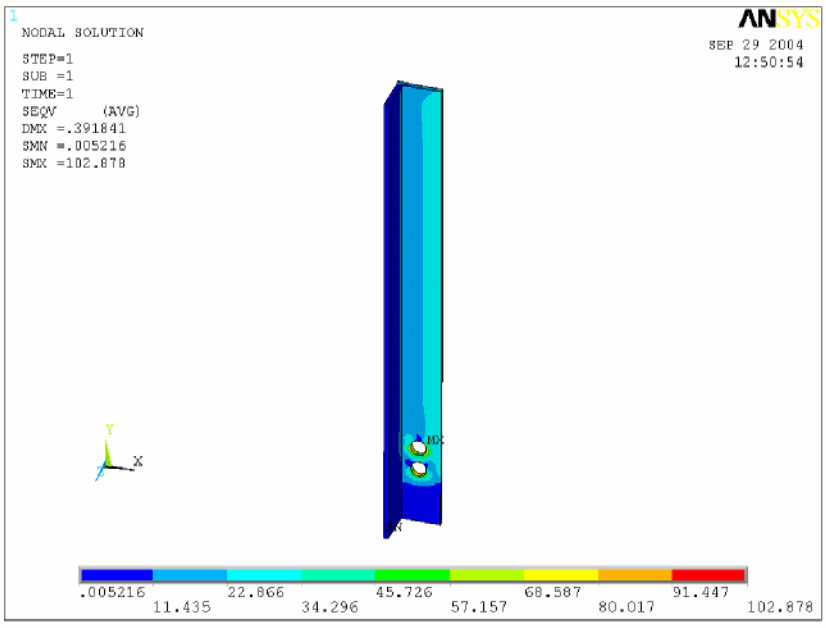

Figure 5.21 Von Mises stress distributions of D3 with 1,5d distance

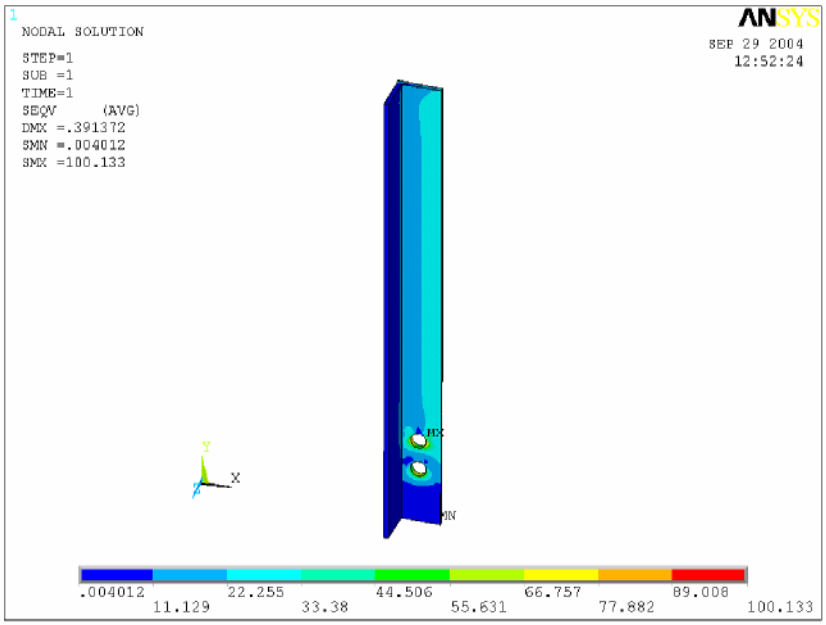

Figure 5.22 Von Mises stress distributions of with 2d distance

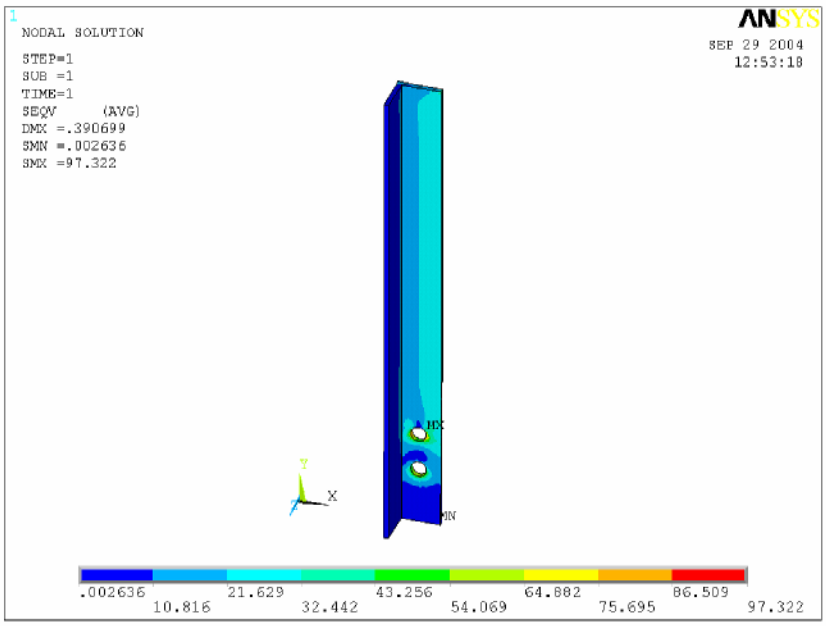

Figure 5.23 Von Mises stress distributions of D3 with 2,5d distance

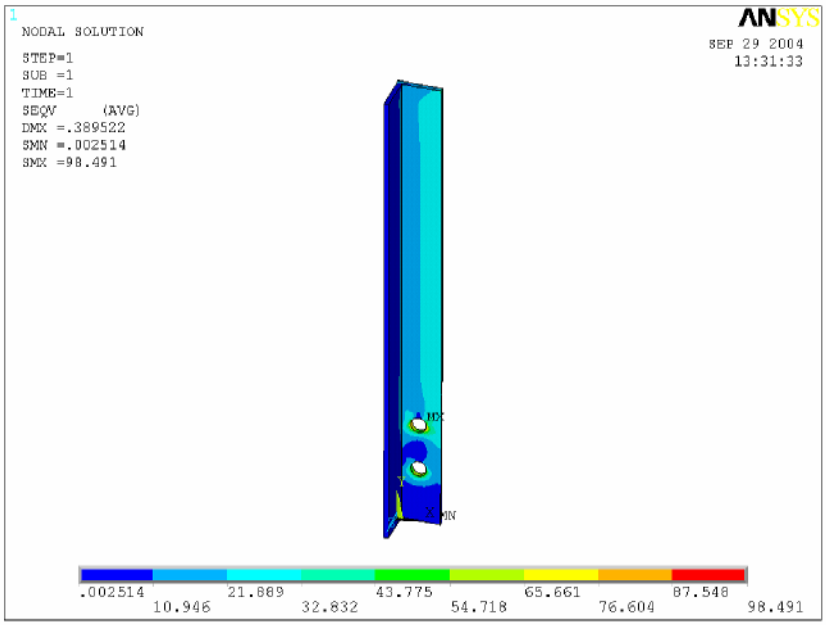

Figure 5.24 Von Mises stress distributions of D3 with 3d distance

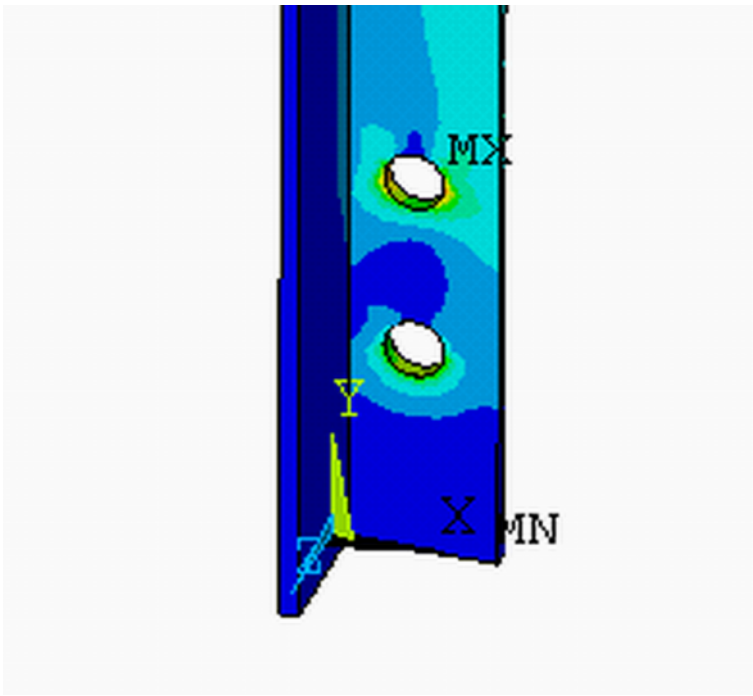

Figure 5.24a

Maximum stress of D3 with 3d distance

This angle carry suppress load. This angle is standard profile which is 50x5 and located diagonally. If distances of two rivet holes are 1,5d, maximum stress value is 73,097 MPa. as seen in figure 5.25. Maximum stress occurs inner surface of top rivet hole. This stress value is safety for this construction.

Second distances of rivet holes is 2d, maximum stress value is 68,504 MPa. as seen in figure 5.26.

When distances of rivet holes are chosen 2,5d, maximum stress value is 65,598 MPa. Another rivet distances is 3d, maximum stress value is 64,526 MPa. in here. Two values are too close each other but not same. Maximum stress occur inner surface of top rivet hole. These values can be seen in figure 5.27, 5.28.

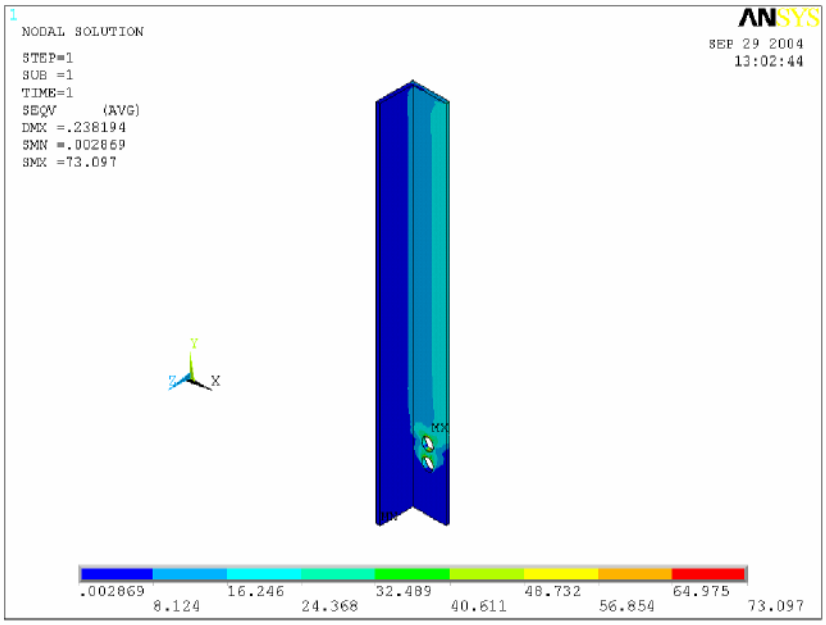

Figure 5.25 Von Mises stress distributions of D4 with 1,5d distance

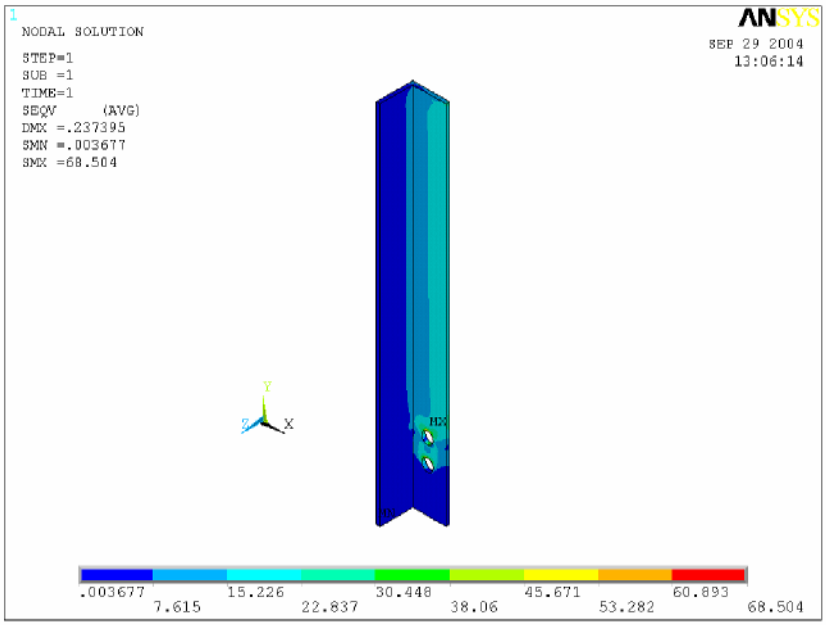

Figure 5.26 Von Mises stress distributions of D4 with 2d distance

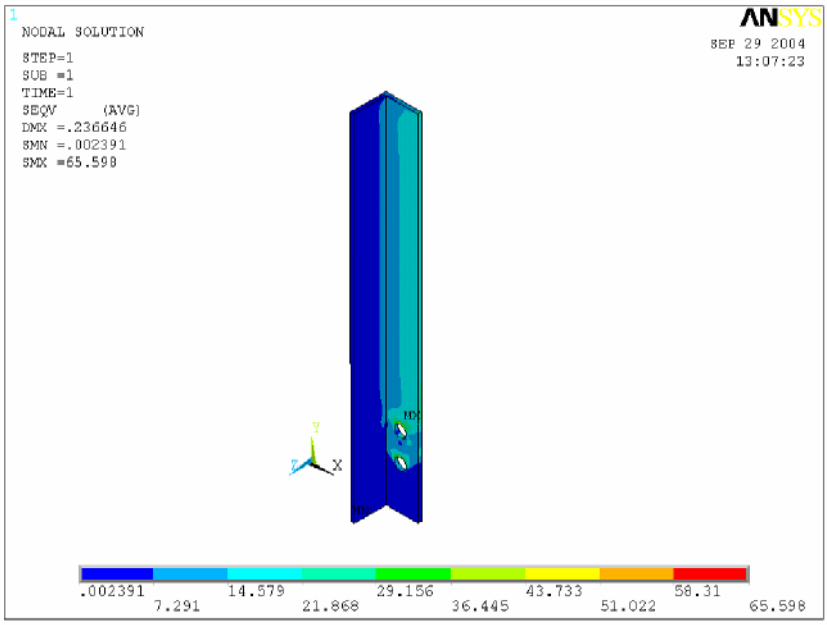

Figure 5.27 Von Mises stress distributions of D4 with 2,5d distance

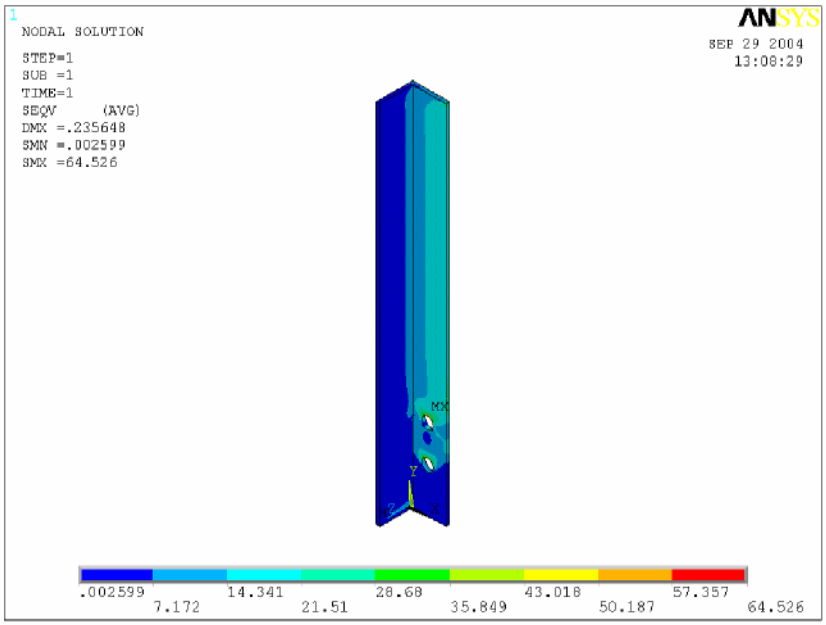

Figure 5.28 Von Mises stress distributions of D4 with 3d distance

This angle carry suppress load. This angle is standard profile which is 50x5 and located vertically. If distances of two rivet holes are 1,5d, maximum stress value is 66,57 MPa. as seen in figure 5.29. Maximum stress occurs inner surface of top rivet hole. This stress value is safety for this construction.

Second distances of rivet holes is 2d, maximum stress value is 62,387 MPa. as seen in figure 5.30.

When distances of rivet holes are chosen 2,5d, maximum stress value is 59,741 MPa. Another rivet distances is 3d, maximum stress value is 58,764 MPa. in here. Two values are too close each other. Every angle has linear stress distributions. Distances of rivet holes increase, maximum stress value decrease. Maximum stress occur inner surface of top rivet hole. These values can be seen in figure 5.31, 5.32.

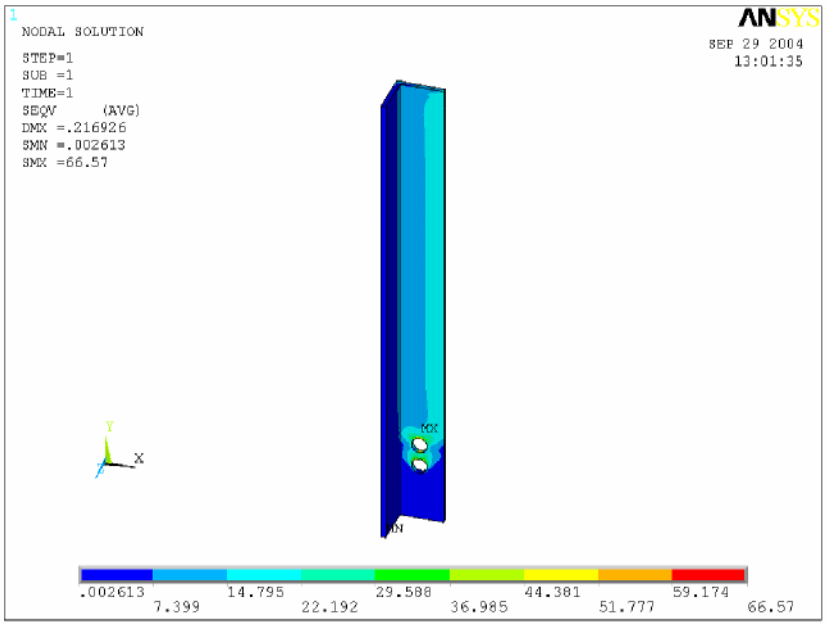

Figure 5.29 Von Mises stress distributions of V2 with 1,5d distance

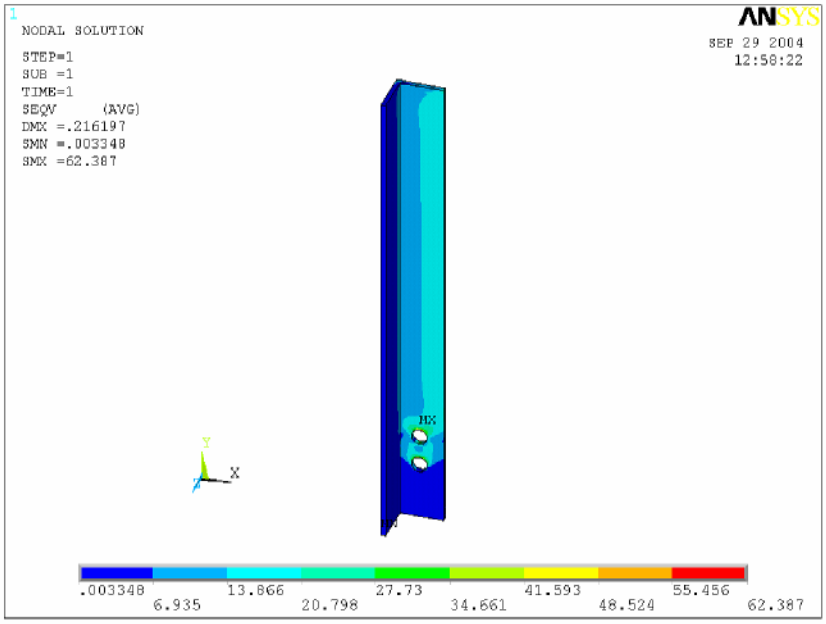

Figure 5.30 Von Mises stress distributions of V2 with 2d distance

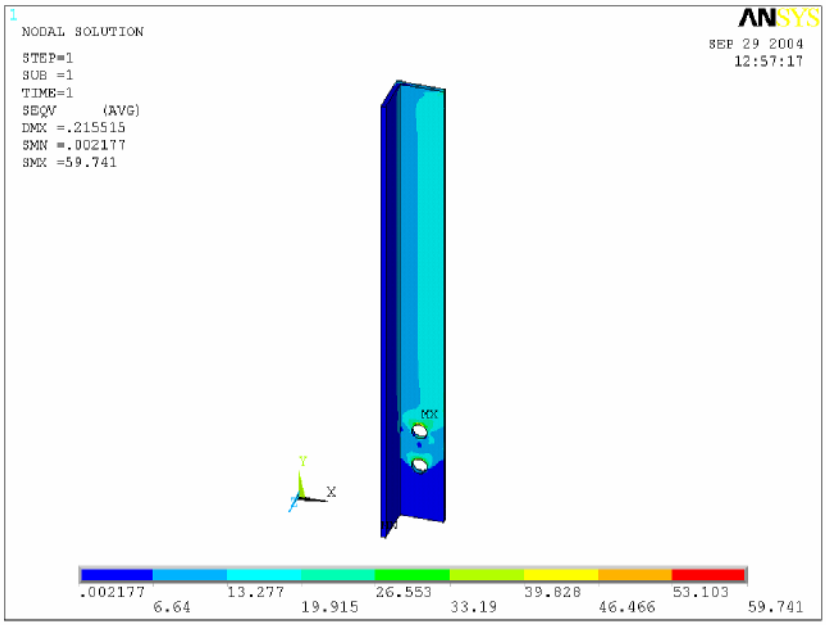

Figure 5.31 Von Mises stress distributions of V2 with 2,5d distance

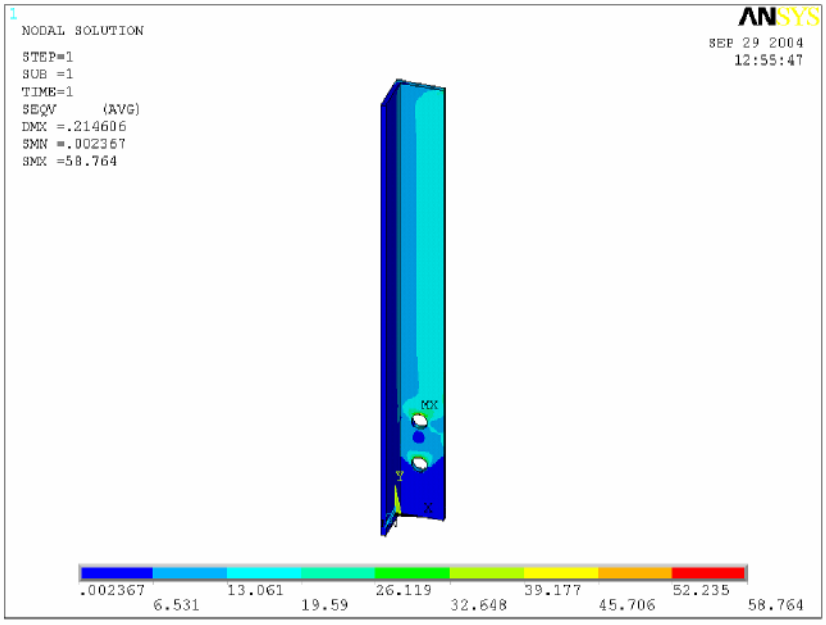

Figure 5.32 Von Mises stress distributions of V2 with 3d distance

This angle is standard profile which is 65x7 and located horizontally. If distances of two rivet holes are 1,5d, maximum stress value is 138,306 MPa. as seen in figure 5.33. There are three rivet holes. Maximum stress occurs inner surface of top rivet hole. This stress value is safety for this construction. But this value is too close maximum safety value.

Second distances of rivet holes is 2d, maximum stress value is 137,198 MPa. as seen in figure 5.34.

When distances of rivet holes are chosen 2,5d, maximum stress value is 133,183 MPa. Another rivet distances is 3d, maximum stress value is 132,326 MPa. in here. Two values are too close each other. Maximum stress occur inner surface of top rivet hole. These values can be seen in figure 5.35, 5.36.

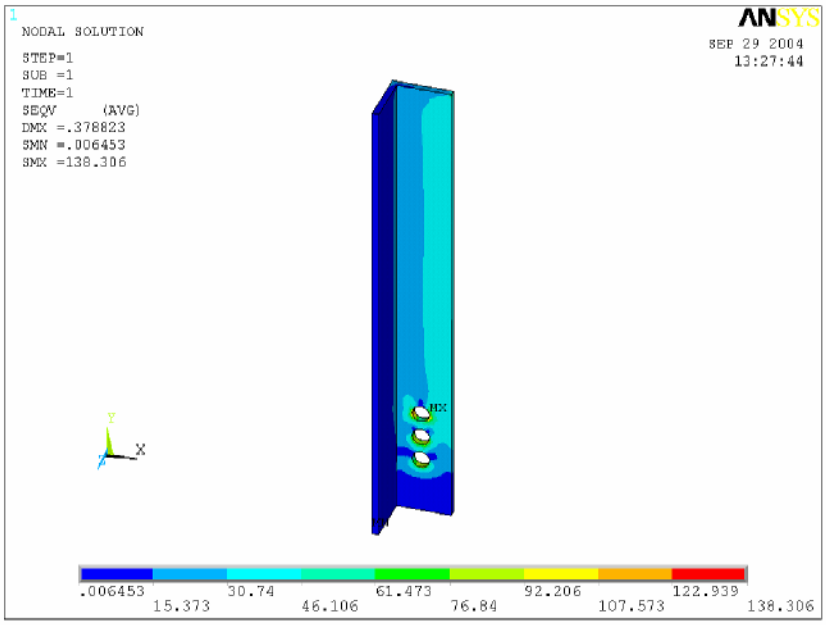

Figure 5.33 Von Mises stress distributions of U2 with 1,5d distance

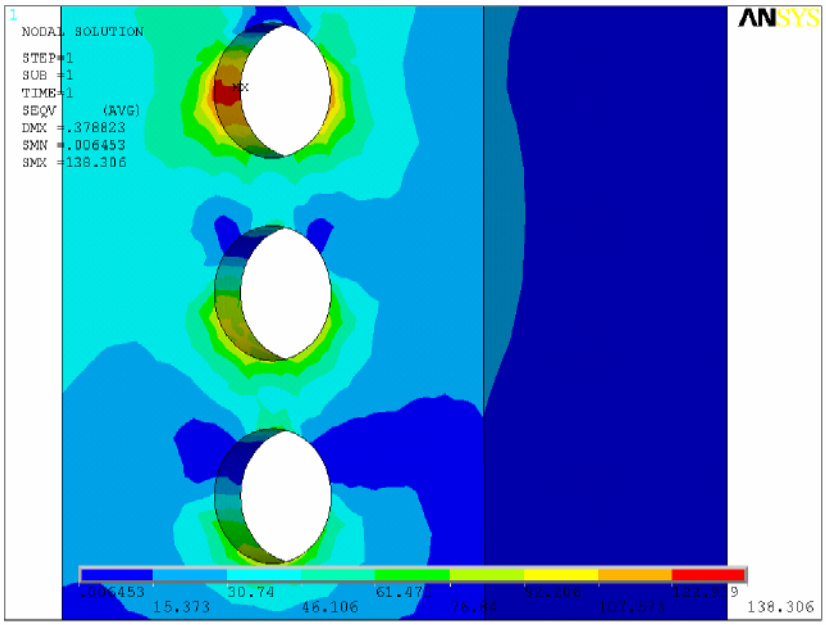

Figure 5.33a Maximum stress of U2 with 1,5d distance

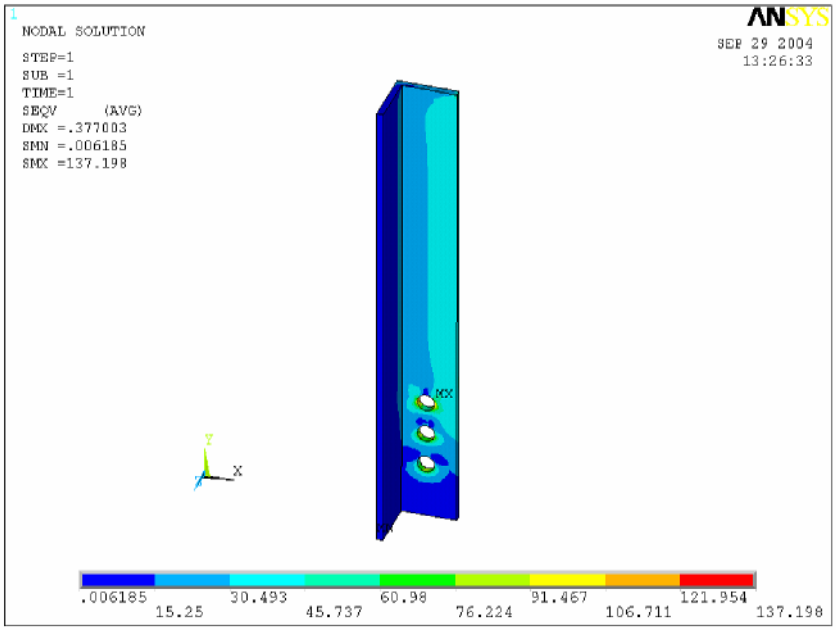

Figure 5.34 Von Mises stress distributions of U2 with 2d distance

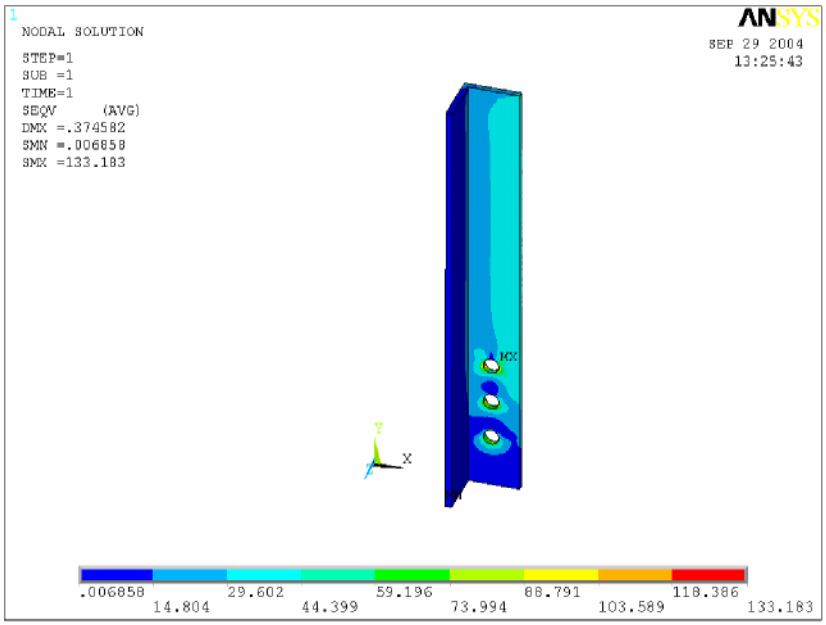

Figure 5.35 Von Mises stress distributions of U2 with 2,5d distance

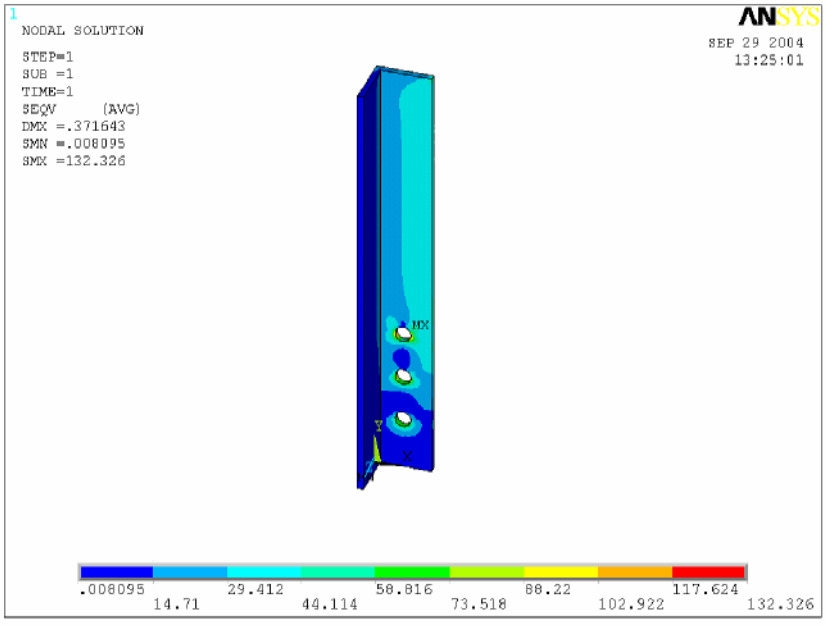

Figure 5.36 Von Mises stress distributions of U2 with 3d distance

This angle is standard profile which is 65x7 and located horizontally. If distances of two rivet holes are 1,5d, maximum stress value is 153,324 MPa. as seen in figure 5.37. There are three rivet holes in here too. Maximum stress occurs inner surface of top rivet hole. This stress value is not safety for this construction. Second distances of rivet holes is 2d, maximum stress value is 153,931 MPa. as seen in figure 5.38. This value is nearly same with 1,5d maximum stress.

When distances of rivet holes are chosen 2,5d, maximum stress value is 145,021 MPa. Another rivet distances is 3d, maximum stress value is 137,49 MPa. Maximum stress occur inner surface of top rivet hole. These values can be seen in figure 5.39, 5.40.

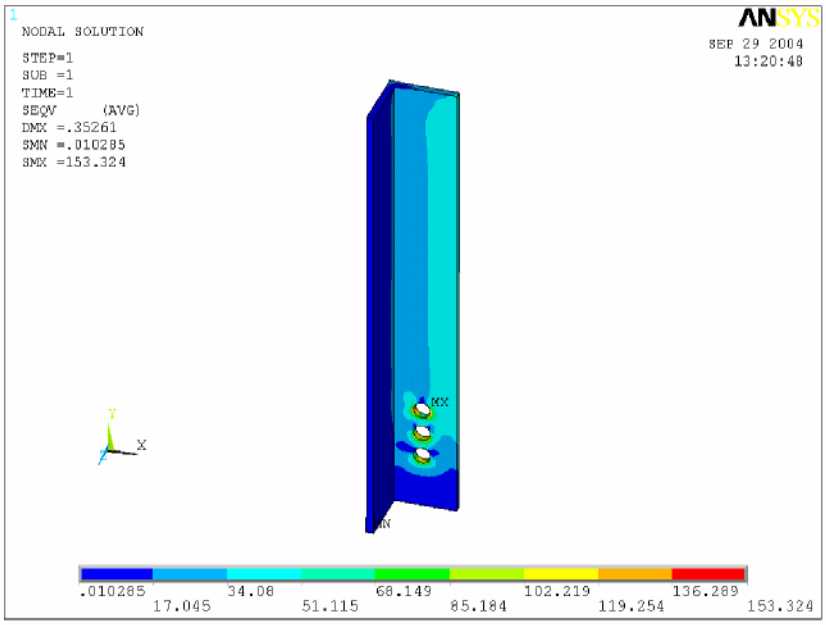

Figure 5.37 Von Mises stress distributions of U3 with 1,5d distance

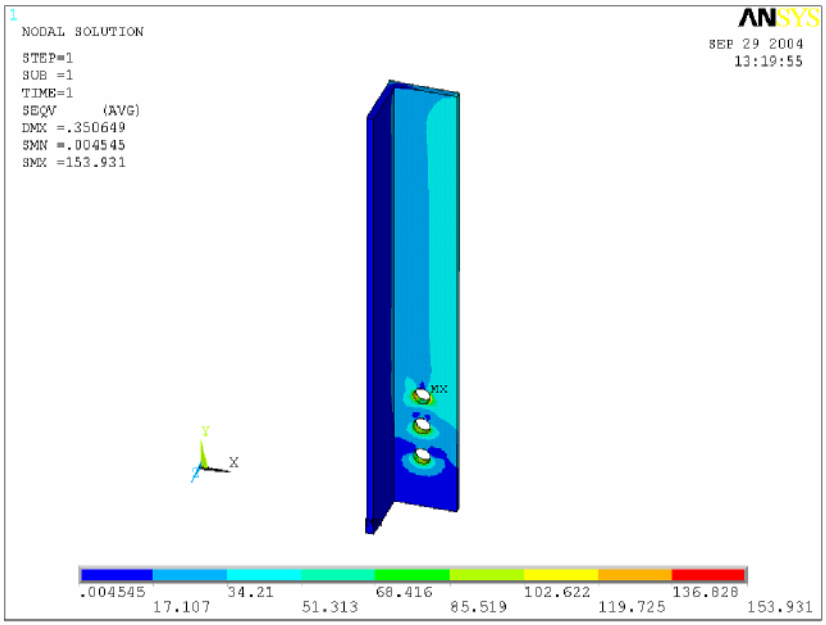

Figure 5.38 Von Mises stress distributions of U3 with 2d distance

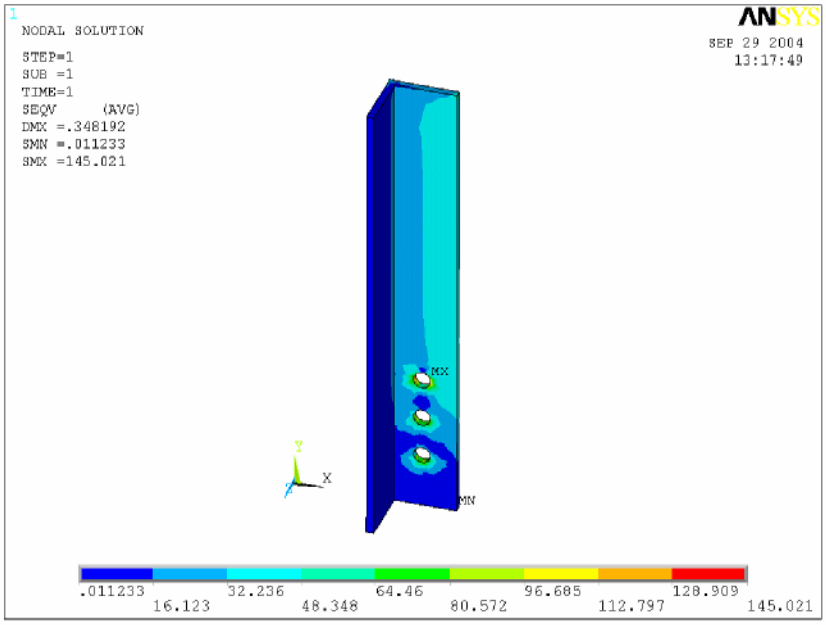

Figure 5.39 Von Mises stress distributions of U3 with 2,5d distance

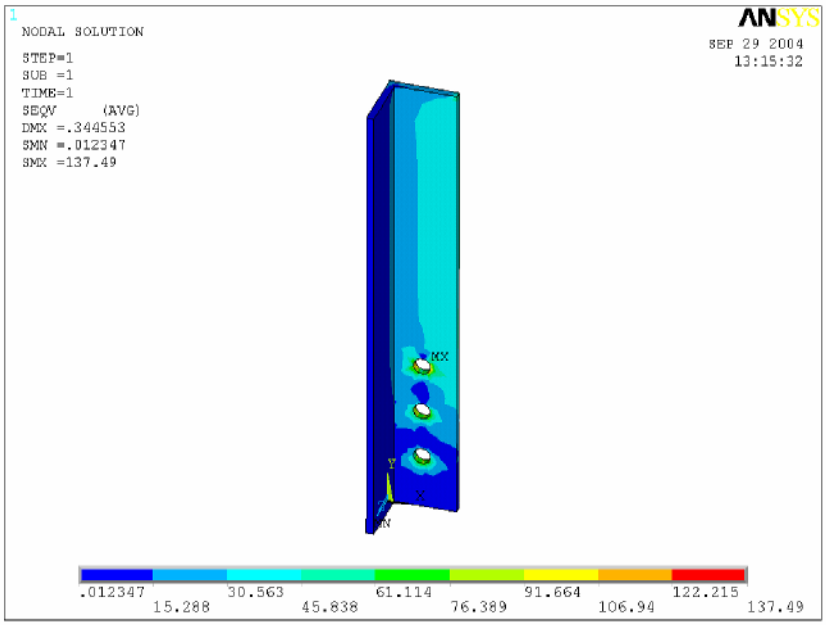

Figure 5.40 Von Mises stress distributions of U3 with 3d distance

5.2 Results of Second Connection Point

5.2.1 Results of Second Connection Point Plate

Thicknesses of second connection point plate were varied from 12mm. to 16mm. Firstly, plate which thickness is 12 mm. was analyzed. If distance between two rivets is 1,5d, maximum stress value is 172,983 MPa. This stress value can be seen in figure 5.41 and 5.41a. Stress distributions generally occur around the rivet holes and these distributions does not spread regular. In this situation, this connection plate is not safety.

If distance between rivet holes is 2d, maximum stress value is 162,86 MPa. This stress value can be seen in figure 5.42. Stress distributions spread more uniform than preceding plate. Although both connection plates have same loads, maximum stress is smaller than preceding connection plate. But this connection plate does not safety.

If distance between rivet holes is 2,5d, maximum stress value is 155,068 MPa. and can be seen in figure 5.43. Stress distributions are getting more uniform and maximum stress value decrease. But this connection plate is not safety too.

If distance between rivet holes is 3d, maximum stress value is 156,224 MPa. Maximum stress value of this connection plate is bigger than the connection plate which has 2,5d rivet holes distances. Both of them have nearly same stress distributions. In this situation, this connection plate thickness is not safety under these load values. This plate stress distributions can be seen in figure 5.44.

In this plate, maximum stress value occurs around angle which is given name U1 in section definition of the problem. Rivet holes of another angles looks under safety stress value according to stress distributions figures. Figure 5.41 show us which rivet region is critical level.

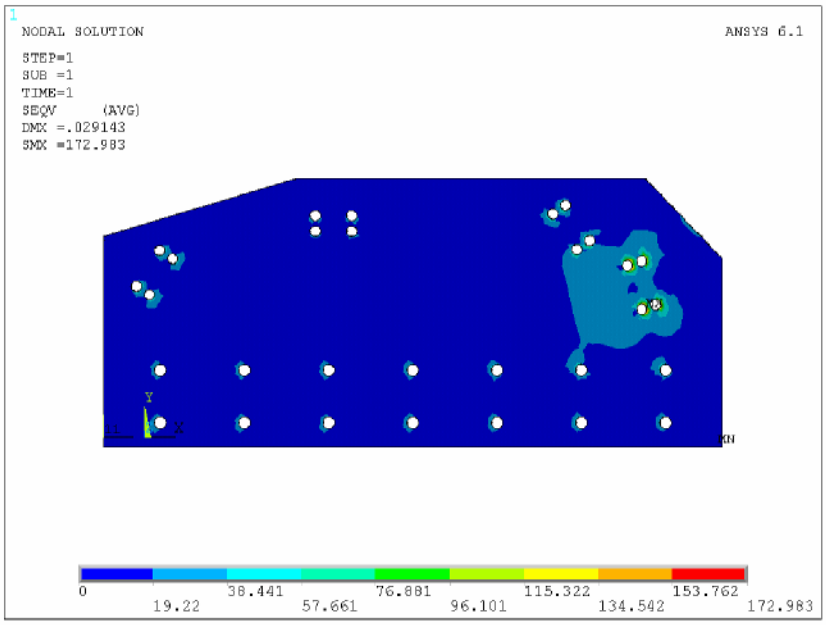

Figure 5.41 Second connection point plate Von Mises stress distributions, thickness of plate 12 mm. and rivets distance 1,5d (Units are MPa)

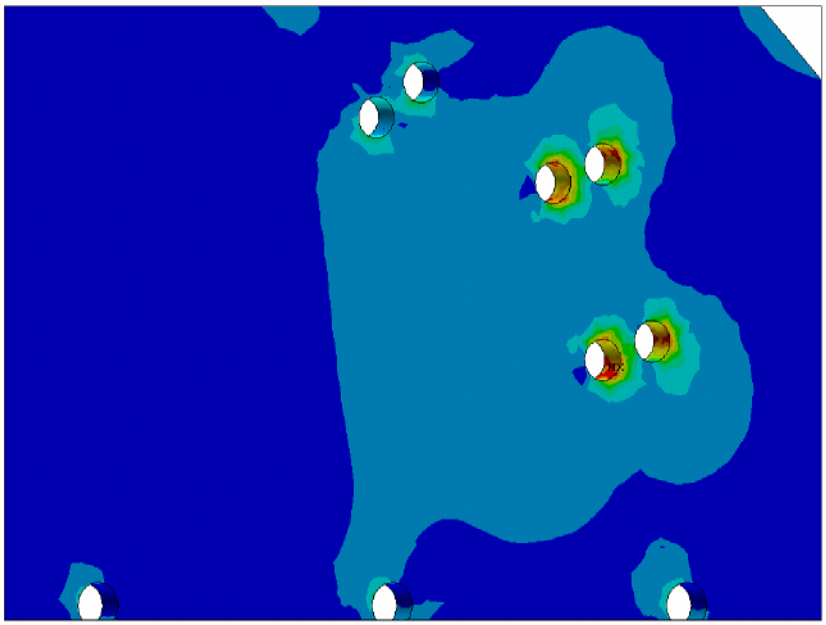

Figure 5.41a Maximum stress of plate 12 mm. and rivets distance 1,5d (Units are MPa)

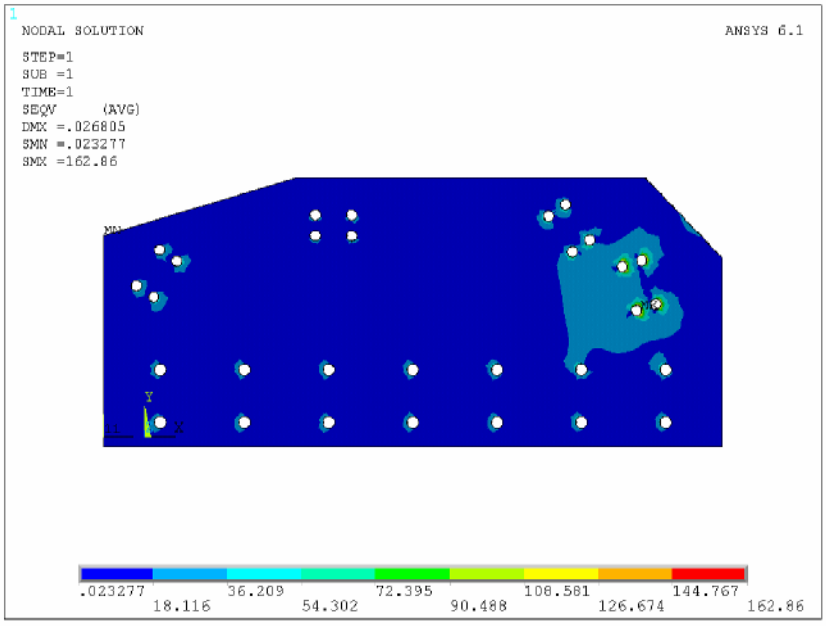

Figure 5.42 Second connection point plate Von Mises stress distributions, thickness of plate 12 mm. and rivets distance 2d (Units are MPa)

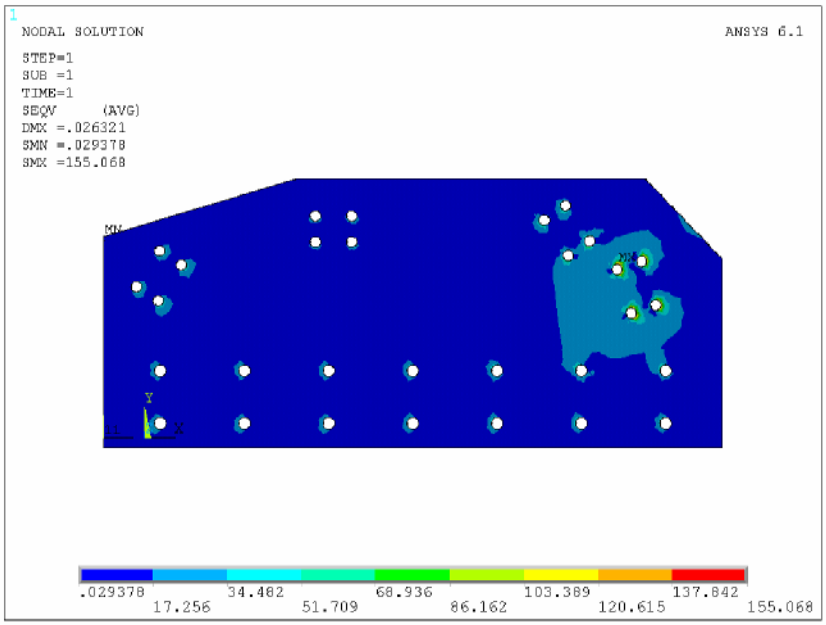

Figure 5.43 Second connection point plate Von Mises stress distributions, thickness of plate 12 mm. and rivets distance 2,5d (Units are MPa)

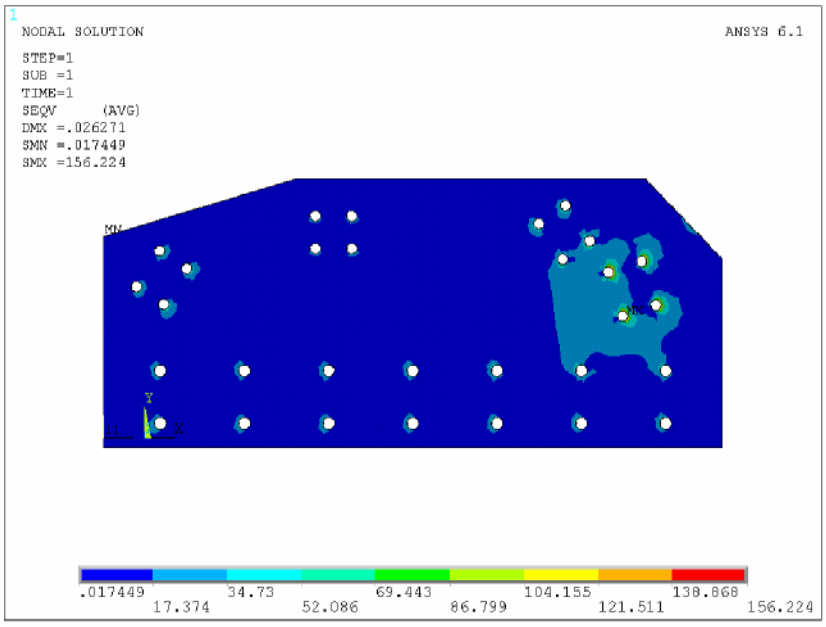

Figure 5.44 Second connection point plate Von Mises stress distributions, thickness of plate 12 mm. and rivets distance 3d (Units are MPa)

Second type of second connection plate thickness is 13 mm. and can be seen in figure 5.45. If rivet holes distances are chosen 1,5d, maximum stress value is 160,941 MPa. Maximum stress value is over safety stress value. But maximum stress value of this connection plate is smaller than connection plate which has same rivet holes distances, thickness 12mm.

If distance between rivet holes is 2d, maximum stress value is 148,029 MPa. Stress distributions can be seen in figure 5.46. Maximum stress value of this plate is too smaller than preceding plate which has 1,5d rivet distances.

If distance between rivet holes is 2,5d, maximum stress value is 159,317 MPa. This plate can be seen in figure 5.47. Despite of increasing thickness of plate, maximum stress value increase.

If distance between rivet holes is 3d, maximum stress value is 144,932 MPa and maximum stress value is over safety stress value, shown in figure 5.48. This plate is not safety. But maximum stresses of 2d and 3d rivet holes distances are too close.

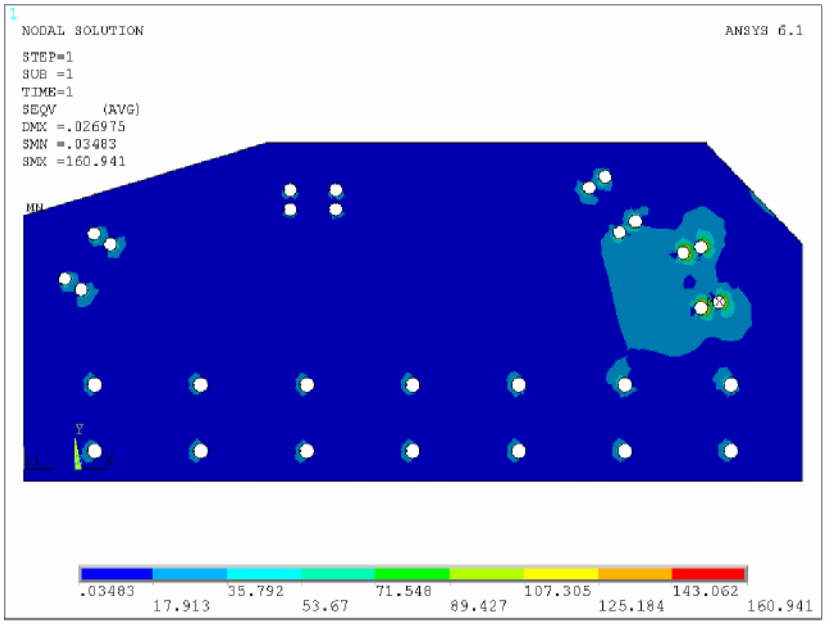

Figure 5.45 Second connection point plate Von Mises stress distributions, thickness of plate 13 mm. and rivets distance 1,5d (Units are MPa)

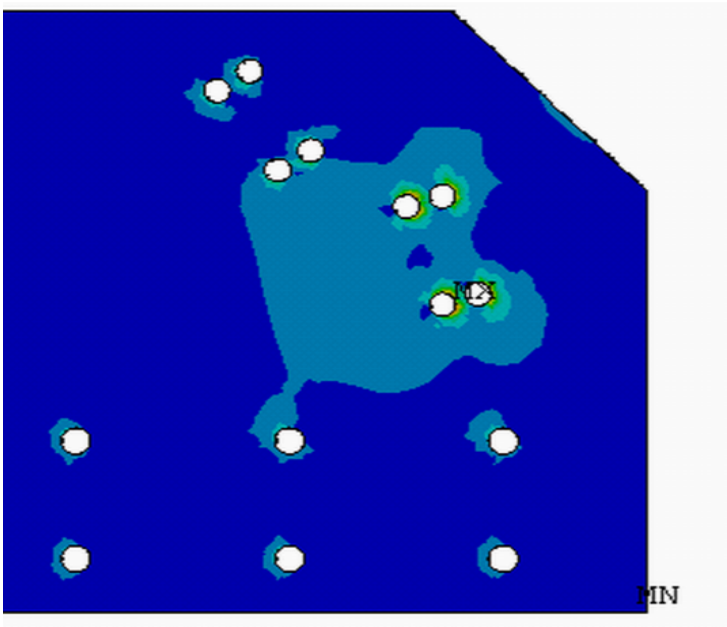

Figure 5.45a Maximum stress

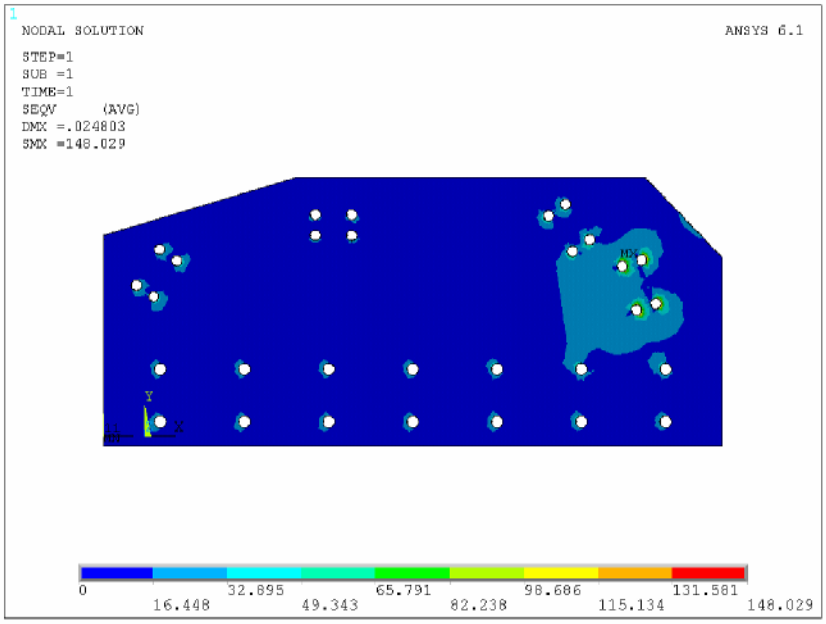

Figure 5.46 Second connection point plate Von Mises stress distributions, thickness of plate 13 mm. and rivets distance 2d (Units are MPa)

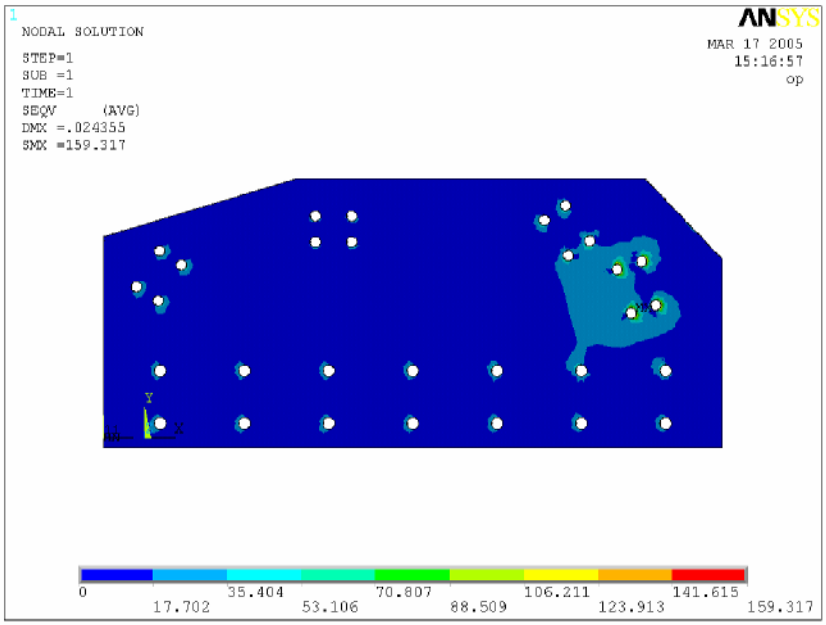

Figure 5.47 Second connection point plate Von Mises stress distributions, thickness of plate 13 mm. and rivets distance 2,5d (Units are MPa)

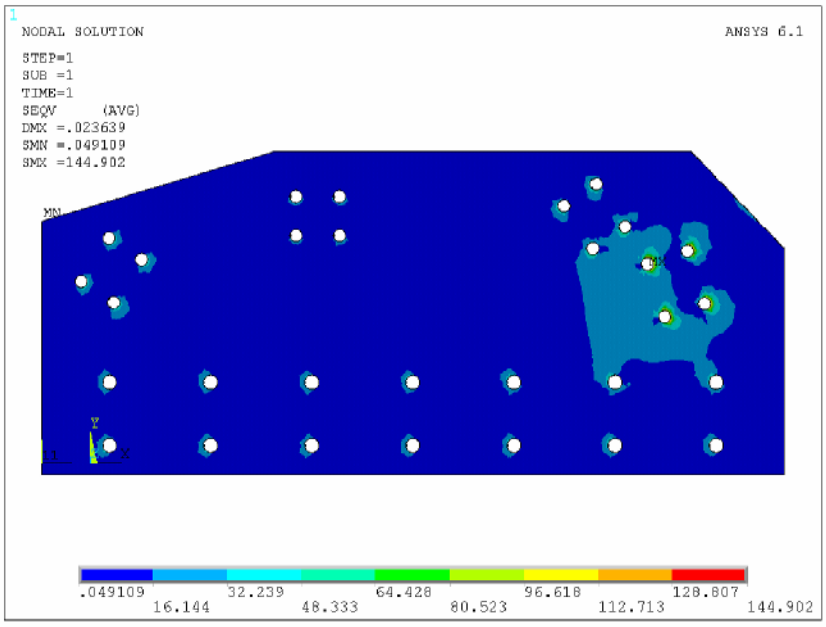

Figure 5.48 Second connection point plate Von Mises stress distributions, thickness of plate 13 mm. and rivets distance 3d (Units are MPa)

Third type of first connection plate thickness is 14 mm. and can be seen in figure 5.49. If rivet holes distances are chosen 1,5d, maximum stress value is 159,098 MPa. Maximum stress occurs the same place as seen in figure 5.49a. Maximum stress values occur around rivet holes. Maximum stress value is over safety stress value.

If distance between rivet holes is 2d, maximum stress value is 149,54 MPa and. stress distributions can be seen in figure 5.50.

If distance between rivet holes is 2,5d, maximum stress value is 138,633 MPa. and can be seen in figure 5.51. Maximum stress occurs same place in this plate. This rivet holes distances is safety.

If distance between rivet holes is 3d, maximum stress value is 135,175 MPa. In this situation, this connection plate thickness is safety under these load values. This plate stress distributions can be seen in figure 5.52.

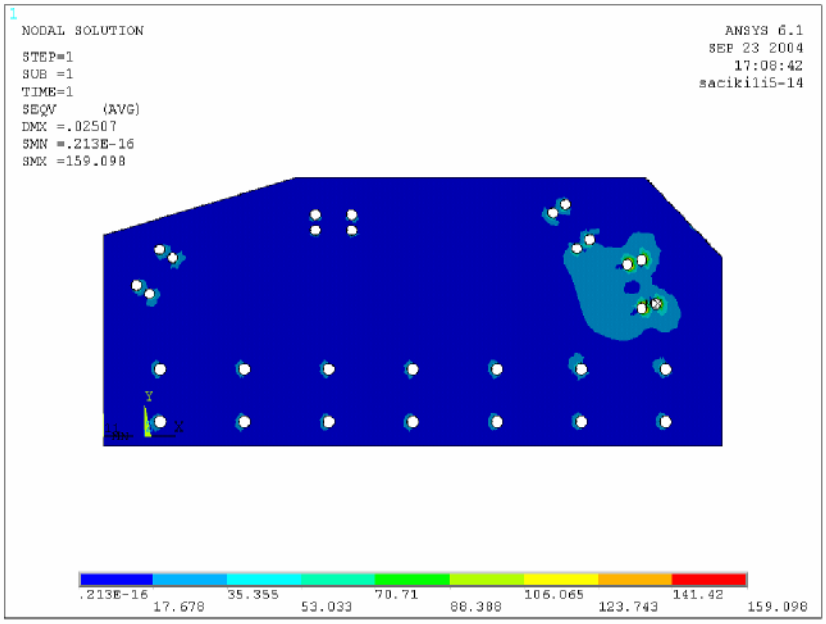

Figure 5.49 Second connection point plate Von Mises stress distributions, thickness of plate 14 mm. and rivets distance 1,5d (Units are MPa)

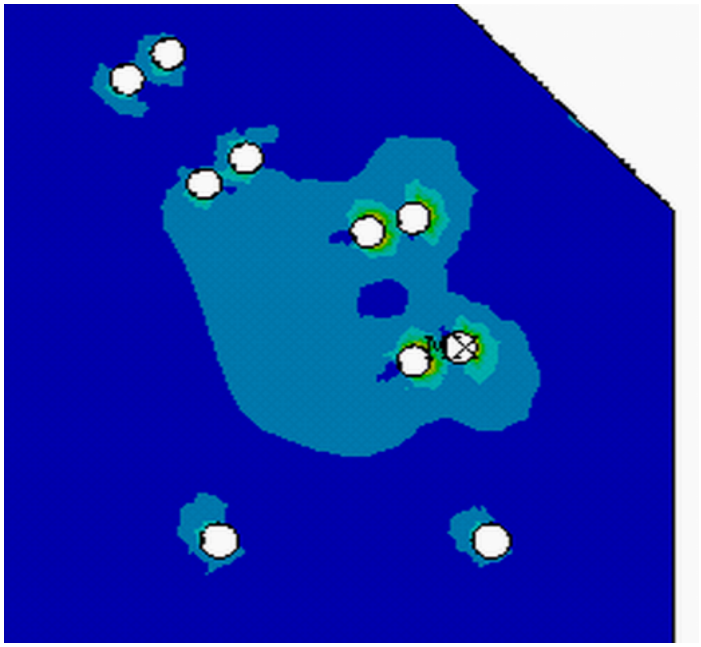

Figure 5.49a Maximum stress

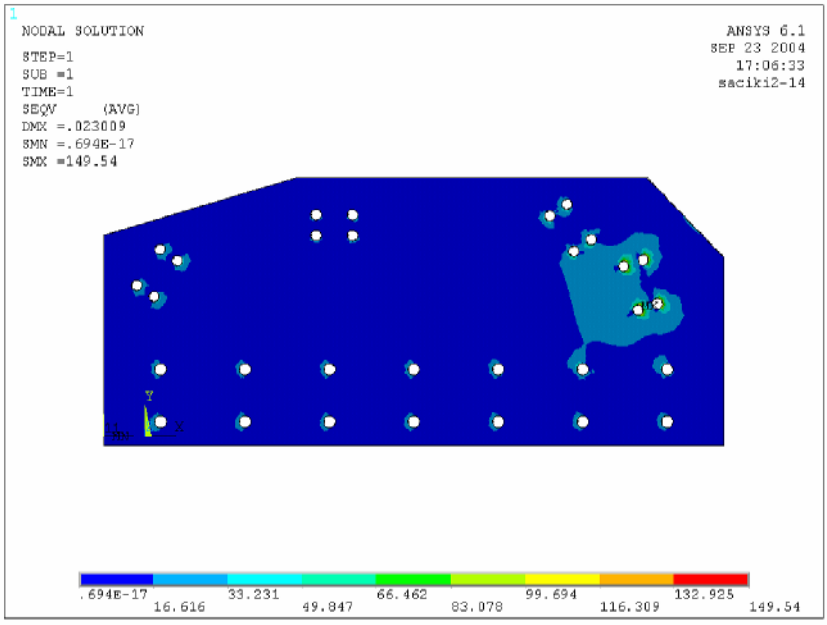

Figure 5.50 Second connection point plate Von Mises stress distributions, thickness of plate 14 mm. and rivets distance 2d (Units are MPa)

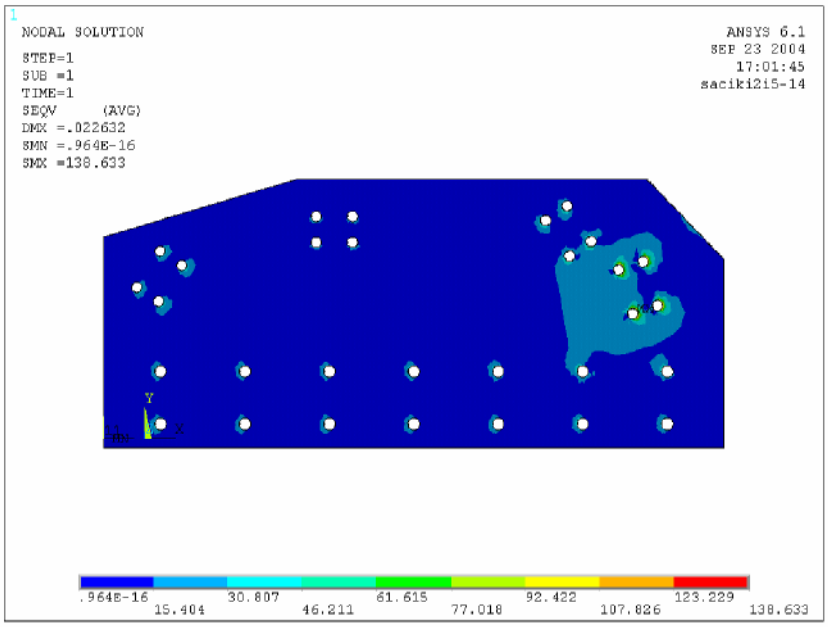

Figure 5.51 Second connection point plate Von Mises stress distributions, thickness of plate 14 mm. and rivets distance 2,5d (Units are MPa)

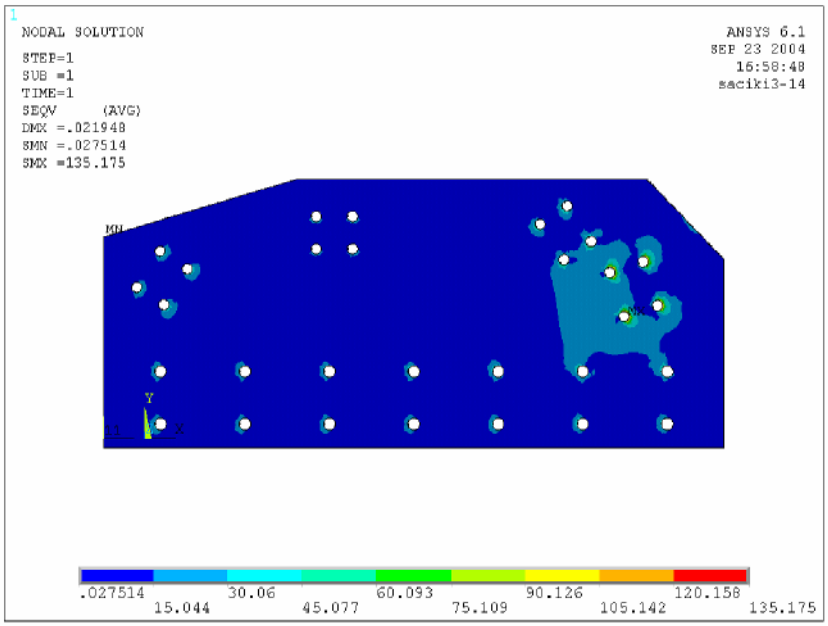

Figure 5.52 Second connection point plate Von Mises stress distributions, thickness of plate 14 mm. and rivets distance 3d (Units are MPa)

This connection plate thickness is 15 mm. and can be seen in figure 5.53. If rivet holes distances are chosen 1,5d, maximum stress value is 158,348 MPa. Maximum stress value occurs inner surface of rivet hole. Maximum stress value is over safety stress value.

If distance between rivet holes is 2d, maximum stress value is 128,587 MPa. Stress distributions can be seen in figure 5.53. If distance between rivet holes is 2,5d, maximum stress value is 128,306 MPa. Stress distributions of this connection plate are more uniform. This plate can be seen in figure 5.54. Both connection plate stress values are too similar. Both of them are safety for this construction.

If distance between rivet holes is 3d, maximum stress value is 126,754 MPa and maximum stress value is under safety stress value, shown in figure 5.55. It can be said that safety stress value obtained by changing distances between rivet holes on same thickness.

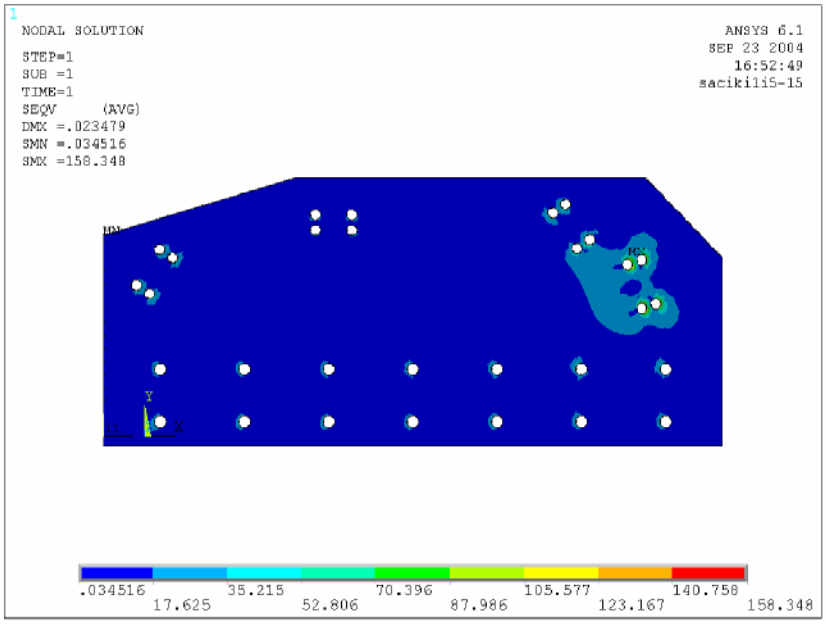

Figure 5.53 Second connection point plate Von Mises stress distributions, thickness of plate 15 mm. and rivets distance 1,5d (Units are MPa)

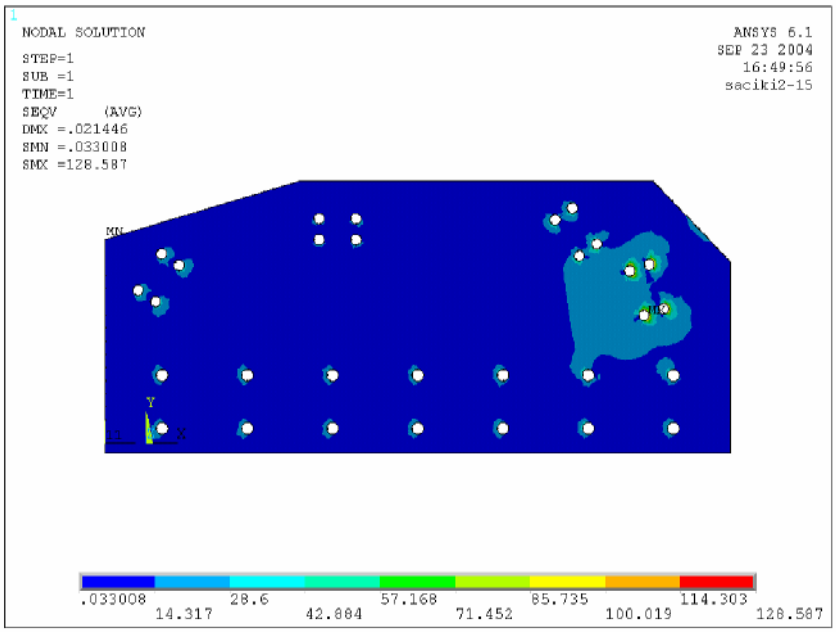

Figure 5.54 Second connection point plate Von Mises stress distributions, thickness of plate 15 mm. and rivets distance 2d (Units are MPa)

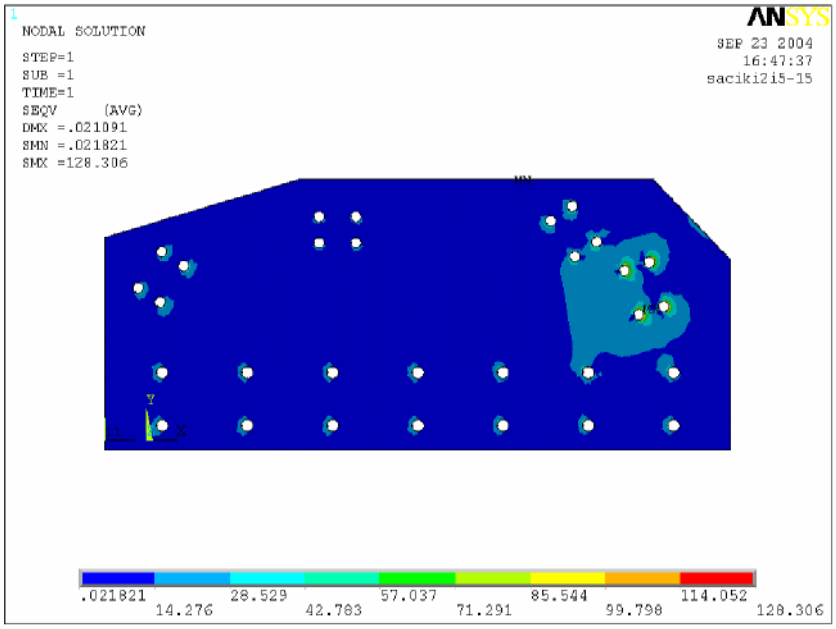

Figure 5.55 Second connection point plate Von Mises stress distributions, thickness of plate 15 mm. and rivets distance 2,5d (Units are MPa)

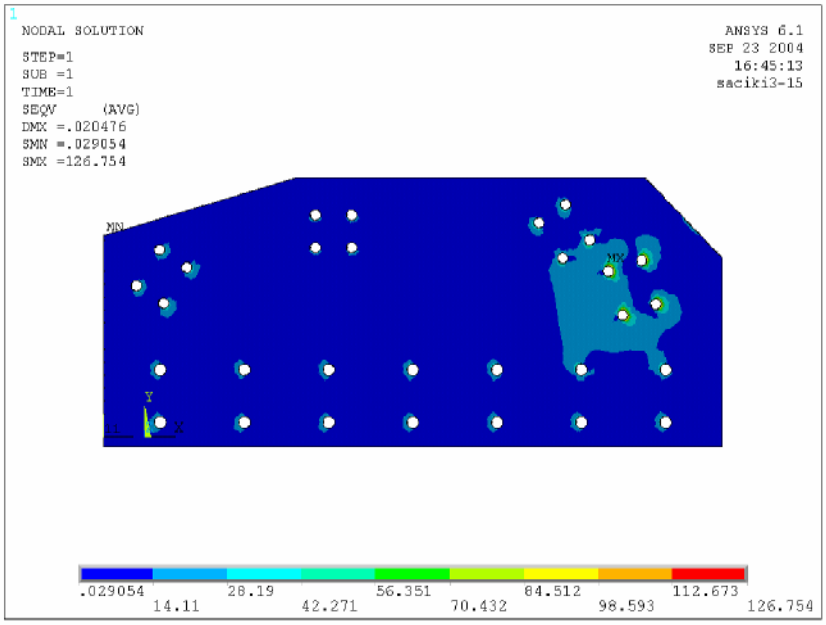

Figure 5.56 Second connection point plate Von Mises stress distributions, thickness of plate 15 mm. and rivets distance 3d (Units are MPa)

Last plate of second connection, thickness is 16 mm. and can be seen in figure 5.57. If rivet holes distances are chosen 1,5d, maximum stress value is 144,951 MPa. Maximum stress values occur around rivet holes. Maximum stress value is under safety stress value. It can be clearly seen that this plate stress value is bigger than preceding plate thickness with 3d rivet distances, last plate also has more 1 mm thickness.

If distance between rivet holes is 2d, maximum stress value is 118,199 MPa and. stress distributions can be seen in figure 5.58. If distance between rivet holes is 2,5d, maximum stress value is 119,510 MPa. and can be seen in figure 5.59. Maximum stress occurs same place in this plate. If distance between rivet holes is 3d, maximum stress value is 119,615 MPa. These three values are too close. In this situation, this connection plate thickness is safety for all distances of rivet holes under these load values. This plate stress distributions can be seen in figure 5.60.

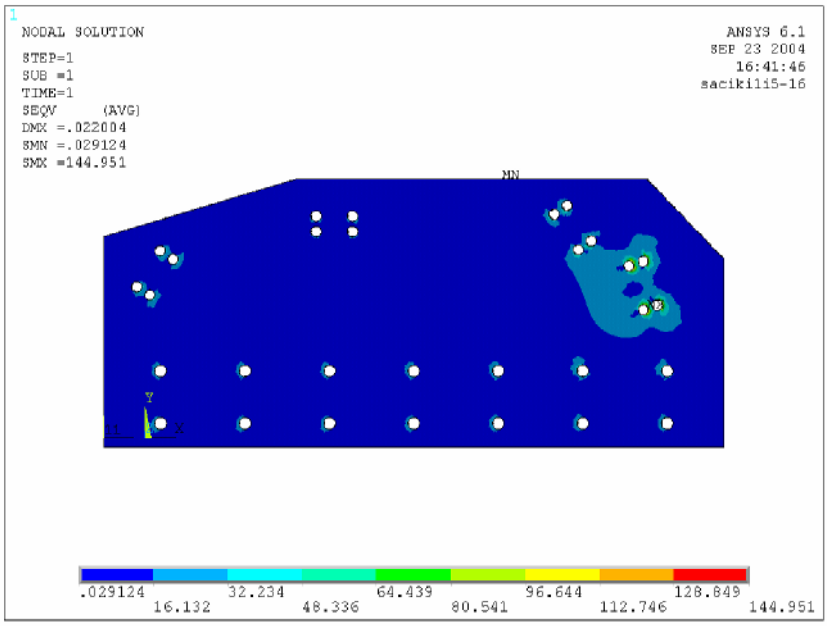

Figure 5.57 Second connection point plate Von Mises stress distributions, thickness of plate 16 mm. and rivets distance 1,5d (Units are MPa)

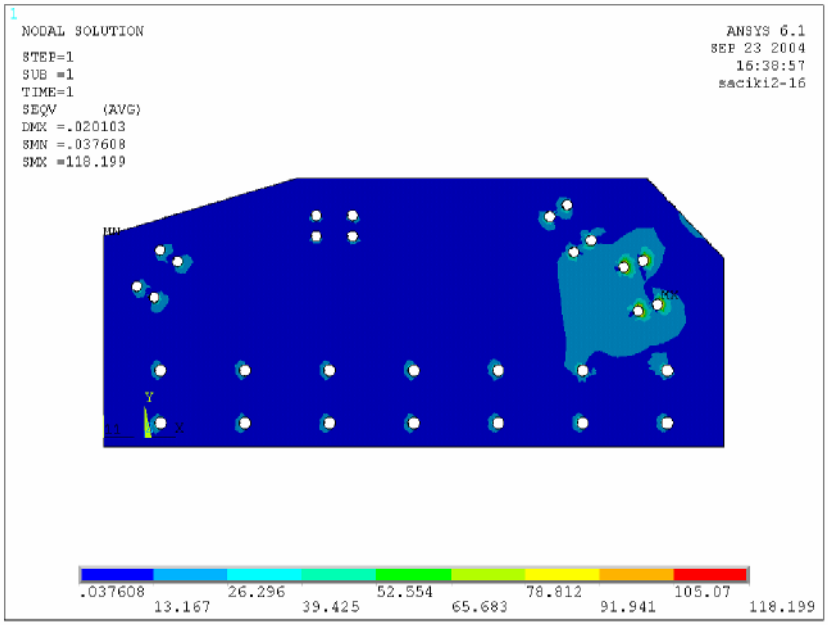

Figure 5.58 Second connection point plate Von Mises stress distributions, thickness of plate 16 mm. and rivets distance 2d (Units are MPa)

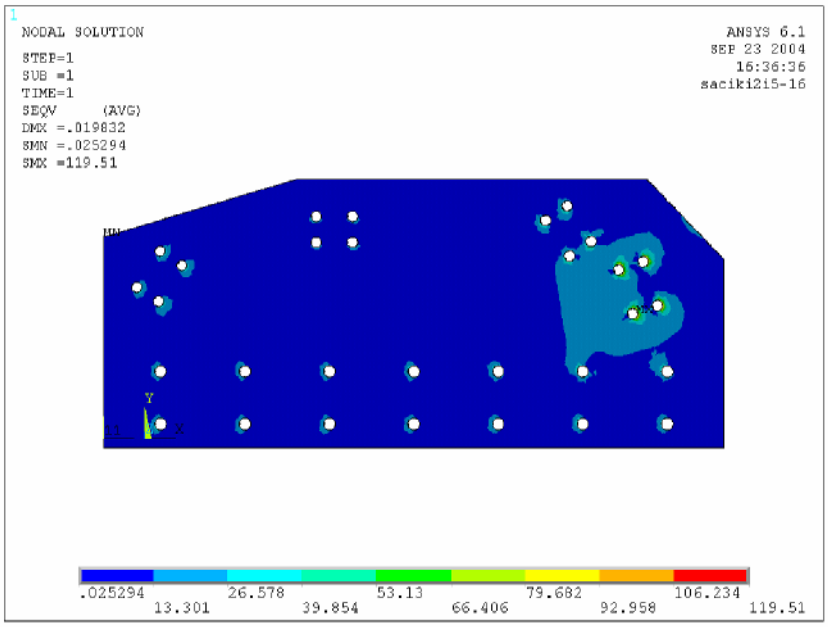

Figure 5.59 Second connection point plate Von Mises stress distributions, thickness of plate 16 mm. and rivets distance 2,5d (Units are MPa)

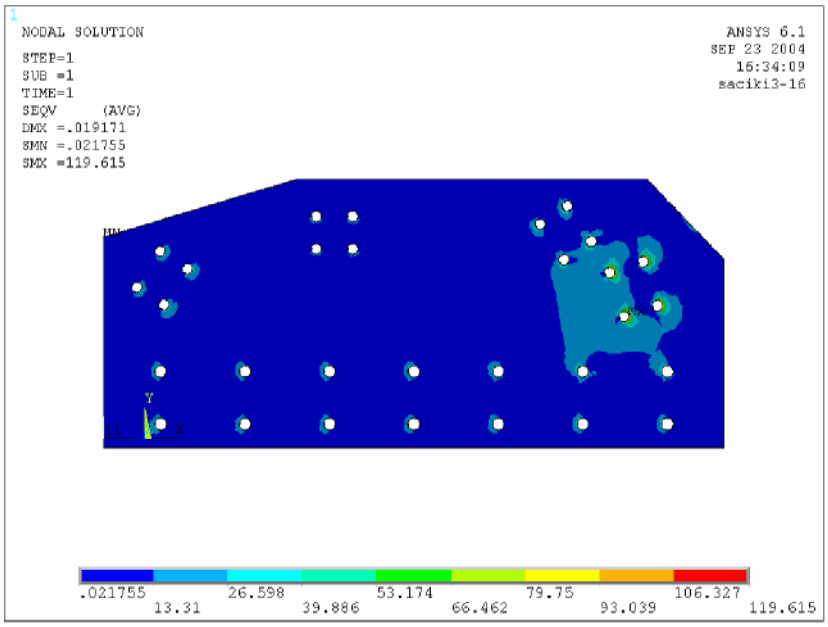

Figure 5.60 Second connection point plate Von Mises stress distributions, thickness of plate 16 mm. and rivets distance 3d (Units are MPa)

5.2.2 Results of Second Connection Point Angles

This angle is standard profile which is 60x6 and located diagonally. If distances of two rivet holes are 1,5d, maximum stress value is 93,382 MPa. as seen in figure 5.61. Maximum stress occurs inner surface of top rivet hole. This stress value is safety for this construction. But other distances of rivet holes will be investigated.

Second distances of rivet holes is 2d, maximum stress value is 91,962 MPa. as seen in figure 5.62. Stress value is decreasing because of rivet holes distances. When distances of rivet holes are chosen 2,5d, maximum stress value is 88,35 MPa. Another rivet distances is 3d, maximum stress value is 86,869 MPa. in here. Two values are too close each other but not same. Maximum stress occur inner surface of top rivet hole. These values can be seen in figure 5.63, 5.64.

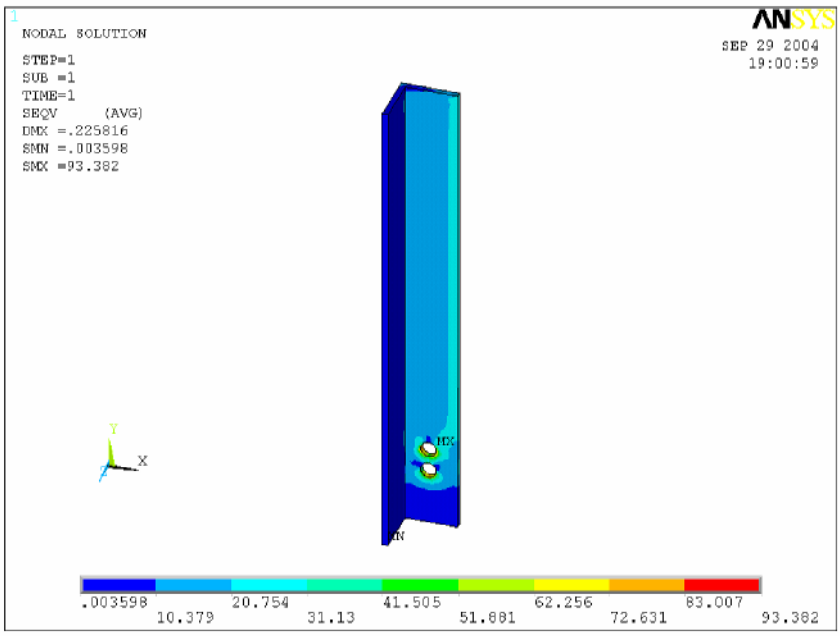

Figure 5.61 Von Mises stress distributions of D1 with 1,5d distance

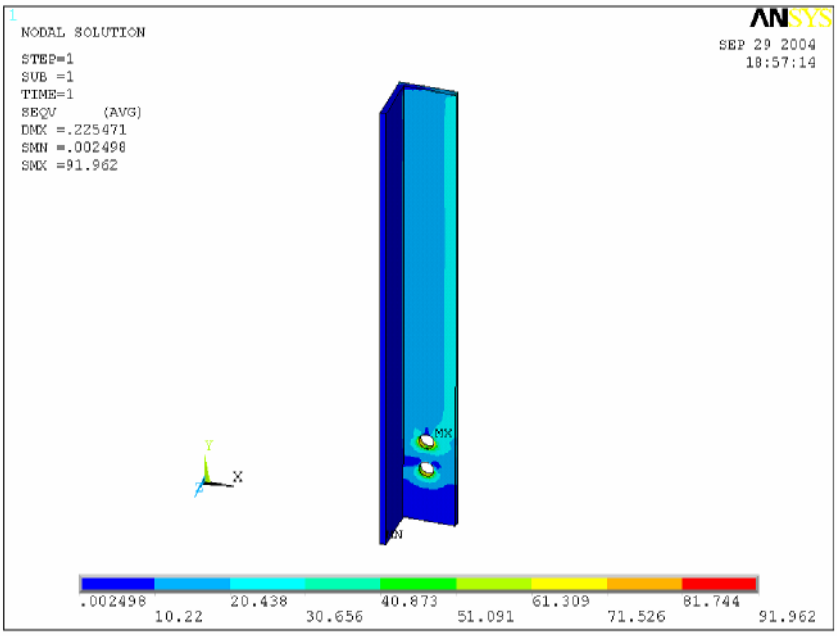

Figure 5. Von Mises stress distributions of D1 with 2d distance

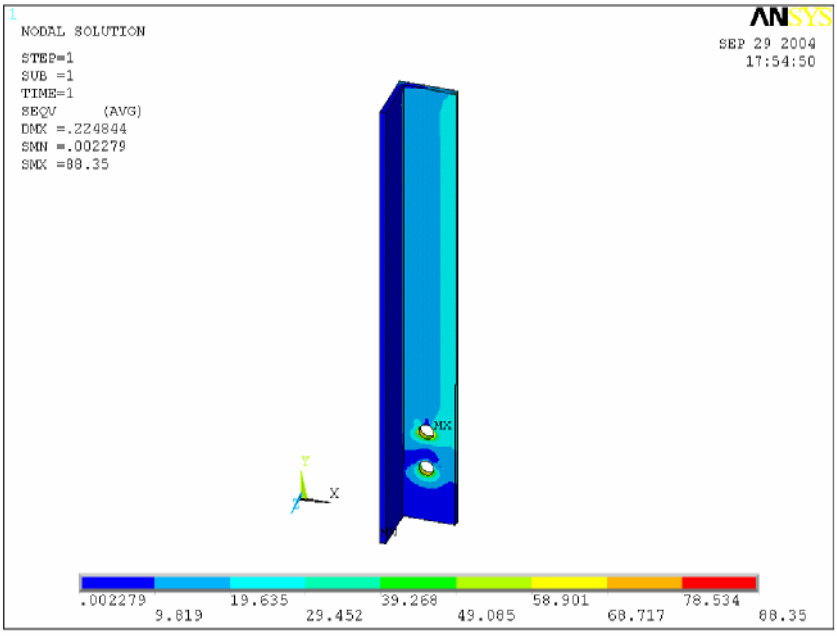

Figure 5.63 Von Mises stress distributions of D1 with 2,5d distance

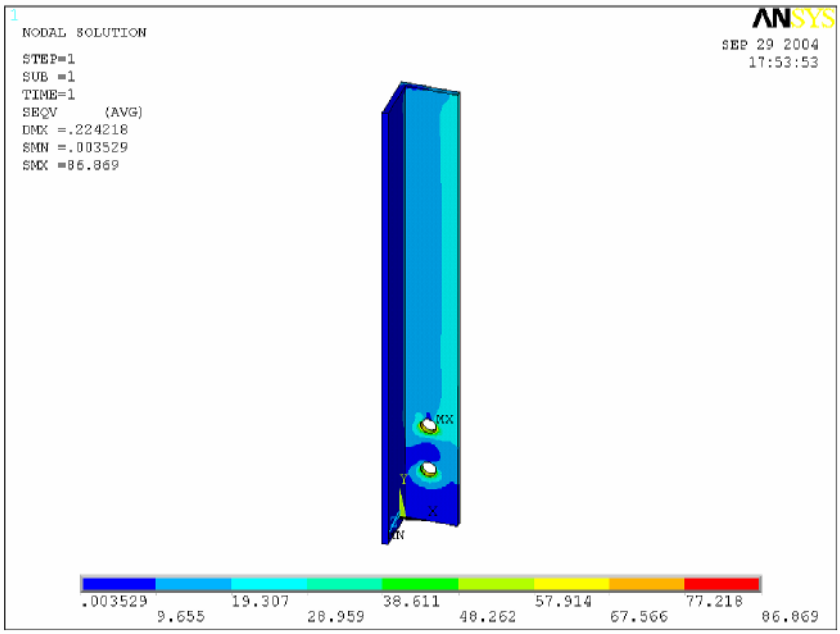

Figure 5.64 Von Mises stress distributions of D1 with 3d distance

This angle is same preceding angle but only load condition is different. If distances of two rivet holes are 1,5d, maximum stress value is 89,646 MPa. as seen in figure 5.65. Maximum stress occurs inner surface of top rivet hole. Second distances of rivet holes is 2d, maximum stress value is 86,492 MPa. as seen in figure 5.66. When distances of rivet holes are chosen 2.5d, maximum stress value is 83,37 MPa. Another rivet distances is 3d, maximum stress value is 79,808 MPa. in here. These values can be seen in figure 5.67, 5.68. It can be clearly seen that this angle and preceding angle results and stress distributions changed determined ratio.

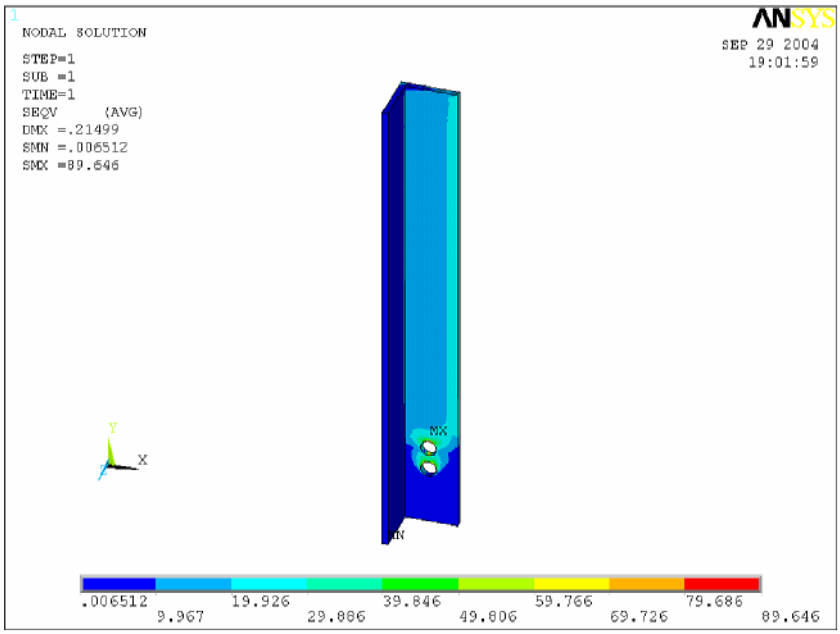

Figure 5.65 Von Mises stress distributions of D2 with 1,5d distance

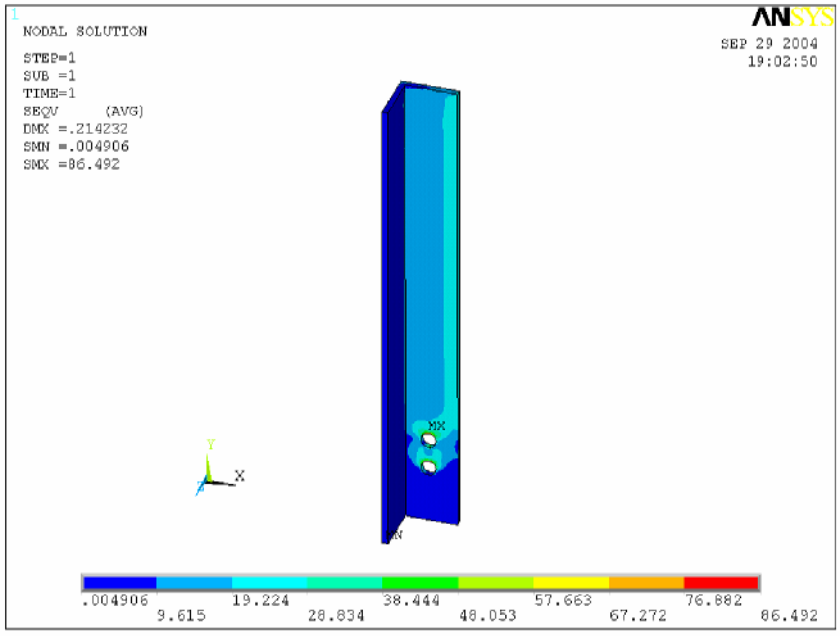

Figure 5.66 Von Mises stress distributions of D2 with 2d distance

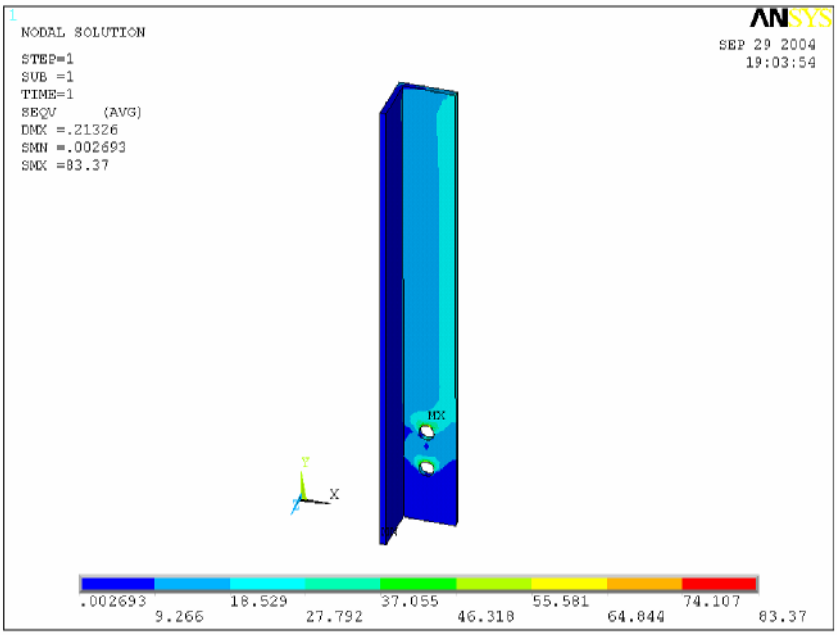

Figure 5.67 Von Mises stress distributions of D2 with 2,5d distance

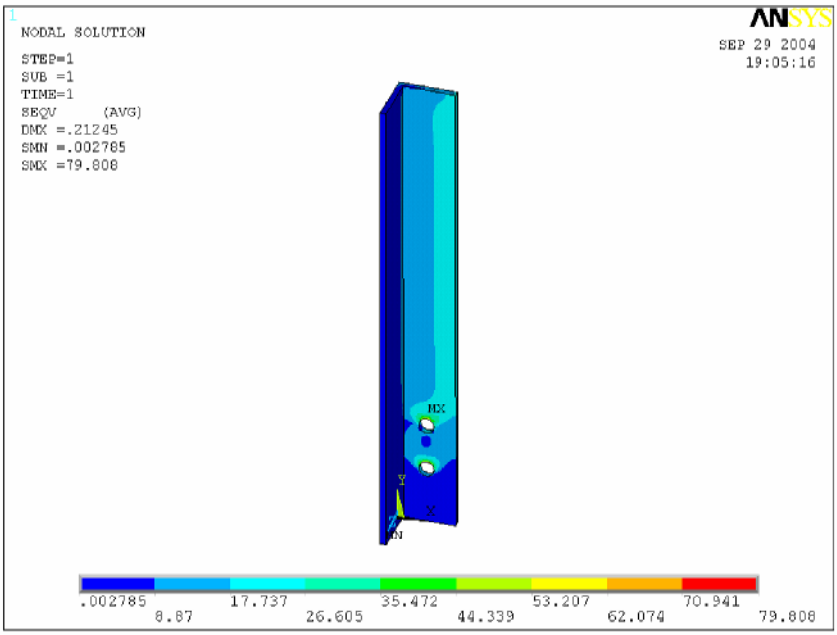

Figure 5.68 Von Mises stress distributions of D2 with 3d distance

This angle is standard profile which is 60x6 and located diagonally. If distances of two rivet holes are 1,5d, maximum stress value is 153,766 MPa. as seen in figure 5.69. Maximum stress occurs inner surface of top rivet hole. This stress value is not safety for this construction.

Second distances of rivet holes is 2d, maximum stress value is 141,127 MPa. as seen in figure 5.70.

When distances of rivet holes are chosen 2,5d, maximum stress value is 138.7 MPa. Another rivet distances is 3d, maximum stress value is 136,99 MPa. in here. Two values are too close each other. Maximum stress occur inner surface of top rivet hole. These values can be seen in figure 5.71, 5.72.

The minimum stress distributions occur by choosing 3d rivet distance. Three of connection points have same angles which are named V1, V2, V3 and the same loads are applied. This angle can be shown in figure 5.29, 5.30, 5.31, 5.32.

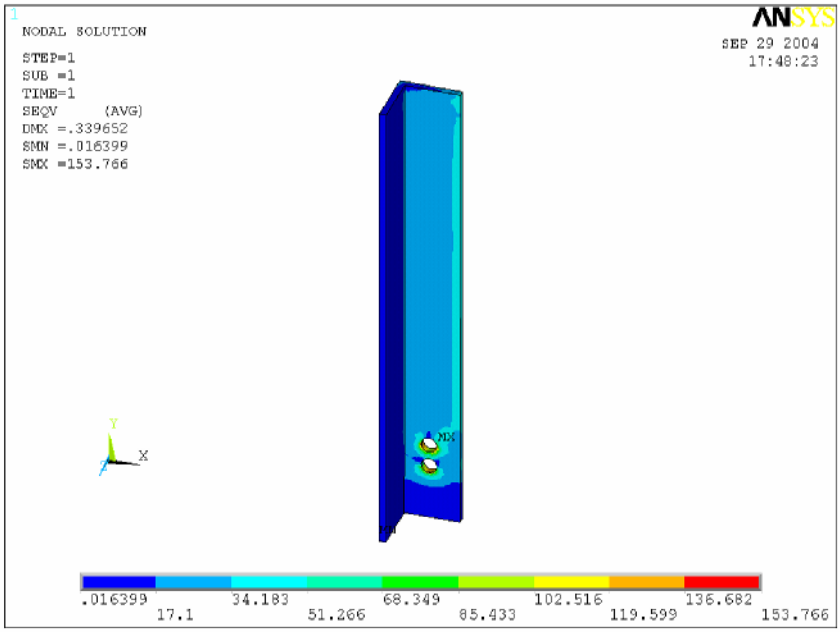

Figure 5.69 Von Mises stress distributions of U1 with 1,5d distance

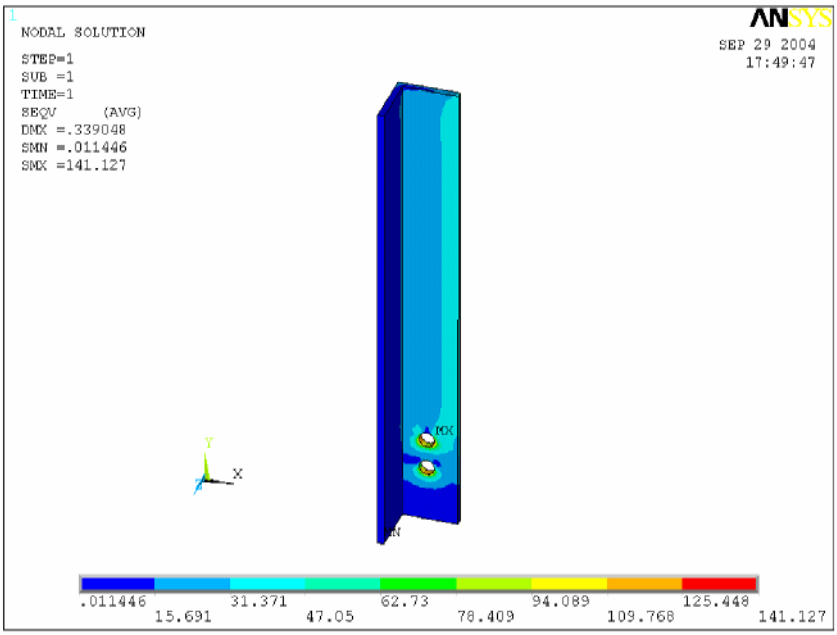

Figure 5.70 Von Mises stress distributions of U1 with 2d distance

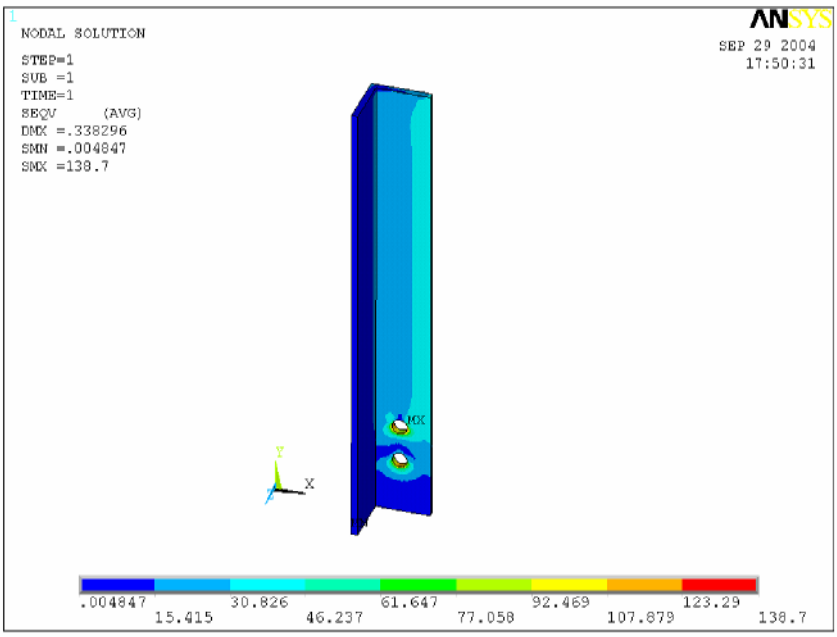

Figure 5.71 Von Mises stress distributions of U1 with 2,5d distance

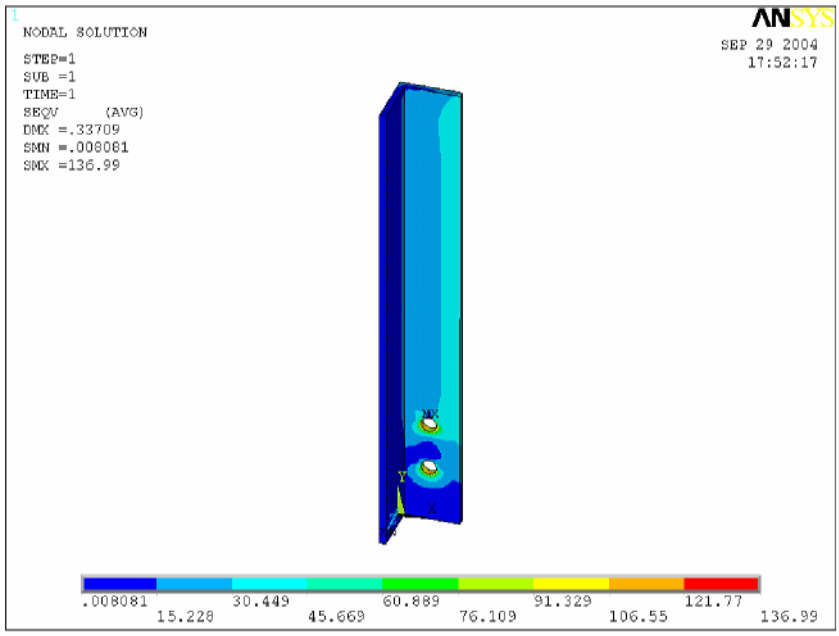

Figure 5.72 Von Mises stress distributions of U1 with 3d distance

5.3 Results of Third Connection Point

5.3.1 Results of Third Connection Point Plate

Thickness of third connection point plate is 7 mm. If distance between two rivets is 1,5d, maximum stress value is 150,818 MPa. This stress value can be seen inner surface of bottom rivet hole. Stress distributions can be seen in figure 5.73. In this situation, this connection plate is not safety.

If distance between rivet holes is 2d, maximum stress value is 146,3 MPa. Maximum stress occurs same place with previous connection plate. This stress value can be seen inner surface of rivet hole. Stress distributions spread more uniform than preceding plate. Because of rivet holes distances are more far away preceding plate, stress spread out much place and stress values which have every mm^2 are decreasing.

Although both connection plates have same loads, maximum stress is smaller than preceding connection plate. But this connection plate does not safety. Stress distributions can be seen in figure 5.74.

If distance between rivet holes is 2,5d, maximum stress value is 143,09 MPa. and can be seen in figure 5.75. Maximum stress place is the same with previous connection plate. This stress value can be seen inner surface of rivet hole. Stress distributions are getting more uniform and maximum stress value decrease. But this connection plate is not safety.

If distance between rivet holes is 3d, maximum stress value is 142,673 MPa. Maximum stress value of this connection plate is similar with the connection plate which has 2,5d rivet holes distances. But these values are too close to each other. Both of them have nearly same stress distributions. Maximum stress occurs inner surface of rivet hole. In this situation, this connection plate thickness is not safety under these load values. This plate stress distributions can be seen in figure 5.76.

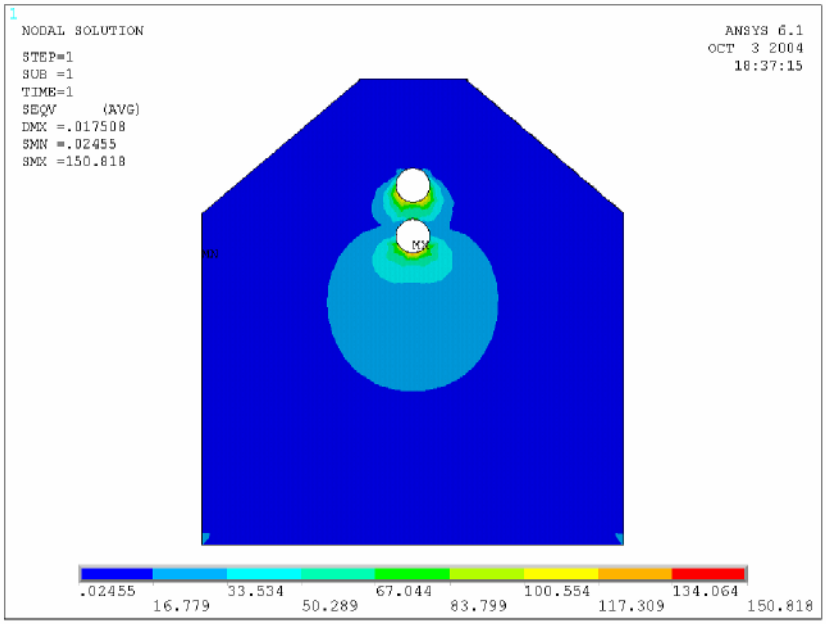

Figure 5.73 Third connection point plate Von Mises stress distributions, thickness of plate 7 mm. and rivets distance 1,5d (Units are MPa)

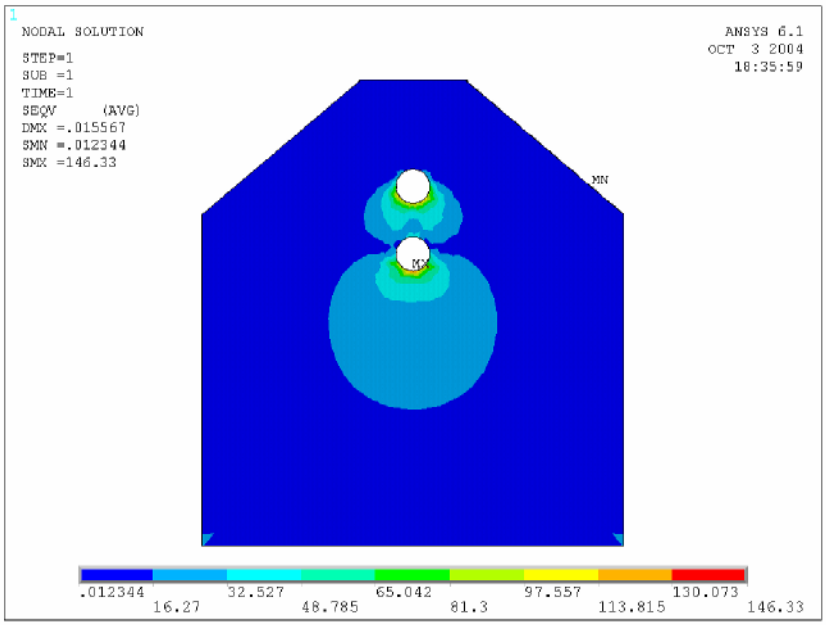

Figure 5.74 Third connection point plate Von Mises stress distributions, thickness of plate 7 mm. and rivets distance 2d (Units are MPa)

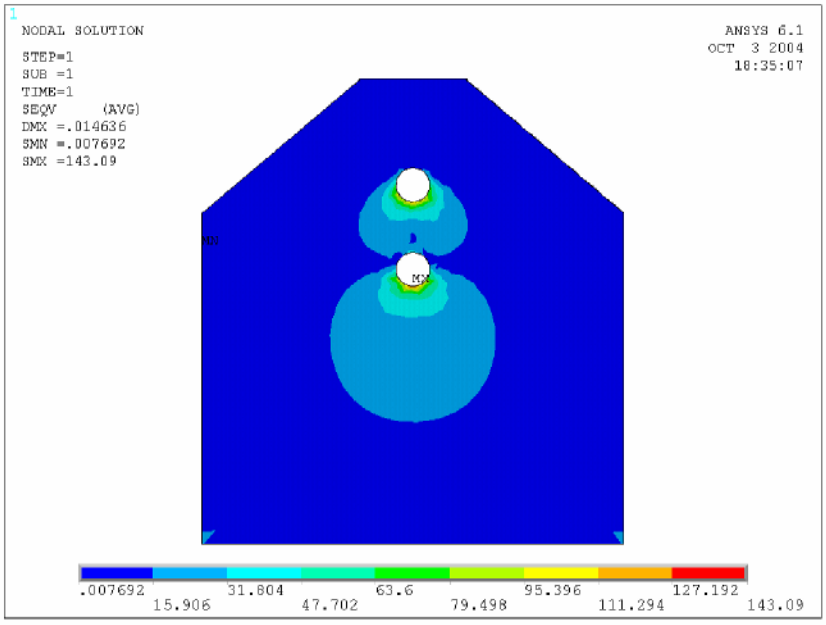

Figure 5.75 Third connection point plate Von Mises stress distributions, thickness of plate 7 mm. and rivets distance 2,5d(Units are MPa)

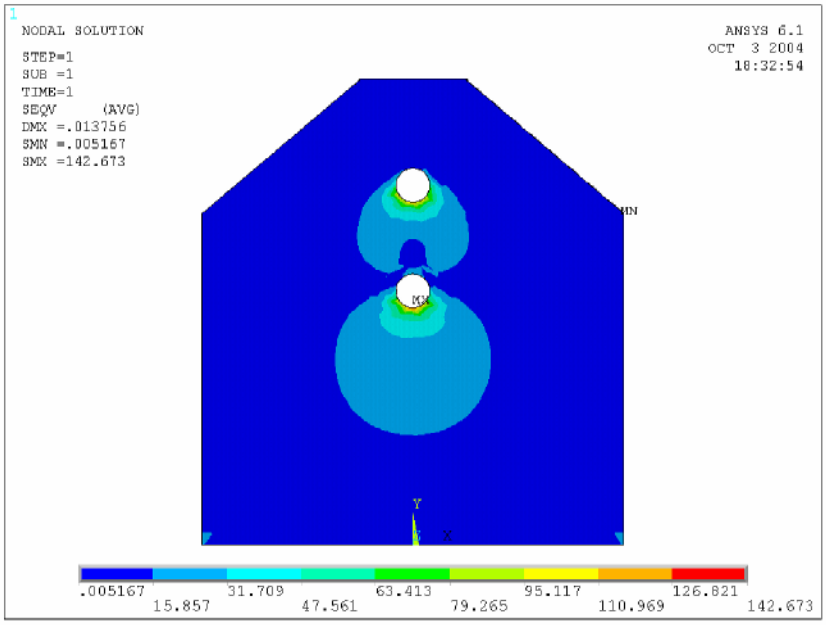

Figure 5.76 Third connection point plate Von Mises stress distributions, thickness of plate 7 mm. and rivets distance 3d (Units are MPa)

Second type of second connection plate thickness is 8 mm. and can be seen in figure 5.77. If rivet holes distances are chosen 1,5d, maximum stress value is 129,877 MPa. Maximum stress value is under safety stress value. If distance between rivet holes is 2d, maximum stress value is 125,509 MPa. Stress distributions can be seen in figure 5.78.

If distance between rivet holes is 2,5d, maximum stress value is 122,469 MPa. This plate can be seen in figure 5.79.

If distance between rivet holes is 3d, maximum stress value is 124,15 MPa and maximum stress value is over safety stress value, shown in figure 5.80. This plate is safety for all rivet distances various.

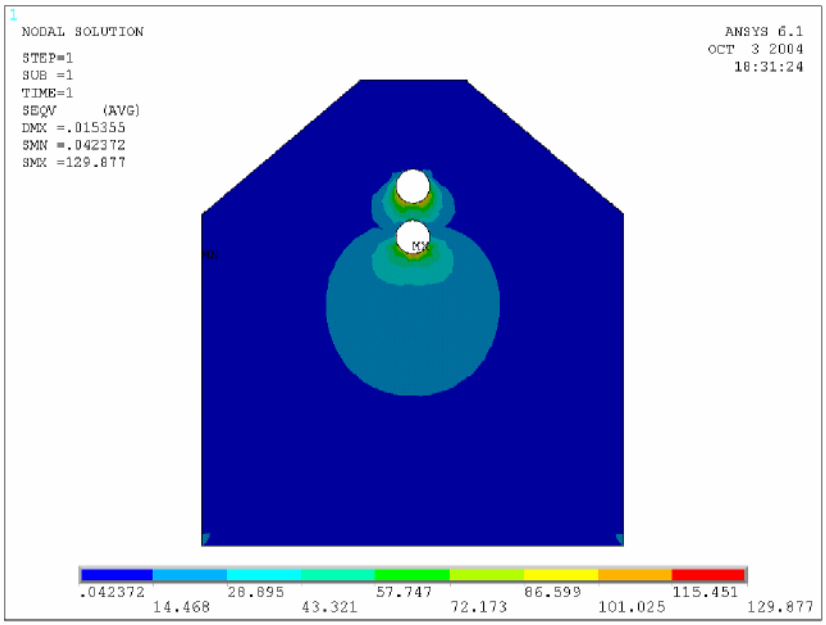

Figure 5.77 Third connection point plate Von Mises stress distributions, thickness of plate 8 mm. and rivets distance 1,5d (Units are MPa)

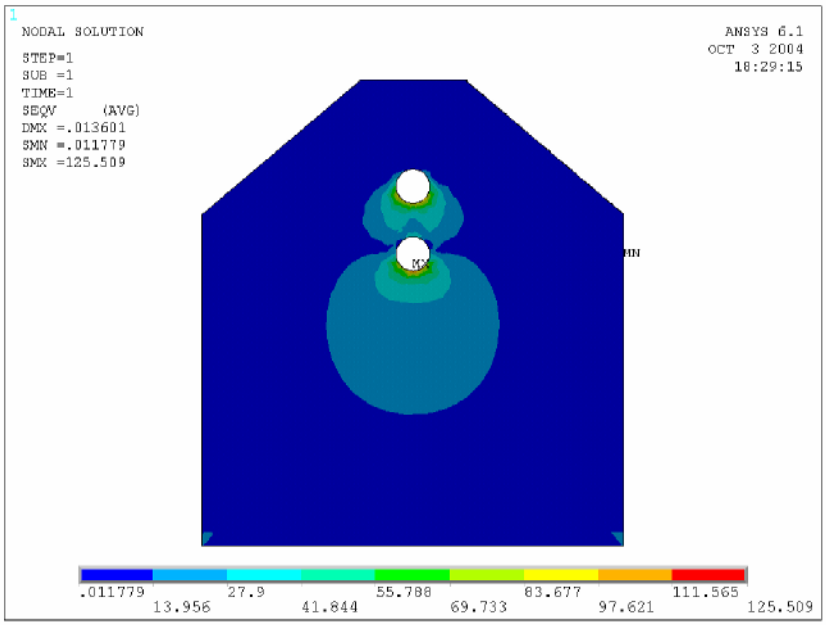

Figure 5.78 Third connection point plate Von Mises stress distributions, thickness of plate 8 mm. and rivets distance 2d (Units are MPa)

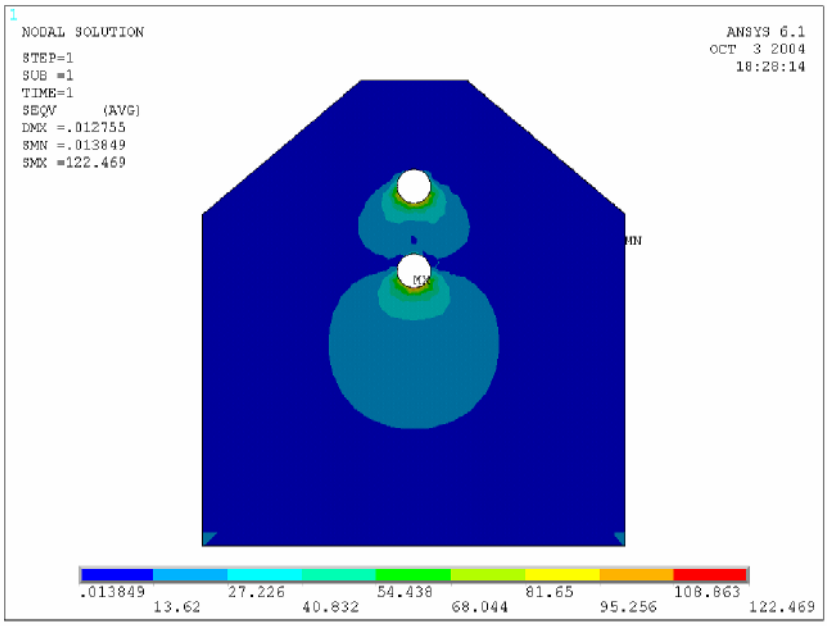

Figure 5.79 Third connection point plate Von Mises stress distributions, thickness of plate 8 mm. and rivets distance 2,5d (Units are MPa)

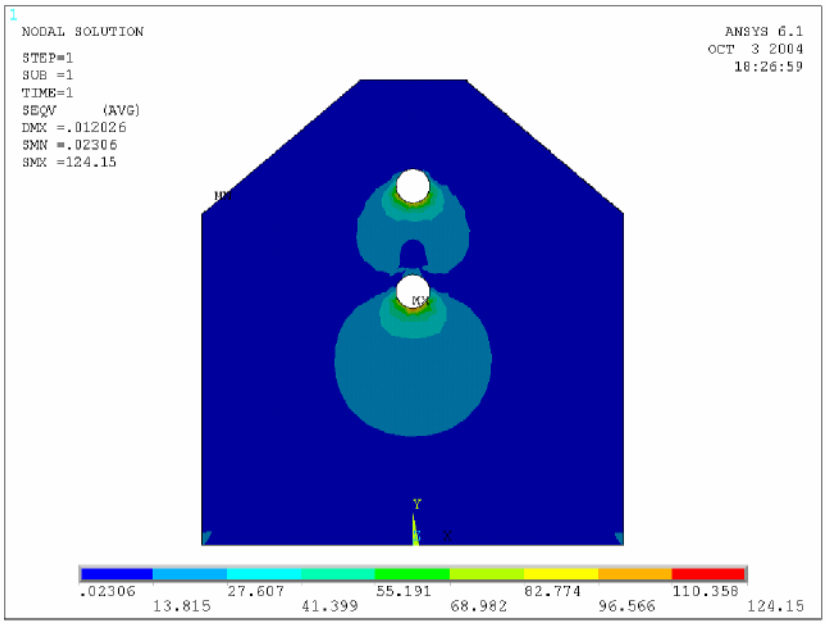

Figure 5.80 Third connection point plate Von Mises stress distributions, thickness of plate 8 mm. and rivets distance 3d (Units are MPa)

5.4 Results of Main Carrying Beam

Main carrying beam consist of two angles and one plate. It takes pressure load. Angles are 80x40x6 and plate thickness is 10 mm. Rivet holes located vertically on plate as seen in figure 5.81. If distance between two rivets is 1,5d, maximum stress value is 179,771 MPa. This stress value can be seen inner surface of bottom rivet hole. Stress distributions can be seen in figure 5.81a. Stress distributions generally can be seen around the rivet holes and these distributions spread on plate surface. In this situation, this connection plate is not safety.

If distance between rivet holes is 2d, maximum stress value is 149,865 MPa. Maximum stress occurs same place with previous main carrying beam. This stress value can be seen same rivet hole. Stress distributions spread more uniform than preceding plate. Because of rivet holes distances are more far away preceding plate, stress spread out much place and stress value is decreasing nearly 30 MPa. But this connection plate does not safety. Stress distributions can be seen in figure 5.82.

If distance between rivet holes is 2,5d, maximum stress value is 130,699 MPa. and can be seen in figure 5.83. Maximum stress place is the same with previous connection plate. This stress value occurs same rivet hole. Stress distributions are getting more uniform and maximum stress value decrease and the stress value is safety.

If distance between rivet holes is 3d, maximum stress value is 114,499 MPa. Maximum stress value is under safety stress value, shown in figure 5.84. It can be said that safety stress value obtained by changing distances between rivet holes on same thickness. Other thicknesses of main carrying beam are given next section as a graphic.

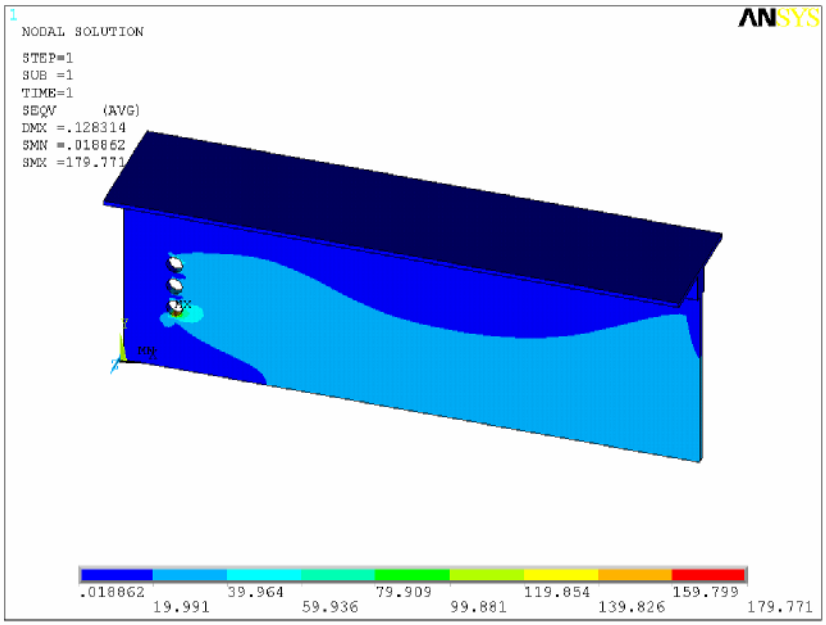

Figure 5.81 Main carrying beam Von Mises stress distributions, thickness of plate 10 mm. and rivets distance 1,5d. (Units are MPa)

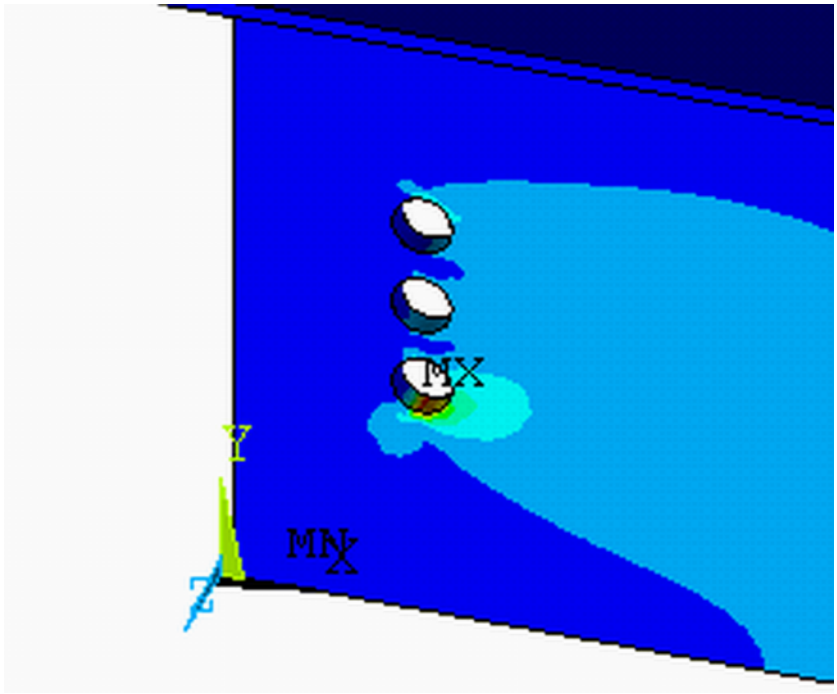

Figure 5.81a Maximum stress

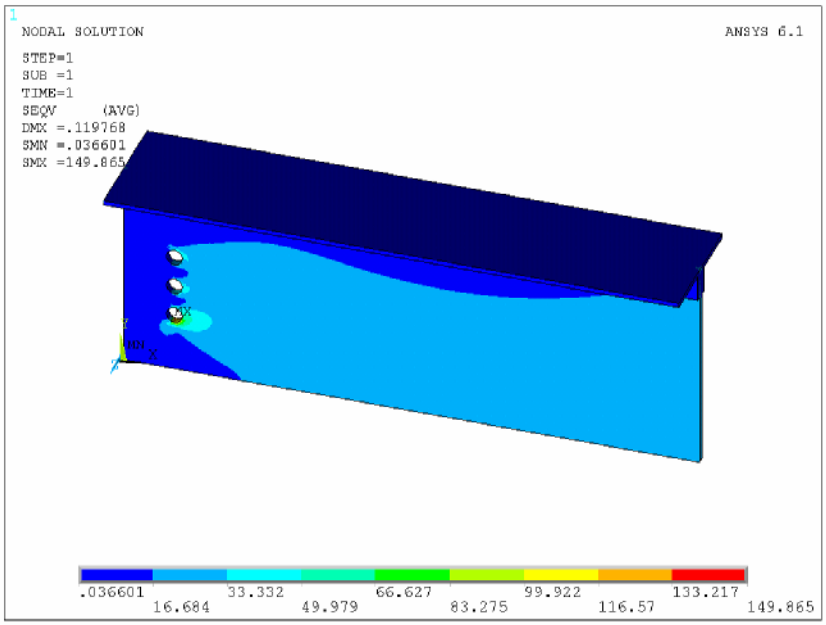

Figure 5.82 Main carrying beam Von Mises stress distributions, thickness of plate 10 mm. and rivets distance 2d. (Units are MPa)

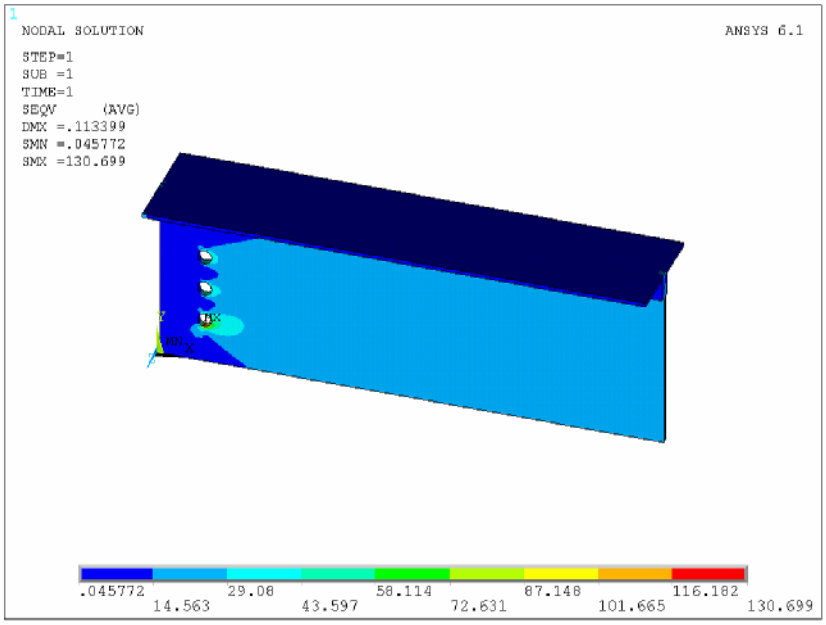

Figure 5.83 Main carrying beam Von Mises stress distributions, thickness of plate 10 mm. and rivets distance 2,5d. (Units are MPa)

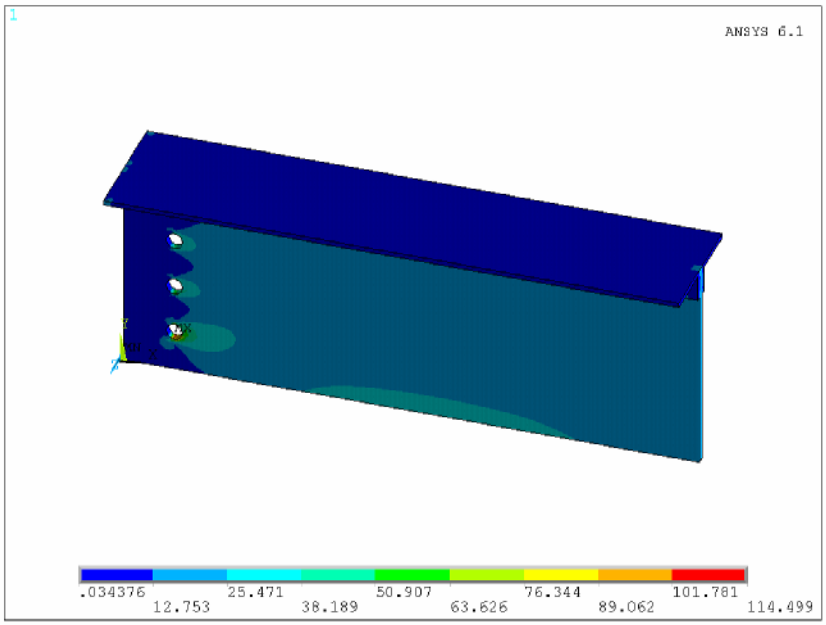

Figure 5.84 Main carrying beam Von Mises stress distributions, thickness of plate 10 mm. and rivets distance 3d. (Units are MPa)

5.5 Result of the Connection Point with Using Contact Element

First connection point was analyzed with angles to investigated behavior of whole component together. Thickness of plate was chosen 13mm. and rivet distances of angles were chosen 3d. Because 3d rivet distance generally gives minimum stress value. Maximum stress value is 133 MPa. It can be said that stress distributions of plate is similar plate which was analyzed as single. Maximum stress value of both plate are to close each other. One of them stress value is 133 MPa. Another one is 134,66 MPa.

Figure 5.85 shows that angles which were named U2 and U3, have much stress value. Green colors show this stress value, because U2 and U3 carry more load than other angles. Load values were given preceding chapter. It can be easily seen that figure 5.85a, first rivet stress value is too much according to second and third rivet.

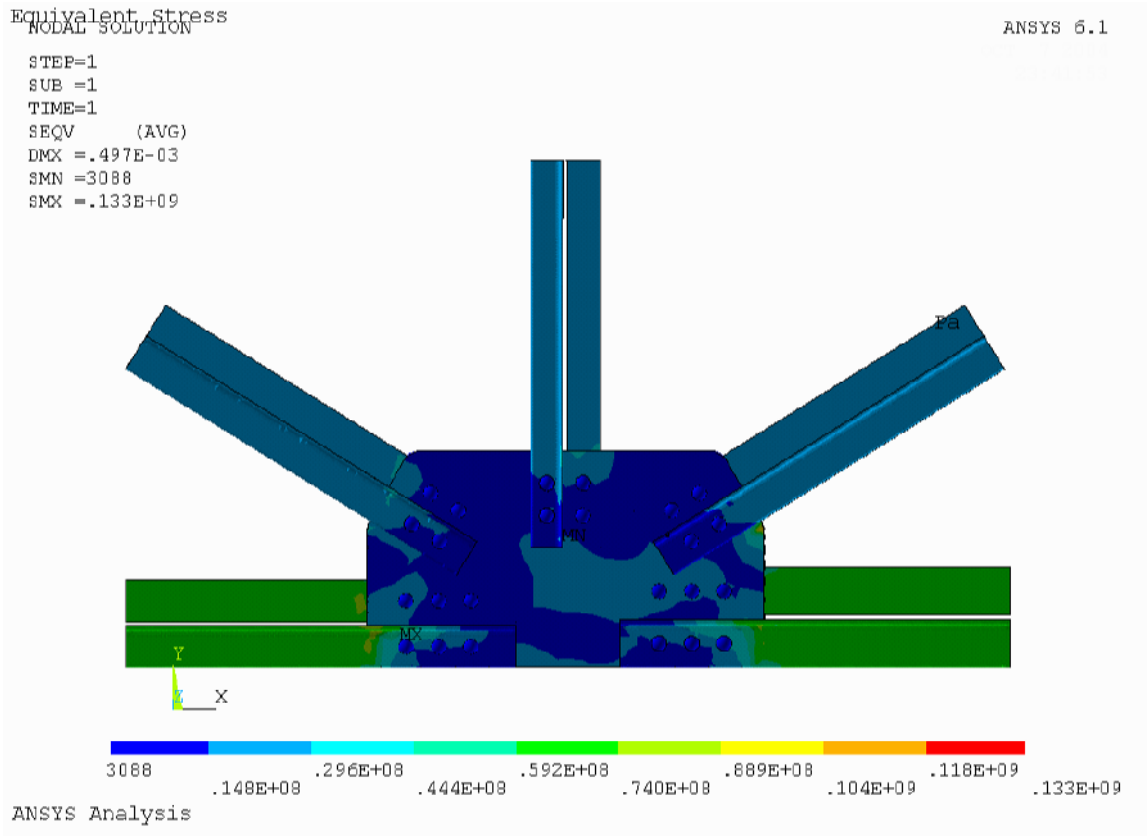

Figure 5.85 Von Mises stress distributions of first connection point. Thickness of plate is 13 mm.

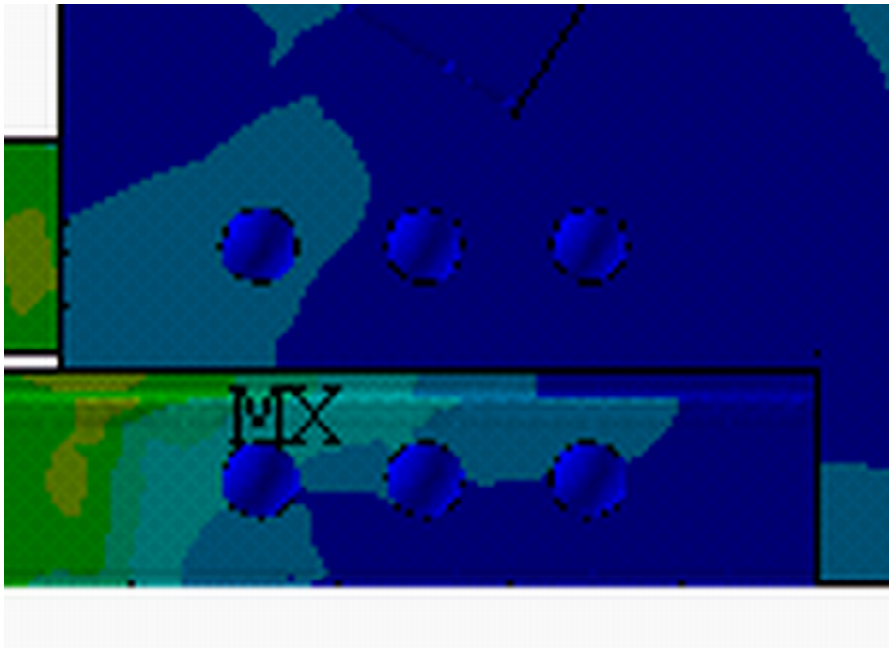

Figure 5.85a Maximum stress

Second connection point components were analyzed together with using contact element like first connection point. Thickness of plate was chosen 13mm. and rivet distances of angles were chosen 3d. Maximum stress value is 140 MPa and it can be seen in figure 5.86. It can be said that stress distributions of this plate and plate which was analyzed as single, are similar. Both of them results are close to each other, 140 MPa. and 135,175 MPa. Another result can be seen in figure 5.52. Maximum stress place is nearly same, shown in figure 5.86b.

Figure 5.86b shows that angles which were named U1 and U3 have much stress value. Green colors show this stress value like first connection point angles. The same stress value can be seen for U3. Load values were given preceding chapter. Stress distributions of angles look safety, they were analyzed one bye one and these values nearly same.

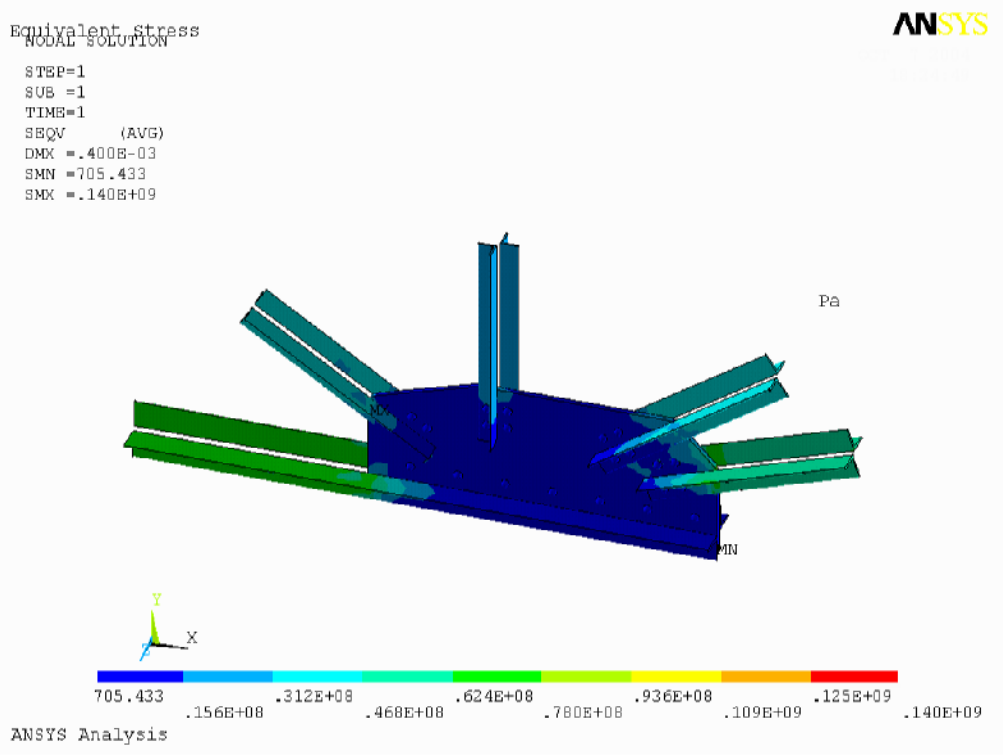

Figure 5.86 Von Mises stress distributions of second connection point.
Thickness of plate is 14 mm.

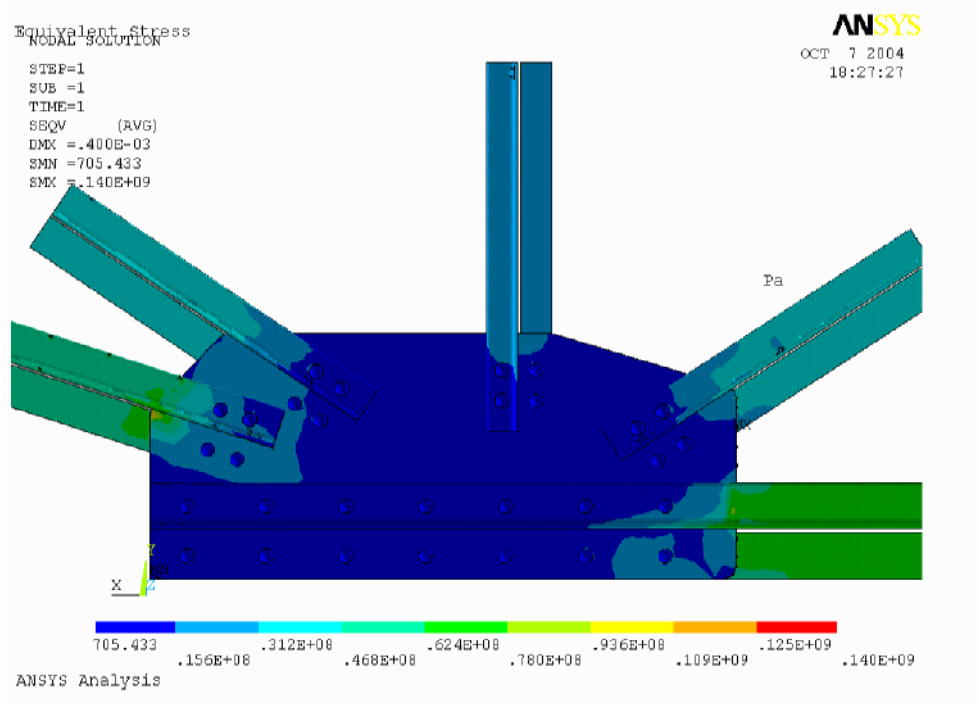

Figure 5.86a Von Mises stress distributions of second connection point. Thickness of plate is 14 mm.

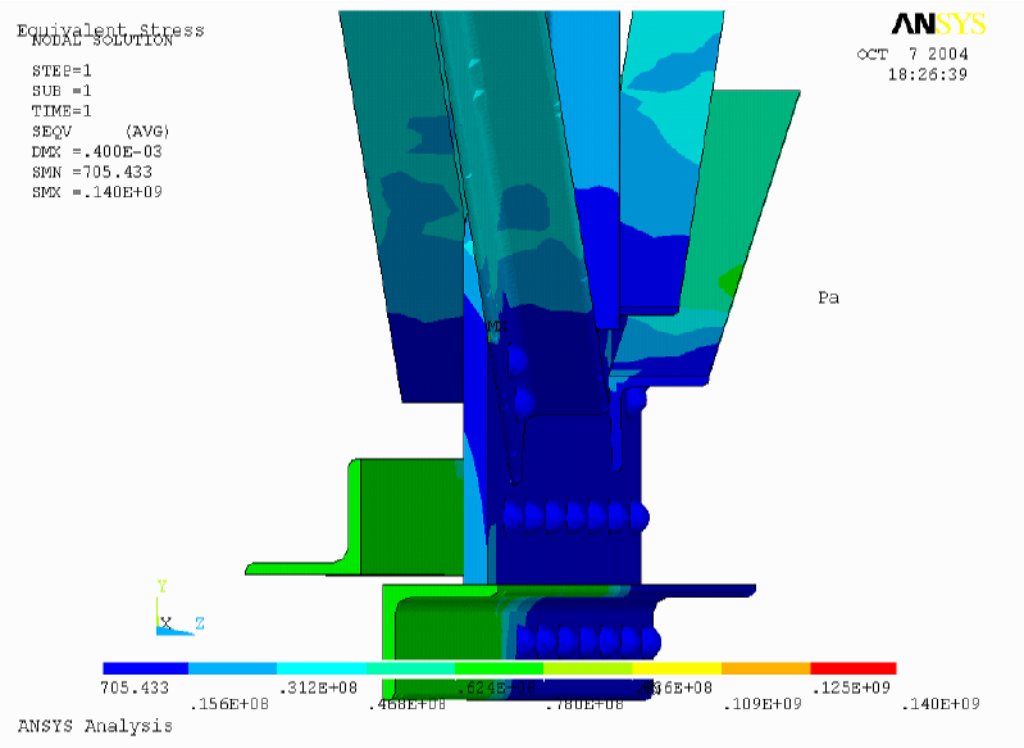

Figure 5.86b Maximum stress

CHAPTER SIX
CONCLUSION

6.1 Conclusion

Figure 6.1 shows that the stress distributions of first connection plate for thicknesses from 12 to 16 mm. It can be easily seen that maximum stress value decrease by choosing 2,5d and 3d rivet distances. Generally minimum stress value occurs 3d rivet distance. Results were obtained by changing rivets distance and thickness of plate for first connection point and the others. Generally, when rivets distance is 3d, stress distribution is minimum for plates of connection points. 2,5d and 3d stress results are very close to each other. Despite of these results, another rivets distance 2d and 1,5d occur higher stress value than 2,5d and 3d. Generally maximum stress occur inner face of rivet holes.

When the stress of connection point angles searched, it has easily seen that increasing rivet distances occurs reducing stress. Figure 6.2 shows stress distributions of the first connection point angles by changing distances between rivets from 3d to 1,5d. Every angles subject to various loads. These loads can be seen as table in last chapter. It can be easily seen that minimum stress distributions of the connection point angles are obtained 3d rivet distance.

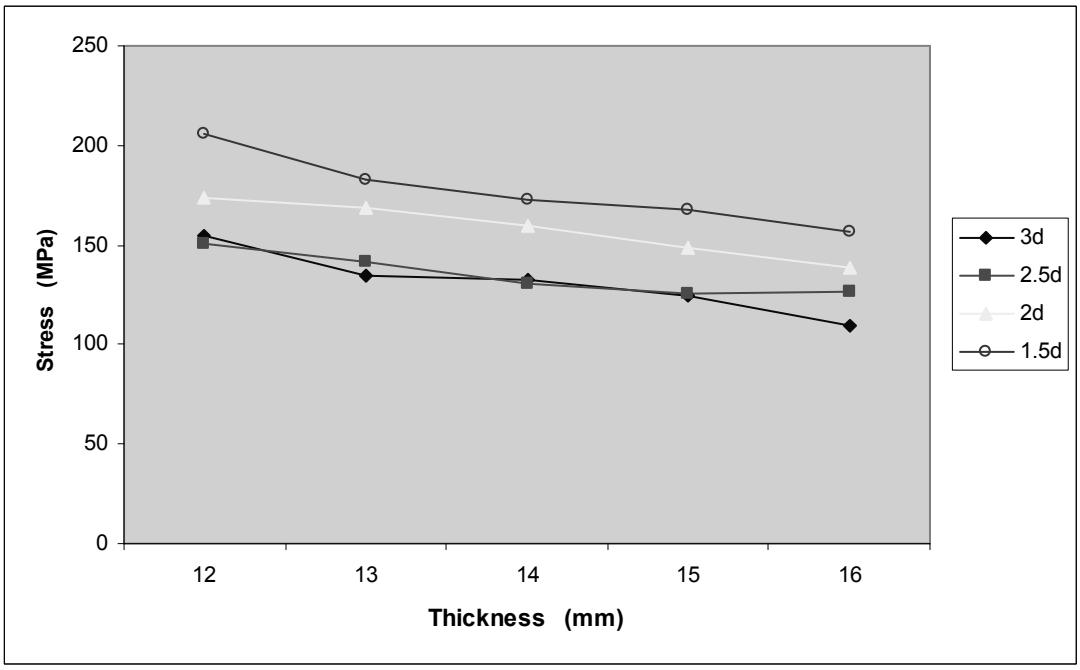

Figure 6.1 Von Mises stress distributions of the first connection point plate

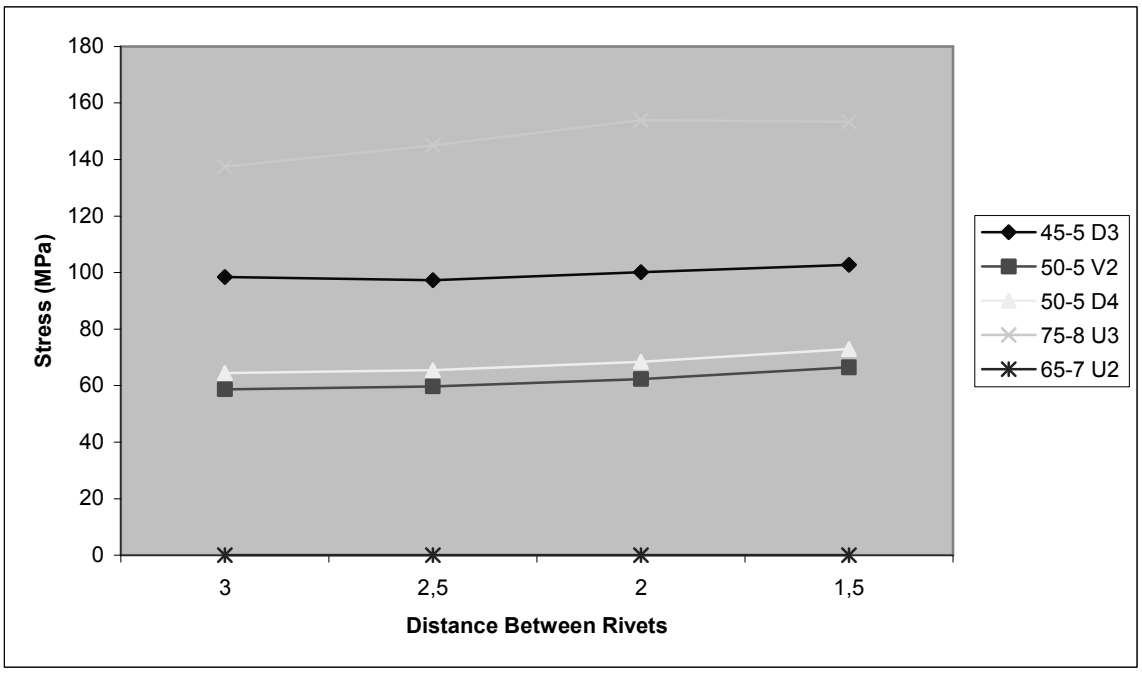

Figure 6.2 Von Mises stress distributions of first connection point angles.
Every angles subject to various loads.

Figure 6.3 shows the stress distributions of second connection plate for the thicknesses from 12 to 16 mm. and the rivet distances were varied 1,5d, 2d, 2,5d, 3d. The stress results of second connection point resemble to first connection point results. The minimum stress value is obtained by choosing 3d rivets distance on plate of second connection point. Loads which are applied on angles are different but 3d rivets distance supply minimum stress distributions. Because, stress can find much place, for this reason stress value decreases. The minimum stress distributions occur by choosing 3d rivet distance. Three of connection points have same angles which are named V1, V2, V3 and the same loads are applied. Stress distributions of these angles shown in figure 6.4. These results are same for sheet iron of third connection point. Results can be shown in figure 6.5. Minimum stress value occurs 2,5d and 3d rivet distances.

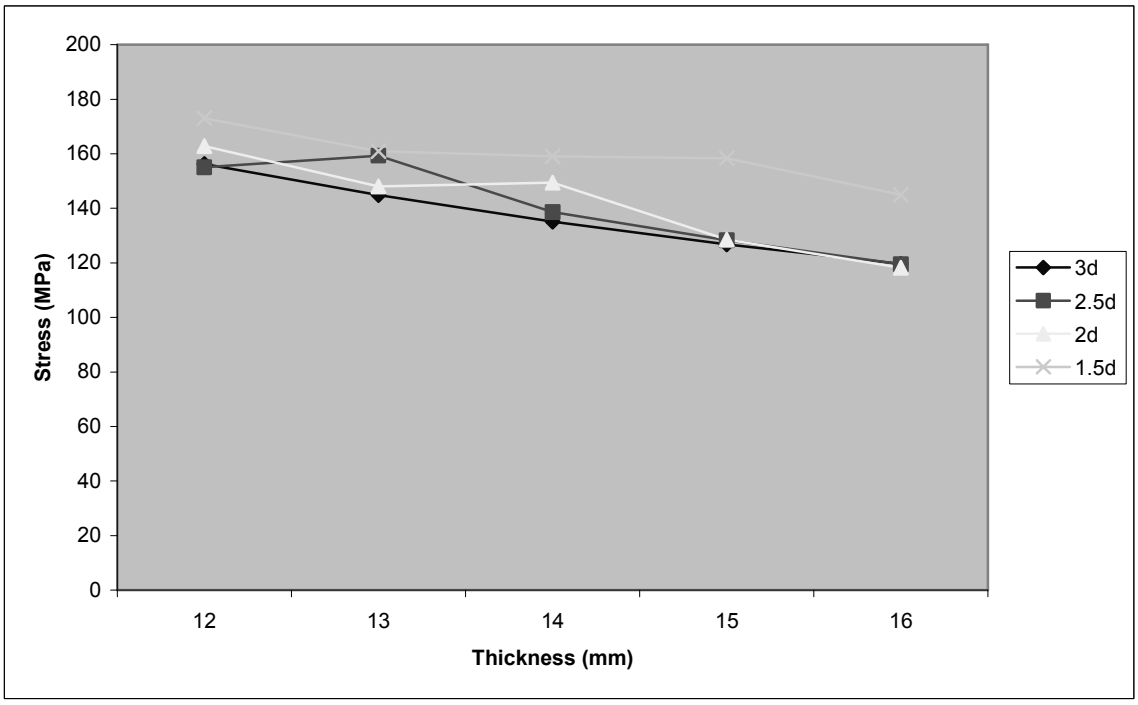

Figure 6.3 Von Mises stress distributions of the second connection point plate

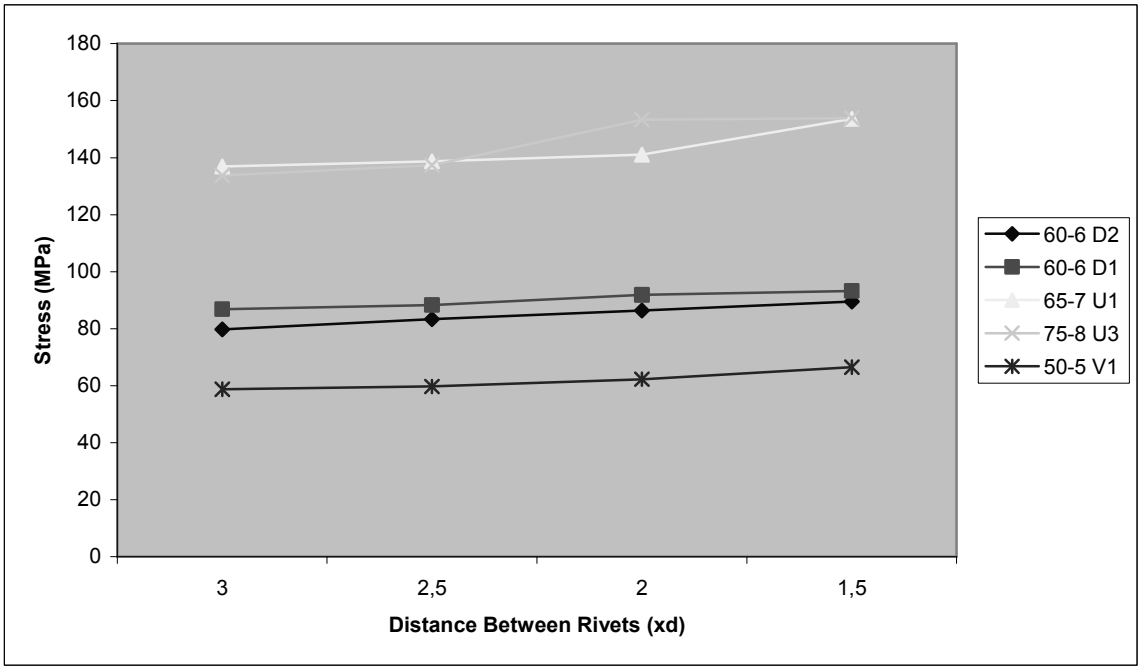

Figure 6.4 Von Mises stress distributions of second connection point angles.
Every angles subject to various loads. (Angle of third connection point is same with V2)

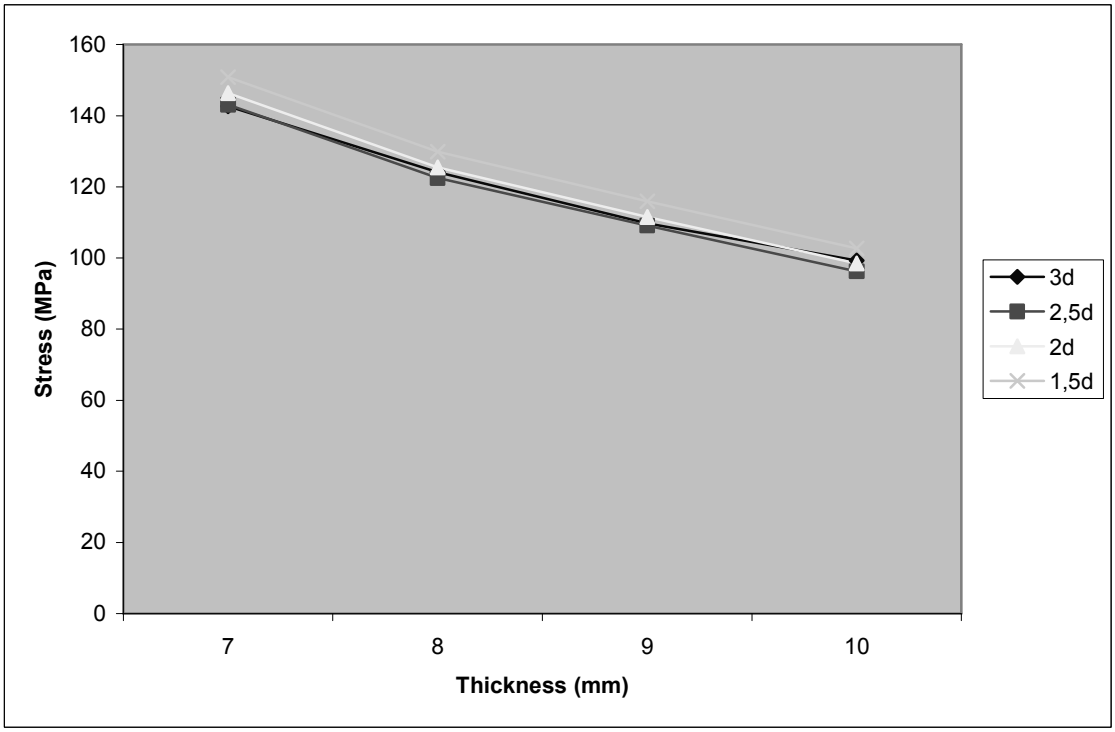

Figure 6.5 Von Mises stress distributions of the third connection point plate

Rivet holes of main carrying beam arranged as a column. Main carrying beam stress results are not different from others. Inner surface of rivet holes is the place where maximum stress distributions formed. It can be easily shown that the stress distributions are getting more uniform by decreasing rivet distances but the minimum stresses occurs approximately by choosing 2,5d and 3d. The importance of stress distributions and displacements on plate and angles are similar for all of analysis. If the rivets distance is chosen 2,5d and 3d, minimum stress distribution on plate and angles are obtained.

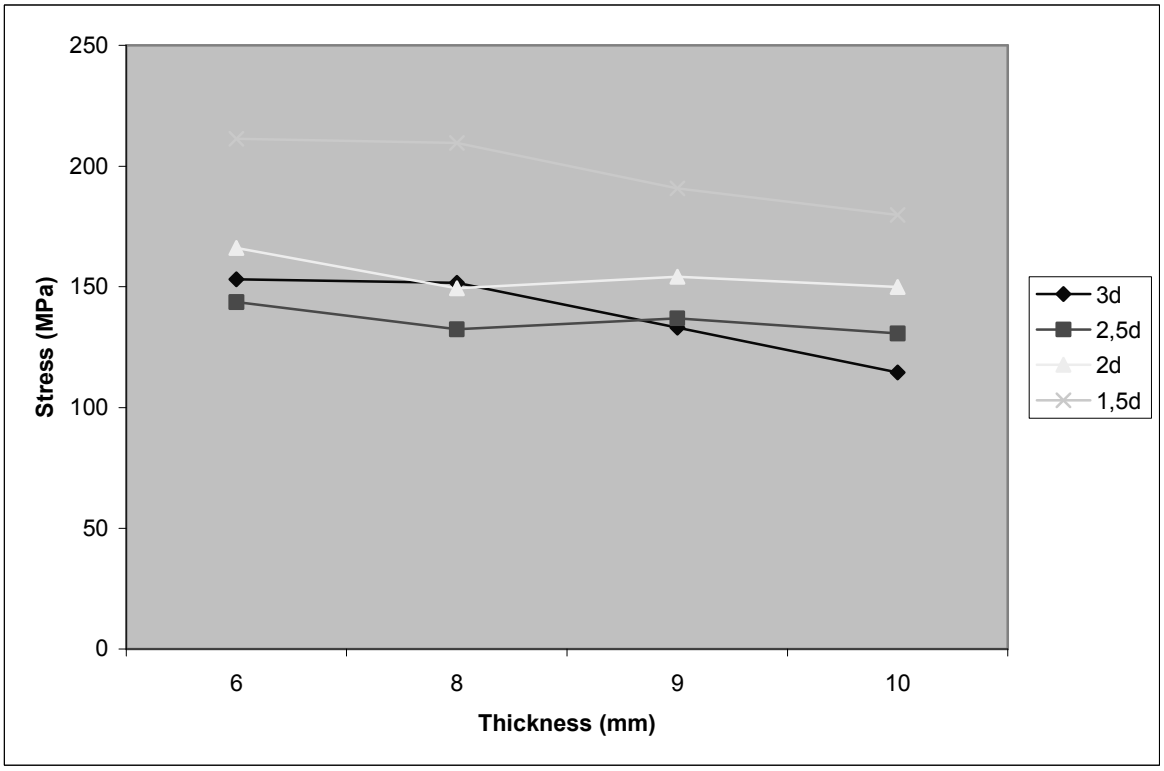

Figure 6.6 Stress distributions of main carrying beam

At the end of these analysis whole connection point analyzed together with using contact element and used element dimensions were chosen according to result of analyses. These result values are under safety value. Results can be seen the last chapter in figure 5.85 – 5.86.

The stress analysis of frame crane connection point has been examined numerically. Increasing the connection plate thickness can reduce stresses in the connection plate. At the all loads and at the all working conditions, the maximum compression stress occurs on the load acting point and inner face of rivet hole.

Table 2 Plate of first connection point Von Mises stress distributions (MPa)

Thickness (mm)					
	12	13	14	15	16
3d	**154,094**	**134,66**	**132,83**	**124,48**	**109,76**
2.5d	**150,68**	**141,38**	**130,15**	**125,28**	**126,59**
2d	**174,09**	**168,97**	**159,5**	**148,23**	**138,45**
1.5d	**205,9**	**182,36**	**173,04**	**168,09**	**156,87**

Table 3 Plate of second connection point Von Mises stress distributions (MPa)

Thickness (mm)					
	12	13	14	15	16
3d	**156,22**	**144,90**	**135,17**	**126,75**	**119,6**
2.5d	**155,06**	**159,317**	**138,63**	**128,3**	**119,51**
2d	**162,86**	**148,02**	**149,5**	**128,5**	**118,199**
1.5d	**175,98**	**160,94**	**159,09**	**158,34**	**144,95**

Table 4 Von Mises stress distributions of plate of third connection point (MPa)

Thickness (mm)				
	7	8	9	10
3d	**142,67**	**124,15**	**109,743**	**99,325**
2,5d	**143,09**	**122,46**	**109,105**	**96,23**
2d	**146,33**	**125,5**	**111,5**	**98,45**
1,5d	**150,81**	**129,87**	**115,93**	**102,71**

Table 5 Von Mises stress distributions of first connection point angles (MPa)

	3d	2,5d	2d	1,5d
45-5 D3	**98,49**	**97,322**	**100,13**	**102,8**
50-5 V3	**58,7**	**59,7**	**62,3**	**66,5**
50-5 D4	**64,5**	**65,5**	**68,5**	**73**
75-8 U3	**137,49**	**145,02**	**153,9**	**153,3**
65-7 U4	**132,3**	**133,1**	**137,1**	**138,3**

Table 6 Von Mises stress distributions of second connection point angles (MPa)

	3d	2,5d	2d	1,5d
60-6 D2	**79**	**83,37**	**86,4**	**89,6**
60-6 D1	**86,86**	**88,35**	**91,9**	**93,3**
65-7 U1	**136,9**	**138,7**	**141,12**	**153,7**
75-8 U3	**137,49**	**145,02**	**153,3**	**153,9**
50-5 V2	**58,7**	**59,7**	**62,3**	**66,5**

Table 7 Von Mises Stress distributions of main carrying beam (MPa)

Thickness (mm)				
	6	8	9	10
3d	**153,07**	**151,65**	**133,03**	**114,49**
2,5d	**143,67**	**132,37**	**136,93**	**130,69**
2d	**166,19**	**149,39**	**154,21**	**149,86**
1,5d	**211,32**	**209,58**	**190,82**	**179,77**

REFERENCES

"*Annual Book of ASTM Standards 2000*" (West Conshohocken, PA: ASTM, 2000). The A502 standard for rivets was withdrawn in 1999.

Ansys 6.1 Documentation

"*American Institute of Steel Construction, Manual of Steel Construction*," latest edition (New York: AISC, 101 Park Avenue, New York NY 10017). Part 4, Connections.

American Railway Engineering Association, "*Specifications for Steel Railway Bridges",* (Chicago: AREA, 59 E. Van Buren St., 1950).

B. Langrand, L. Patronelli, E. Deletombe, E. Markiewicz and P. Drazétic*,"Full scale experimental characterisation for riveted joint design".* Aerospace Science and Technology, volume 6, Issue 5, Sepetember 2002, Pages 333-342.

Brebbia, C. A., & Cnnor, J. (1969). "*Geometrically non-linear finite element analysis*". U.S. Department of Commerce, National Technical Information Service.

C. Carmichael, ed., "*Kent's Mechanical Engineer's Handbook"*, 12th ed. (New York: John Wiley & Sons, 1950). Design and Production volume, Section 10.

C.P. Fung and J. Smart , "*An experimental and numerical analysis of riveted single lap joints"*, J. Aerospace Eng. 208 (1994), 70-79.

Ghali, A., & Neville, A.M. (1978) "*Structural Analysis",* (2nd ed.) London and Southampton, Printed in Great Britain by the Comelet Press Ltd.

G. Harish, T.N. Farris, "*Modeling of skin/rivet contact: application to fretting fatigue"*, collection of Technical Papers, Proceedings of 38th

AIAA/ASME/ASCE Structures, "*Structural Dynamics and Material Conference"*, Vol. 4, 1997, pp. 2761–277.

H. Tada, P.C. Paris and G.R. Irwin, "*The stress analysis of cracks handbook*", ASME Press (2000)

Engineers Edge Solutions by Design(2000). *Rivet Application&Intallation* Retrieved November 13, 2004, from *http://www.engineersedge.com*

Jaroslav Mackerle, "*Finite element analysis of fastening and joining"*: A bibliography (1990–2002). International Journal of Pressure Vessels and Piping. (April 2003)

J. Moreno and A. Valiente, "*Stress intensity factors in riveted steel beams"*, Engineering Failure Analysis, Volume 11, Issue 5, October 2004, Pages 777-787.

Kumar V, German MD, Shih CF. "*An engineering approach for elastic–plastic analysis"*, EPRI NP-1931, EPRI; 1981.

K. Iyer, "*Solutions for contact in pinned connections"*. Int J Solids Struct 38 50 (2001), pp 9133–9148.

Nath B. (1974) "*Fundamentals of Finite Elements for Engineers",* New York: Humanities Press Inc.

Pál Tomka, "*Lateral stability of coupled simply supported beams"*. Journal of Constructional Steel Research, Volume 57, Issue 5, May 2001, Pages 517-523.

P.F.P. de Matos, M.G.P. Moreira, J.C.P. Pina, A.M. Dias and P.M.S.T. de Castro, "*Residual stress effect on fatigue striation spacing in a cold-worked rivet hole"*.

Poceski, A., & Smonce, V. (1972). "*The Finite Element Method and its Applications"*, Haarlem –Holland, The Technical Publishing Company Stam H.

Roeder, Charles W.; Knechtel, Brett; Thomas, Eric; Vaneaton, Anne; Leon, Roberto T.; Preece, F.Robert, "*Seismic behavior of older steel structures",* USA, 1996.

Tarantine G. & Nimmer R. (1994), "*Structural Analysis of Thermoplastic Components*", Mc Graw-Hill, Inc.

Timoshenko, S. (1956). "*Strength of Materials",* Printed in the United States of America, Mc Graw-Hill Book Company, Inc.